

EGE UNIVERSITY
GRADUATE SCHOOL OF NATURAL AND APPLIED SCIENCE
(MSc THESIS)

**SYNTHESIS, CHARACTERIZATION,
FUNCTIONALIZATION AND TUNABLE
CATALYTIC PROPERTIES OF BIMETALLIC
METAL ORGANIC FRAMEWORKS FOR
GLYCEROL OXIDATION**

Hülya AÇAR KILIÇ

Supervisor: Assoc. Prof. Dr. Emine SERT

Department of Chemical Engineering

Presentation Date: 07.12.2018

Bornova-İZMİR

2018

Hülya Açar Kılıç tarafından **Yüksek Lisans** tezi olarak sunulan “SYNTHESIS, CHARACTERIZATION, FUNCTIONALIZATION AND TUNABLE CATALYTIC PROPERTIES OF BIMETALLIC METAL ORGANIC FRAMEWORKS FOR GLYCEROL OXIDATION” başlıklı bu çalışma EÜ Lisansüstü Eğitim ve Öğretim Yönetmeliği ile EÜ Fen Bilimleri Enstitüsü Eğitim ve Öğretim Yönergesi'nin ilgili hükümleri uyarınca tarafımızdan değerlendirilerek savunmaya değer bulunmuş ve 07.12.2018 tarihinde yapılan tez savunma sınavında aday oybirliği/oyçokluğu ile başarılı bulunmuştur.

Jüri Üyeleri:

Jüri Başkanı

: Prof.Dr. Ferhan S.Atalay

İmza

.....


Raportör Üye

: Doç.Dr. Emine Sert

.....


Üye

:Doç.Dr. Aslı Yüksel Özşen

.....


EGE ÜNİVERSİTESİ FEN BİLİMLERİ ENSTİTÜSÜ

ETİK KURALLARA UYGUNLUK BEYANI

EÜ Lisansüstü Eğitim ve Öğretim Yönetmeliğinin ilgili hükümleri uyarınca Yüksek Lisans Tezi olarak sunduğum “SYNTHESIS, CHARACTERIZATION, FUNCTIONALIZATION AND TUNABLE CATALYTIC PROPERTIES OF BIMETALLIC METAL ORGANIC FRAMEWORKS FOR GLYCEROL OXIDATION” başlıklı bu tezin kendi çalışmam olduğunu, sunduğum tüm sonuç, doküman, bilgi ve belgeleri bizzat ve bu tez çalışması kapsamında elde ettiğimi, bu tez çalışmasıyla elde edilmeyen bütün bilgi ve yorumlara atıf yaptığımı ve bunları kaynaklar listesinde usulüne uygun olarak verdiğimi, tez çalışması ve yazımı sırasında patent ve telif haklarını ihlal edici bir davranışımın olmadığını, bu tezin herhangi bir bölümünü bu üniversite veya diğer bir üniversitede başka bir tez çalışması içinde sunmadığımı, bu tezin planlanmasından yazımına kadar bütün safhalarda bilimsel etik kurallarına uygun olarak davrandığımı ve aksinin ortaya çıkması durumunda her türlü yasal sonucu kabul edeceğimi beyan ederim.

07/12/2018

Hülya Açar Kılıç

ÖZET**GLİSEROL OKSİDASYONU İÇİN BİMETALİK METAL
ORGANİK AĞ YAPILARIN SENTEZLENMESİ,
KARAKTERİZASYONU, KATALİK ÖZELLİKLERİNİN
MODİFİKASYONU VE İŞLEVSELLENDİRİLMESİ**

AÇAR KILIÇ, Hülya

Yüksek Lisans Tezi, Kimya Mühendisliği Anabilim Dalı

Tez Danışmanı: Doç. Dr. Emine SERT

Aralık 2018, 84 sayfa

Bu çalışmada; gliserol, zirkonyum bazlı metal organik ağ yapıları (MOF) kullanılarak dihidroksi aseton, gliseraldehid, gliserik asit, formik asit, laktik asit ve asetik asit gibi değerli kimyasallara dönüşümü incelenmiştir. Gliserol oksidasyon reaksiyonu Zr bazlı metal organik ağ yapıları olan UiO-66 ve UiO-66-NH₂ varlığında incelenmiştir. UiO-66 sentezinde terefitalik asit, UiO-66-NH₂ sentezinde ise amino terefitalik asit kullanılmıştır. Yapıya eklenen amino grubunun ve farklı miktarlarda yüklenen magnezyumun gliserol dönüşümü ve ürünlerin seçimliliği üzerindeki etkileri incelenmiştir. Sentezlenen metal organik ağ yapıları XRD, SEM, TGA ve BET analizleri ile karakterize edilmişlerdir. Tüm katalizörler TGA sonuçlarına göre termal olarak kararlı bulunmuştur. Katalizörün kristal yapısı (XRD), literatürdeki UiO-66'ya benzer elde edilmiştir. Saf UiO-66'nın yüksek kristallik derecesi, magnezyum ilavesinden sonra hafifçe azalmıştır. SEM sonuçlarına göre, küçük parçacıklar homojen bir şekilde eşit dağılmışlardır. Magnezyum ilavesi aglomerasyona neden olmuştur. Gliserol oksidasyon, reaksiyonu üç saat boyunca atmosferik basınç altında 70°C'de gerçekleştirilmiştir. En aktif katalizör Mg_{0.3}@UiO-66-NH₂ olarak bulunmuştur. Gliserol dönüşümü %21.7 olarak hesaplanmış ve formik asit, laktik asit ve dihidroksi aseton seçiciliği sırasıyla % 42.2, % 21.9 ve % 20.3 olarak hesaplanmıştır. Deneysel tasarım çalışmaları da Anova yazılımı kullanılarak gerçekleştirilmiştir. Parametrik çalışma, Mg_{0.3}@UiO-66-NH₂ kullanılarak farklı sıcaklıklarda, katalizör yükleme ve hidrojen peroksit / gliserol molar oranlarında incelenmiştir.

Anahtar Kelimeler; Metal organik ağ yapıları, gliserol oksidasyonu, oksidasyon, kataliz, bimetalik



ABSTRACT**SYNTHESIS, CHARACTERIZATION, FUNCTIONALIZATION
AND TUNABLE CATALYTIC PROPERTIES OF BIMETALLIC
METAL ORGANIC FRAMEWORKS FOR GLYCEROL
OXIDATION**

AÇAR KILIÇ, Hülya

MSc in Chemical Eng.

Supervisor: Assoc. Prof. Dr. Emine SERT

December 2018, 84 pages

In this study, glycerol was oxidized to valuable chemicals which were dihydroxy acetone, glyceraldehyde, glyceric acid, formic acid, lactic acid and acetic acid by using the Zr based metal organic frameworks (MOF). Glycerol oxidation was performed using UiO-66 and UiO-66-NH₂. In the synthesis of UiO-66 and UiO-66-NH₂, terephthalic acid and amino terephthalic acid were used as ligand, respectively. The effect of amino groups and the effect of magnesium addition on the glycerol conversion and product selectivity were investigated for both MOFs. The synthesized MOFs were characterized using XRD, SEM, TGA and BET analysis. All the catalysts were found as thermally stable according to TGA results. Crystallinity (XRD) of the catalyst were obtained similar to the UiO-66 in literature. High crystallinity of pure UiO-66 reduced the slightly after magnesium addition. According to SEM results, small particles were observed having a uniform distribution at homogeneity. Magnesium addition caused agglomeration. Glycerol oxidation reaction was carried out at 70°C under atmospheric pressure for three hours. The most active catalyst was found as Mg_{0.3}@UiO-66-NH₂. The conversion of glycerol was calculated as 21.7 % and selectivity of formic acid, lactic acid and dihydroxy acetone was found as 42.2 %, 21.9 % and 20.3 %, respectively. The experimental design studies were also performed by using Anova software. The parametric study was investigated using Mg_{0.3}@UiO-66-NH₂ at different temperatures, catalyst loading and hydrogen peroxide/glycerol molar ratios.

Keywords; Metal organic frameworks, glycerol oxidation, oxidation, catalysis, bimetallic



ACKNOWLEDGEMENT

I would like to thank to my supervisor, Assoc. Prof. Dr. Emine Sert, for the continuous support, her patience, motivation, encouragement and enthusiasm. I have been extremely lucky to have a supervisor who cared so much about my work and who steered me in the right direction whenever I needed it.

I would also like to acknowledge Prof. Dr. Ferhan Atalay and I am gratefully indebted to his very valuable comments on this thesis.

I also would like to thank for the financial support provided by Ege University Science Research Project -16MÜH124.

I am also grateful to Gökçe Anılır and Esra Yılmaz for their friendship, help and supports.

Finally, I must express my very profound gratitude to my husband Dr. Emre Kılıç, to my daughter Eylül Kılıç and to my parents for providing me with unfailing support and continuous encouragement throughout study and writing this thesis.



TABLE OF CONTENTS

	<u>Page</u>
ÖZET.....	vii
ABSTRACT.....	ix
ACKNOWLEDGMENT.....	xi
LIST OF FIGURES.....	xv
LIST OF TABLES.....	xix
1. INTRODUCTION.....	1
2. REVIEW ON METAL ORGANIC FRAMEWORK.....	3
2.1 Definition of Metal Organic Framework.....	3
2.2 Synthesis Methods of Metal Organic Framework.....	4
2.3 Bimetallic Metal Organic Frameworks.....	8
2.4 Zirconium Based Metal Organic Frameworks.....	11
3. REVIEW ON GLYCEROL OXIDATION.....	13
3.1 Properties, Uses and Applications of Glycerol.....	13
3.2 Glycerol Oxidation Mechanism.....	15
4. LITERATURE REVIEW.....	19
4.1 Use of UiO-66 as catalyst.....	19
4.2 Use of UiO-66-NH ₂ as catalyst.....	22
4.3 Studies on the Synthesis of Bimetallic Metal Organic Frameworks.....	23
4.4 Catalysts in Glycerol Oxidation.....	26

TABLE OF CONTENTS (continued)

	<u>Page</u>
5. MATERIALS AND METHOD.....	30
5.1 Chemicals.....	30
5.2 Synthesis of Zr based Metal Organic Frameworks.....	32
5.2.1 Synthesis of UiO-66.....	32
5.2.2 Synthesis of UiO-66-NH ₂	32
5.2.3 Synthesis of Mg@UiO-66 and Mg@UiO-66-NH ₂	32
5.3 Characterization Methods.....	35
5.4 Glycerol Oxidation.....	36
5.5 Analysis.....	40
6. RESULTS AND DISCUSSION.....	42
6.1 Characterization of Zr Based Metal Organic Frameworks.....	42
6.2 Catalytic Activities of Zirconium Based Metal Organic Frameworks in Glycerol Oxidation.....	58
7. CONCLUSION.....	68
REFERENCES.....	70
CURRICULUM VITAE.....	81

LIST OF FIGURES

<u>Figure</u>	<u>Page</u>
2.1. Different Types of Metal Organic Frameworks.....	4
2.2. Conventional solvothermal synthesis of MOF.....	5
2.3. Microwave solvothermal synthesis of MOF.....	5
2.4. Sonochemical synthesis of MOF.....	6
2.5. Electrochemical synthesis method of MOF.....	7
2.6. Mechanochemical synthesis of MOF.....	7
2.7. Mixed-metal MOF-74 structure and styrene oxidation products organic structure.....	10
2.8. Molecular shape of Zr containing NH ₂ functionalized monometallic UiO-66 type metal organic framework.....	10
2.9. Molecular shape of Zr and Ti containing NH ₂ functionalized bimetallic UiO-66 type metal organic framework.....	11
2.10. Representation of a) [Zr ₆ -O ₄ (OH ₄)] ¹²⁺ , b) Crystalline structure of UiO-66.....	12
2.11. The structure of UiO-66 and UiO-66 derivatives.....	12
2.12. Molecular structure of organic linker. (Terephthalate).....	12
3.1. Transesterification of vegetable oils with methanol.....	13

LIST OF FIGURES (Continued)

<u>Figure</u>	<u>Page</u>
3.2. Some valuable products obtained from glycerol.....	15
3.3. Glycerol Oxidation Pathway.....	16
3.4. Possible Glycerol Oxidation Reaction Mechanism in Alkaline Medium.....	17
3.5. Possible Glycerol Oxidation Reaction Mechanism in Neutral Medium.....	17
3.6. Possible Glycerol Oxidation Reaction Mechanism in Acidic Medium.....	18
5.1. The schematic description of preparation steps.....	34
5.2. Molecular structures of metal precursor, linker and building unit of UiO-66.....	34
5.3. Molecular structures of metal precursor, linker and building unit of UiO-66-NH ₂	35
5.4. Molecular structure of UiO-66-frameworks.....	35
5.5. The scheme of experiment setup.....	37
5.6. Schematic representation of UiO-66 and UiO-66-NH ₂	38
5.7. The sample HPLC chromatogram.....	40
6.1. TGA and DTG curves for UiO-66.....	43

LIST OF FIGURES (Continued)

<u>Figure</u>	<u>Page</u>
6.2. TGA and DTG curves for Mg _{0.15} @UiO-66.....	44
6.3. TGA and DTG curves for Mg _{0.225} @UiO-66.....	44
6.4. TGA and DTG curves for Mg _{0.3} @UiO-66.....	45
6.5. TGA and DTG curves for UiO-66-NH ₂	46
6.6. TGA and DTG curves for Mg _{0.15} @UiO-66-NH ₂	47
6.7. TGA and DTG curves for Mg _{0.225} @UiO-66-NH ₂	47
6.8. TGA and DTG curves for Mg _{0.3} @UiO-66-NH ₂	48
6.9. XRD pattern for synthesized UiO-66 and UiO-66 by loading different amount of Mg.....	50
6.10. XRD pattern for synthesized UiO-66-NH ₂ and UiO-66-NH ₂ by loading different amount of Mg.....	51
6.11. SEM image of UiO-66.....	53
6.12. SEM image of Mg _{0.15} @UiO-66.....	53
6.13. SEM image of Mg _{0.225} @UiO-66.....	54
6.14. SEM image of Mg _{0.3} @UiO-66.....	54
6.15. SEM image of UiO-66-NH ₂	55

LIST OF FIGURES (Continued)

<u>Figure</u>	<u>Page</u>
6.16. SEM image of Mg _{0.15} @UiO-66.....	56
6.17. SEM image of Mg _{0.225} @UiO-66-NH ₂	56
6.18. SEM image of Mg _{0.3} @UiO-66-NH ₂	57
6.19. Catalytic activities of zirconium based metal organic frameworks.....	59
6.20. The product distribution of glycerol oxidation using Mg _{0.3} @UiO-66-NH ₂ after 3 hours.....	61
6.21. The proposed mechanism of glycerol oxidation.....	62
6.22. Main effects of parameters.....	63
6.23. The effects of the reaction time on the conversion of glycerol.....	66
6.24. The selectivity of products with different reaction time.....	67

LIST OF TABLES

<u>Table</u>	<u>Page</u>
3.1. Physical properties of glycerol.....	14
4.1. Textural properties of the catalysts.....	25
4.2. Glycerol oxidation studies from literature results.....	29
5.1. Chemicals used in synthesis of different MOFs.....	30
5.2. The chemicals used in this study.....	31
5.3. The synthesis conditions of Zr based metal organic frameworks.....	33
5.4. The parameters for catalyst screening experiments.....	38
5.5. Design experiments. with three parameters at three levels for glycerol oxidation.....	39
5.6. The experimental plan for glycerol oxidation catalysed by Mg _{0.3} @UiO-66-NH ₂	39
6.1. The weight losses of zirconium-based metal organic frameworks including terephthalic acid.....	45
6.2. The weight losses of zirconium-based metal organic frameworks including amino terephthalic acid.....	49
6.3. Surface area of the synthesis Zr-based metal organic frameworks.....	58

LIST OF TABLES (Continued)

<u>Table</u>	<u>Page</u>
6.4. The results of parametric study performed using $Mg_{0.3}@UiO-66-NH_2$	63
6.5. Anova Results for conversion of limiting reactant.....	64
6.6. Product selectivity of liquid phase glycerol oxidation catalysed by $Mg_{0.3}@UiO-66-NH_2$	65



1. INTRODUCTION

World's population and energy demand have been rising steadily. At the same time pollution from petroleum-based products growing day by day due to the bad waste disposal and especially lack of the sustainable processes in most part of the world. Using fossil fuels as starting material is still the most economical way to produce many valuable chemicals. That's why people have been searching alternative new methods and techniques. These alternative roads will be used for the sustainable and renewable productions to reach a green future and to meet the demand of this new world. On the other hand, it still a big engineering challenge to develop environmentally friendly processes with an economical way to improve the wealth of the developing countries by rapid growth.

Glycerol is the most crucial sustainable and renewable resources as being alternative to petroleum-based ones and also it is side product of the biodiesel industry. It is low toxic biodegradable chemical and also has high boiling point which makes the use of glycerol convenient as a starting material in reactions (Pagliaro, 2010). Glycerol is commonly used in many industries such as pharmaceuticals, cosmetics, paints, paper, textile and food industries. Although its usage areas are very large and it is currently being used in high quantities, there is still huge amount of excess glycerol (from fuel industries) to be utilized as a feed stock. Glycerol is a highly functionalized molecule when compared to petroleum-based hydrocarbons. Glycerol, having three very reactive hydroxyl groups, can be converted to many valuable products and intermediates (Pagliaro, 2010). It is a major challenge to improve the product selectivity in these reactions by designing a suitable catalyst. The most common glycerol reactions are oxidation, hydrogenolysis, pyrolysis/gasification, etherification, (trans) esterification, polymerization/oligomerization, dehydration and carboxylation. One of the most important reactions with glycerol is oxidation of glycerol. Large number of the products can be obtained from oxidation. It is directly oxidized to very valuable products such as dihydroxyacetone and glyceryl aldehyde in the presence of suitable catalyst and these products are sometimes converted to the valuable acids (e.g. tartronic acid, glyceric acid) (Pagliaro, 2010). However, there is still a search to find an active and selective catalyst for glycerol oxidation. Current catalysts are not active or not reusable.

In recent years, porous materials have attracted attentions of engineers, chemists' and physicists' due to their big potential properties of their large pores

(Davis, 2002). These materials can be effectively used in reactions as a catalyst, in adsorption, separation, purification and any other applications. Activated carbons, zeolites, molecular sieves, mesoporous silicas and carbon nanotubes are commonly used conventional porous materials in industry for gas adsorption studies (Yu et al., 2017, Nale et al. 2016, Plerdsranov et al. 2017, Wang et al. 2015, Javadian et al., 2015 and Surrey et al., 2016). Among these materials, the most common ones are activated carbons. Although they have high adsorption capacities and large surface areas, they do not have regular structures. Inorganic materials like zeolites have regular structures and high stability at high temperatures. However, they have low stabilities in aqueous systems due to dealumination (Muller, 2000, Silaghi, 2014). These problems lead researchers to synthesize novel porous materials synthesis. Metal organic frameworks (MOF's) with high stability, regular pore structure and high surface areas were developed to overcome these problems and meet the demands of industry (Lee et al, 2009, Falcaro et al., 2016). Unsaturated surface sites and excess charge from metal ions form new active sites for many reactions and make MOFs suitable catalyst. The main reactions using MOFs are oxidation, hydrogenation and photocatalytic reactions (Bai et al., 2016). They are also used as an adsorbent in gas storage systems (especially for hydrogen storage), adsorption and separation studies owing to their high surface area and large pores. Use of metal organic frameworks in fuel cells (as an electrode materials or super-capacitor) rapidly increased in recent years (Ponomareva et al., 2012). High porosity and tunable properties make them suitable for fast mass transport in fuel cell application. One of the other important area that uses MOFs are drug delivery systems.

In this study, different types of mono and bimetallic metal organic frameworks were synthesized. They were characterized and tested in glycerol oxidation, products were analysed to determine the activity and selectivity of the catalyst.

2. REVIEW ON METAL ORGANIC FRAMEWORKS

2.1 Definition of Metal Organic Frameworks

One of the most promising and the new porous materials MOFs are formed from metal cations or metal clusters bonded to poly-functional organic ligands in the form of one, two or three-dimensional structures. They are crystalline coordination polymers having excellent porous structures and very high surface areas. They have tunable surface, pore and acid properties; they also could be modified for special uses. These properties can be achieved by attaching functional groups (in different acidities, hydrophilicities) (Oozeerally et al., 1999) and by tuning coordination numbers of metal ions, type of the metal(s) and symmetries of organic structure. MOFs are also exhibited high hydrothermal stability in many studies. These advantages have significantly increased the studies on MOFs in a few years.

Almost hundred types of metal organic frameworks are mentioned in literature, each of them is used for different purposes. Given these wide variety of MOFs, the most used MOF types are given in Figure 2.1. These MOFs can be synthesized with an organic ligand such as 1,4-benzenedicarboxylic acid (H_2BDC) or terephthalic acid; sometimes their functionalized derivatives: 2-amino-1,4-benzenedicarboxylic acid ($H_2BDC-(OH)_2$) and metal precursor. MOF-5, synthesized using H_2BDC , is a Zn containing MOF having an open framework structure. Although MOF-5 has rigid structure (Li et al., 1999) and seems to be stable in many gas phase applications, its slow stability limits usage in aqueous systems. After these outcomes were observed, researchers tended to HKUST-1, which is a copper-based metal organic framework synthesized by using tricarboxylic acid (Chui et al., 1999). HKUST-1 exhibited good hydrothermal stabilities in many applications and can be synthesized practically with an easy procedure. Recent advances showed an increase in the use of MIL-101 for catalysis and adsorption studies (Férey et al., 2005) MIL-101, synthesized by with a chromium salt and H_2BDC , is a stable MOF in water, active for many reactions and has very high adsorption capacities due to its unsaturated Cr^+ centers. MIL-101 has also very high surface area. ZIF-8 (Zeolitic imidazolate frameworks) is an amine containing microporous MOFs, having similarities with zeolite topology. ZIF-8 is generally used for many reactions, fuel cell applications and some adsorption studies. MIL-53, carboxylic acid-amine groups containing MOFs are commonly used for gas storage. Among these mentioned MOFs, UiO-66, Zr-based MOFs have

an excellent hydrothermal stability. It has also good shape selectivity due to its pore structure and it is very active since it has high amount of Lewis acid sites. UiO-66 can be functionalized easily to change the nature of the surface acid sites; some Bronsted acid creating groups (sulphate, germinal etc.) can be added by applying some easy modifications.

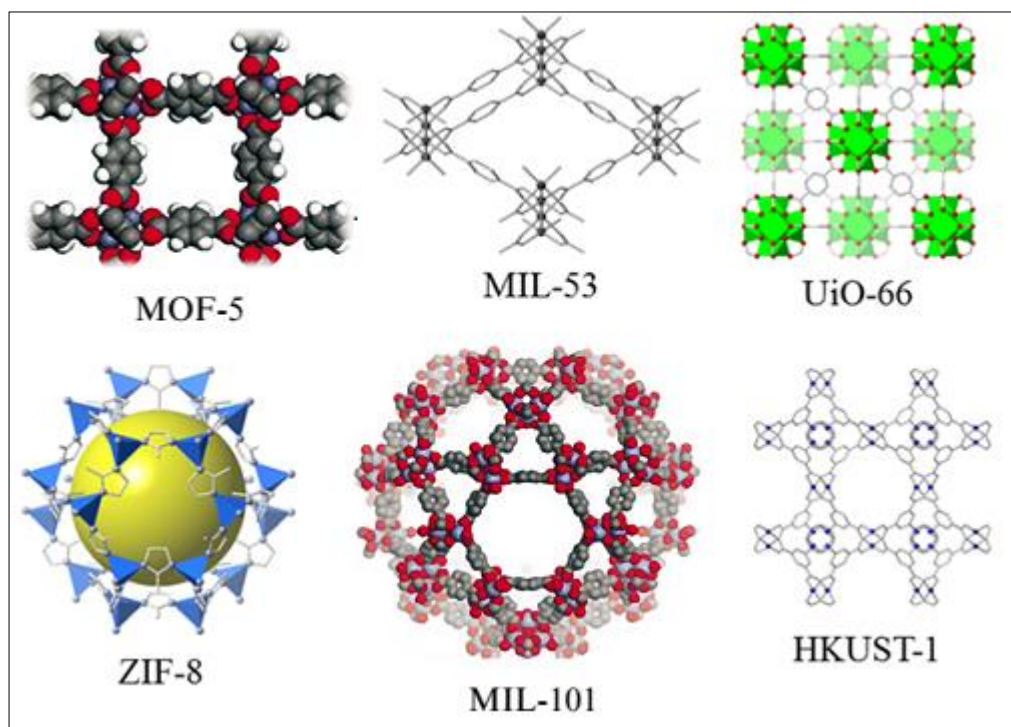


Figure 2.1. Different Types of Metal Organic Frameworks (Lee et al., 2013).

2.2 Synthesis Methods of Metal Organic Frameworks

There are many methods to synthesize metal organic frameworks such as solvothermal/hydrothermal, microwave, sonochemical, electrochemical and mechanochemical methods.

In conventional solvothermal synthesis, metal salt, organic ligand and suitable solvent (water or DMF) are put into the vials and the mixture are heated with conventional electric. Then, waste products are removed by washing using solvent, heat or vacuum treatment. The schematic diagram of this method is given in Figure 2.2. The most common example to this method is UiO-66 synthesis. In the study of Eddaoudi et al (2002) UiO-66 catalyst was prepared by conventional solvothermal method at 120 °C for 24 h. $Zn(NO_3)_2 \cdot 4H_2O$ metal salt and H_2BDC

ligand were mixed in DMF solvent. This material was used in methane storage at 25 °C and 40 bars (Eddaoudi et al., 2002).

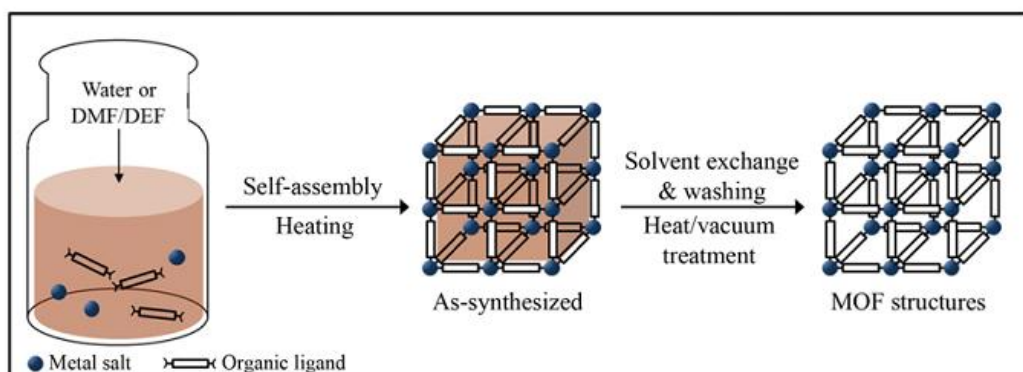


Figure 2.2. Conventional solvothermal synthesis of MOF (Lee et al., 2013).

In microwave synthesis method, metal salt, organic ligand and a suitable solvent are loaded into Teflon vessel. This mixture is heated under microwave at a specific temperature. This was followed by washing, heating and vacuum treatments (Lee et al., 2013). The schematic diagram of this method is given in Figure 2.3. When compared to other methods, synthesis reaction was occurred in shorter times (Ni et al., 2006). For instance, Cr-MIL-101 catalyst was synthesized both conventional and microwave solvothermal methods. $\text{Cr}(\text{NO}_3)_3 \cdot 9\text{H}_2\text{O}$ metal salt, H_2BDC ligand were mixed in H_2O at 220 °C. Cr-MIL-101 catalyst was synthesized for 8 h by conventional solvothermal method (Ferey et al., 2005) where it was synthesized by microwave method for 4 h (Jhung et al., 2007).

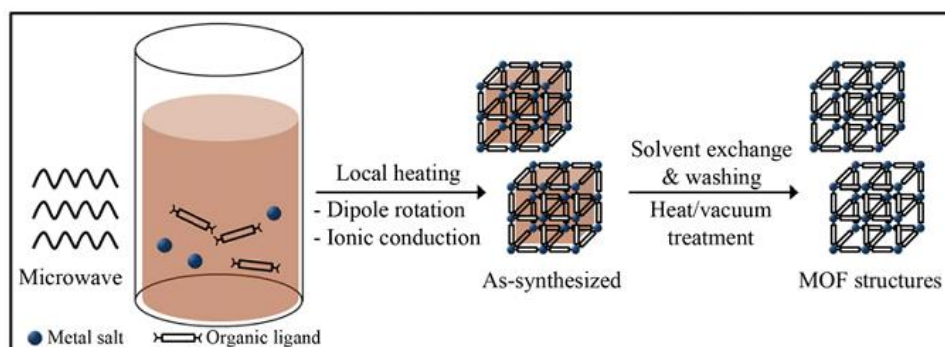


Figure 2.3. Microwave solvothermal synthesis of MOF (Lee et al., 2013).

Sonochemical method is pursued by mixing metal salts and organic ligands in horn-type reactor with suitable solvent. Ultrasonic wave is applied to the mixture.

After sonication, bubbles are formed and collapsed in the solution. Scheme of this synthesis is given in Figure 2.4. Due to the ultrasonic waves high temperatures and pressures are formed during the synthesis (approximately 5000 K and 1,000 bar) (Stock et al., 2012). This fast heating and cooling provided to obtain a fine crystallite in MOF structure (Stock et al., 2012). Sonochemical method is advantageous for reducing the crystallization time and producing the smaller particle size MOF than conventional solvothermal synthesis method (Suslick et al., 1991, Gedanken, 2004).

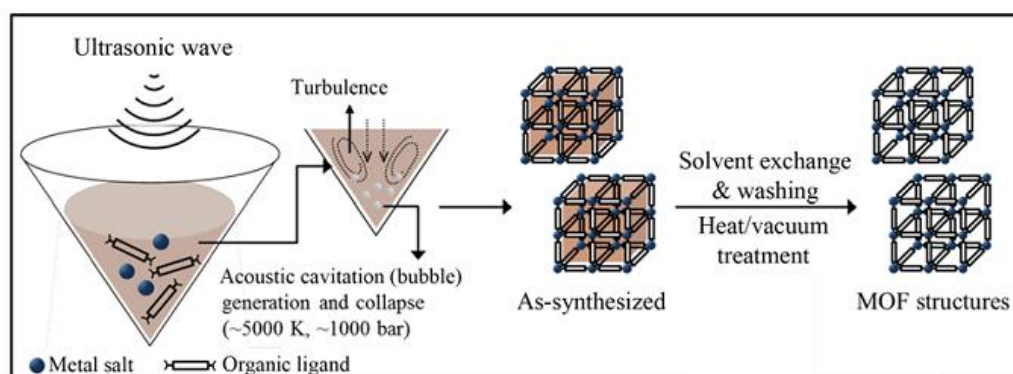


Figure 2.4. Sonochemical synthesis of MOF (Lee et al., 2013).

In electrochemical synthesis, different from the other methods, metal ions are continuously supplied through an anodic dissolution. Then, metal ions react with an organic linker by conducting salt in the solution (Mueller et al., 2006). Voltage or reaction time was found affecting the crystal size (Zhang et al., 2017). Cation(M^+) releases from anode slice when the voltage is applied. Cation reacts with the ligand to synthesise MOFs. The advantages of this method are working at lower temperatures, faster synthesise times and high purity MOFs (system works without using salts, separation of anions (NO_3^- or Cl^-) is not necessary) (Eddaoudi et al., 2011; Tranchemontagne et al., 2009). The scheme is shown in Figure 2.5.

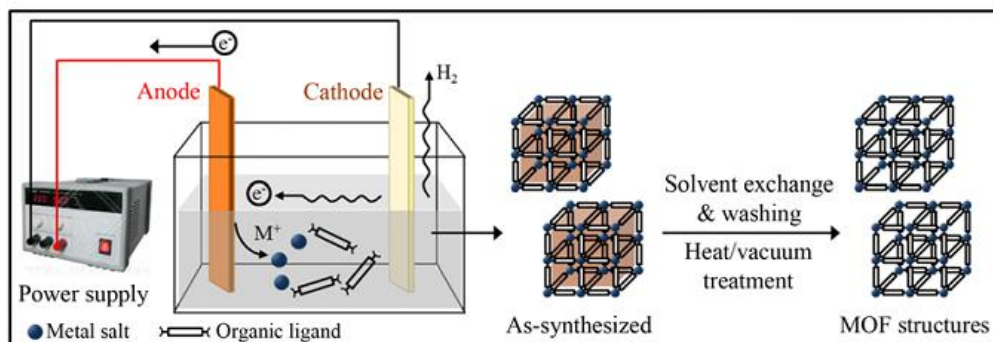


Figure 2.5. Electrochemical synthesis method of MOF (Lee et al., 2013).

The mechanochemical synthesis of MOFs is carried out in a ball mill under solvent-free condition at room temperature (Rademann et al., 2010). Ball mill grind the metal salt and organic ligand (Rademann et al., 2010). Intermolecular bonds of molecules are broken by mechanically and chemical transformation is occurred (Stock et al., 2012). Although this method is effective due to the solvent-free condition, a few types of MOFs could be synthesized, and largescale synthesis is not practical by using mechanochemical synthesis. In some cases, very small amount of solvents can be used to accelerate the reaction via mobility of reactants. For instance, ZIF-8 was produced by mechanochemical synthesis. ZnO and HIm (imidazole) were grinded in DMF solvent. Schematic diagram of mechanochemical synthesis is given in Figure 2.6.

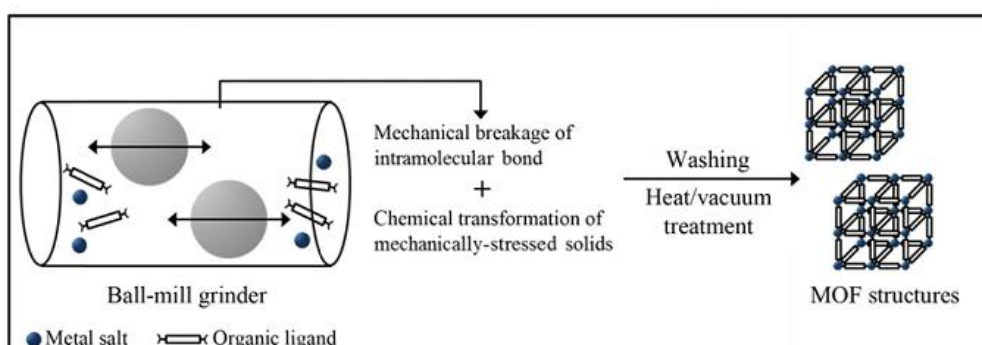


Figure 2.6. Mechanochemical synthesis of MOF (Lee et al., 2013).

2.3 Bimetallic Metal Organic Frameworks

Bimetallic catalysts contain two metals in their structures incorporated or loaded by modification after synthesis. Type of these metals and their particle size's affect the structure of the catalyst (Sharma et al., 2017). These metals are sometimes loaded with isomeric substitution or loaded by impregnation on the surface of the MOFs. Loading of these metals improve the mechanical, thermal, conductive, adsorption or catalytic properties of these organic materials. Bimetallic nanoparticles show better catalytic activity and specific properties such as catalytic, electrical, chemical, biological, mechanical and thermal because of composition and synergistic effects (Sharma et al., 2017). In addition, organic (carbon or graphene) or inorganic (zeolites) supported bimetallic nanoparticles enhanced the effectiveness of the catalyst (Sharma et al., 2017). For instance, Au/Pt-C nanoparticles exhibited higher catalytic activity than pure bimetallic nanoparticles. Gold and platinum were uniformly distributed on the carbon by the way the rate of glucose electro-oxidation reaction increased (Sharma et al., 2017).

Wang et al. (2016) studied with monometallic Cu-C catalyst and bimetallic Cu/Ni(0.5)-C bimetallic catalyst in hydrogenation furfural to cyclopentanone reaction. They obtained higher conversion and selectivity by using the bimetallic Cu/Ni(0.5)-C catalyst. Conversion increased 20 % (from 80 % to 100 %) where cyclopentanone selectivity increased 45 % by the addition of Ni ion (from 52 % to 97 %). The interaction between Cu and Ni increased the catalytic activity.

MOFs are highly crystalline porous materials having tunable properties (Lu et al, 2014). When metal clusters connect to organic groups, these materials gain multidimensional structure, larger inner pore volume and micro- or meso- porosity (Stock et al., 2011; Furukawa et al., 2013). In addition, MOFs supported active bimetallic nanoparticles provide stabilization due to regular pore structure. (Rösler et al., 2017). Adding a metal to monometallic catalysts enhance the catalytic activity of catalyst due to the change in the structure and electronic effects. Bimetallic MOFs can have in intra-framework or extra-framework structures. Extra-framework bimetallic MOFs contains one metal incorporated and exist in the structure, other metals exist on the outer surface or in the pores which were present in the form of counter-ion or polyoxymetalate clusters. Counter-ion MOFs are same with zeolites frameworks. In the zeolites, a cation is required to balance the negative charge for the neutralization. This case is also same in counter-ion MOFs, alkali metal cations are used to balance the charge of the MOF framework and MOFs have generally cationic framework. Polyoxymetalate cluster containing MOFs uses

from polyoxometalate as a secondary building unit. In this type of the material an organic ligand and metal clusters are combined to form a MOF framework. Transition or lanthanide type metals are used for the metal part where organic linkers are the other part of the framework.

Bimetallic MOFs are used in some cases; if the amount or type of the acid sites on the monometallic MOFs are not sufficient, new acid sites are created by synthesizing these MOFs with two different metals. Sometimes two different functions are required during catalysis such as oxidation and dehydration at the same time; in these cases, second metal may be loaded to overcome this issue. Support-metal interaction, which is very important in some cases, could be enhanced by using bimetallic MOFs formed from one metal (active site) and second metal (promoter).

Synergetic effects of multi-metals in MOFs are very important and affect the product distribution significantly. A good example can be given to this situation from the study of Fu et al (2016). Fu et al. studied with monometallic (Cu or Co-MOF74) and bimetallic organic frameworks (Cu/Co-MOF74) for aerobic styrene oxidation under mild condition. Using the bimetallic catalyst provided higher styrene epoxide selectivities (18 % higher than Co, 35 % higher than Cu) than monometallic organic frameworks (Cu-MOF74 or Co-MOF74). This was attributed to the incorporation chemistry. Incorporation of Cu ions into Co-MOF-74 prevented the polymerization of styrene where incorporation of Co ions into Cu-MOF-74 significantly enhanced the conversion of styrene to benzaldehyde, styrene epoxide and phenylacetaldehyde. The structure of this used MOF-74 and formed products are given in Figure 2.7.

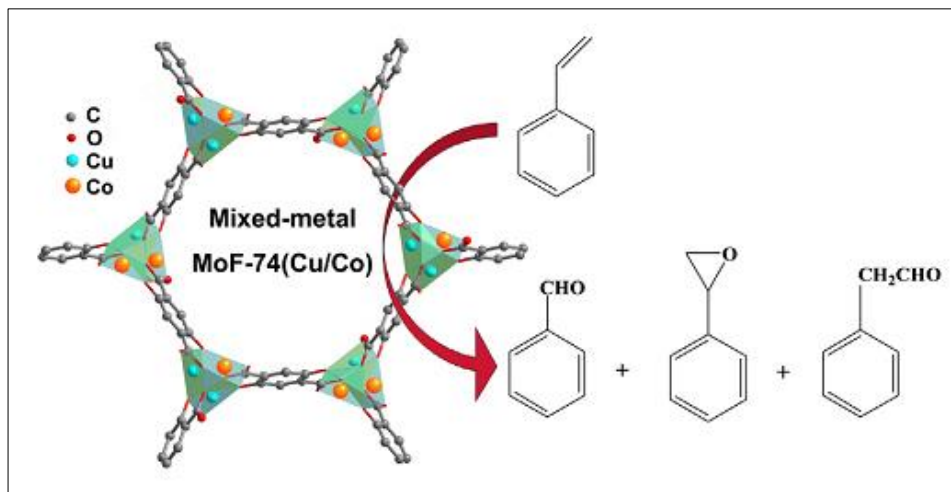


Figure 2.7. Mixed-metal MOF-74 structure and styrene oxidation products organic structure (Fu et al., 2016).

Molecular geometries of monometallic and bimetallic UiO-66 type metal organic frameworks are given in Figures 2.8 and 2.9, respectively. (Kim et al., 2012-modified) UiO-66 is a Zr containing MOFs. NH_2 functionalized form of this catalyst is given in Figure 2.7. In Figure 2.8, Ti incorporated and NH_2 functionalized UiO-66 is shown. Ti containing UiO-66 catalysts are generally used in photocatalytic studies due to the excellent photocatalytic properties of Ti ions.

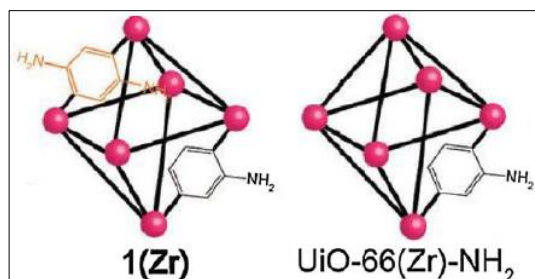


Figure 2.8. Molecular shape of Zr containing NH_2 functionalized monometallic UiO-66 type metal organic framework.

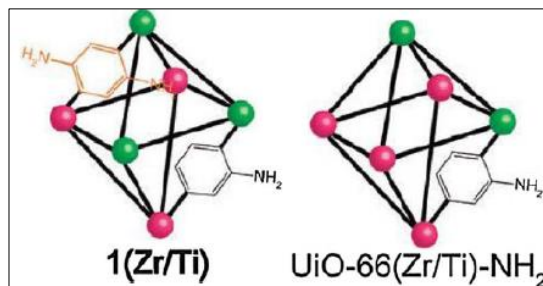


Figure 2.9. Molecular shape of Zr and Ti containing NH_2 functionalized bimetallic UiO-66 type metal organic framework.

2.4 Zirconium Based Metal Organic Frameworks

Metal organic frameworks (MOFs) are highly crystalline porous materials and their crystallinities and porosities can be modified by chemically for various applications (Ferey, 2008; Kitagawa et al., 2004; Yaghi et al., 2003). However, MOFs have weak stabilities (Ferey, 2008). For this reason, high valent metal ions (Zr^{4+} , Fe^{3+} , Al^{3+} , and Cr^{3+}) can be used to obtain stable metal cluster (Zheng et al., 2015).

UiO-66 materials which are Zr containing MOFs have hydrothermal, chemical and thermal (up to 450 C) stabilities (Cavka et al., 2008; Mondloch et al., 2013; Feng et al., 2012). Bonds between the inorganic and organic part of the MOFs determine stability of the catalyst. UiO-66 are formed by binding of $[\text{Zr}_6\text{O}_4(\text{OH}_4)]^{12+}$ with an organic linker (BDC-given in Figure 2.12) (Taddei, 2017). Octahedral $\text{Zr}_6\text{O}_4(\text{OH})_4$ clusters combine with 12-connected terephthalate ligands to form UiO-66 (Kim et al., 2012; Yee et al. 2013). $\text{Zr}_6\text{O}_4(\text{OH})_4$ clusters contain six-centered Zr cations, four -O bridges and four -OH groups (Zhu et al., 2015). Benzene rings and carboxyl group bond in the Zr-based MOFs are the weakest bonds. (Cavka et al., 2008). Longer the bonds in the linker improve the surface area of the material. (Cavka et al., 2008). The BET surface of UiO-66 catalyst is approximately 1200 m^2/g (Yuan et al., 2018). UiO-66 can be generated two isostructures which are UiO-67 and UiO-68 (Yuan et al., 2018). Figure 2.10 shows $[\text{Zr}_6\text{O}_4(\text{OH}_4)]^{12+}$ and UiO-66 structures and Figure 2.11 shows UiO-66 derivatives which contain $-\text{NH}_2$, $-\text{OH}$, and $-\text{SO}_2$ groups.

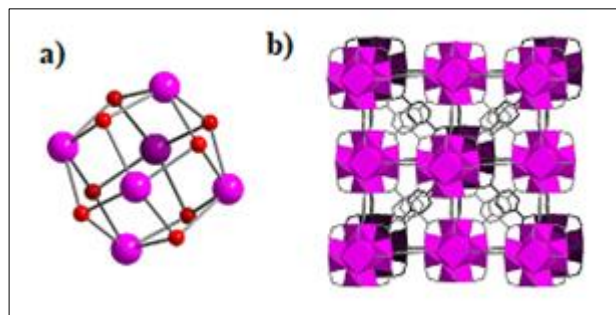


Figure 2.10. Representation of a) $[\text{Zr}_6\text{-O}_4(\text{OH}_4)]^{12+}$, b) Crystalline structure of UiO-66 (Taddei, 2017).

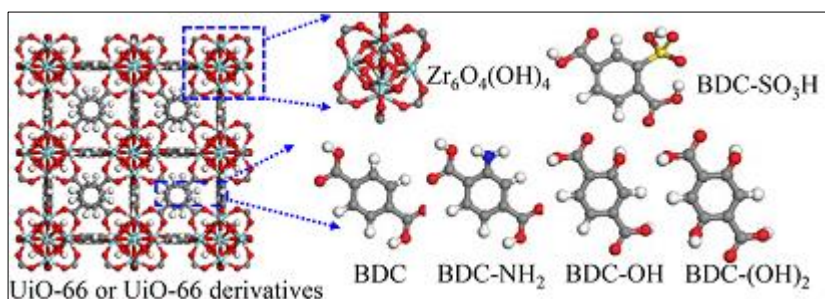


Figure 2.11. The structure of UiO-66 and UiO-66 derivatives (Li et al., 2017).

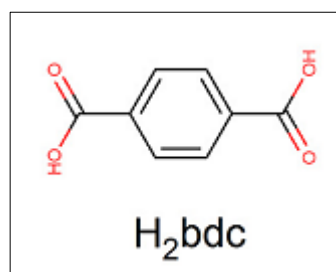


Figure 2.12. Molecular structure of organic linker (Terephthalate) (Taddei, 2017).

3. REVIEW ON GLYCEROL OXIDATION

3.1 Properties, Uses and Applications of Glycerol

Rapid rise in the energy demand in the last decades and decrease in oil and petroleum reserves push people to find an alternative resource for the sustainable clean energy production.

Among these alternatives, biomass sources (obtained from plant residues, such as: wheat straw, corn and nutshell etc.) or side products from other processes are good options for the sustainable future. Glycerol (1, 2, 3-propanetriol) is a by-product of biodiesel production; it is formed after trans-esterification of oils (Triglycerides) with alcohols. In this process, vegetable oils are trans-esterified with and alcohol (ethanol or methanol; generally, methanol due to its high reactivity) in the presence of a catalyst. (M) ethyl esters (called as biodiesel) and glycerol are formed as products. The main reaction pathway is given in Figure 3.1 below.

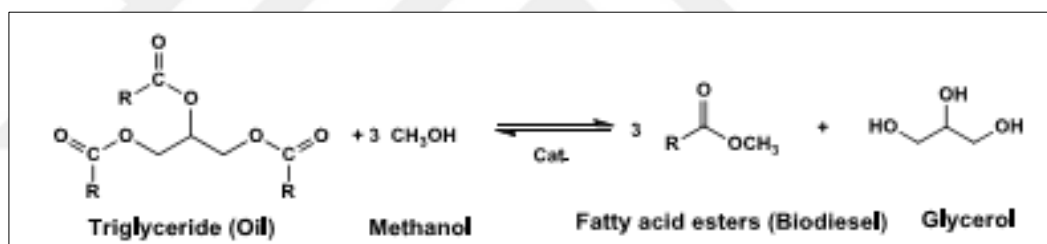


Figure 3.1. Transesterification of vegetable oils with methanol (Purushothaman., 2014).

Glycerol is a colourless, low toxic, biodegradable and viscous chemical having high boiling point, which makes it very favourable to be used as a raw material. It is generally used as humectant, sweetener, solvent or raw material to produce some valuable intermediates. Glycerol is soluble in water and alcohols, slightly soluble in other organic solvents. It is very stable under normal conditions. The organic structure of glycerol is given in Figure 3.1. Some physical properties of glycerol are given in Table 3.1 (Purushothaman., 2014).

Table 3.1. Physical properties of glycerol

Chemical Formula	$C_3H_5(OH)_3$
Molecular Mass	92.09382 g/mole
Density	1.261 g/cm ³
Viscosity	1.5 Pa.s
Melting Point	18.2°C
Boiling Point	290°C

Some valuable chemicals obtained from glycerol and reactions starting from glycerol are given in Figure 3.2. Glycerol can be polymerized to poly-glycols. Acrolein and 3-hydroxypropionaldehyde are produced by the dehydration of glycerol. Acrolein is oxidized to acrylic acid which is polymerized to acrylic resins (Pagliaro., 2010). Glycerol can be also etherified to some -mono, -di -tri ether groups, hydrogenated to ethylene glycol and 1,3-propane diols over metallic catalysts. Esterification of glycerol with carboxylic acids results in monoacylglycerols (MAGs) and diacylglycerols (DAGs) which are used as emulsifier (Pagliaro., 2010). Both MAGs and DAGs are widely used as food additives in bakery products, margarines, dairy products and sauces. In addition, owing to their excellent lubricant and plasticizing properties MAGs are used in textile processing oils on various types of machinery.

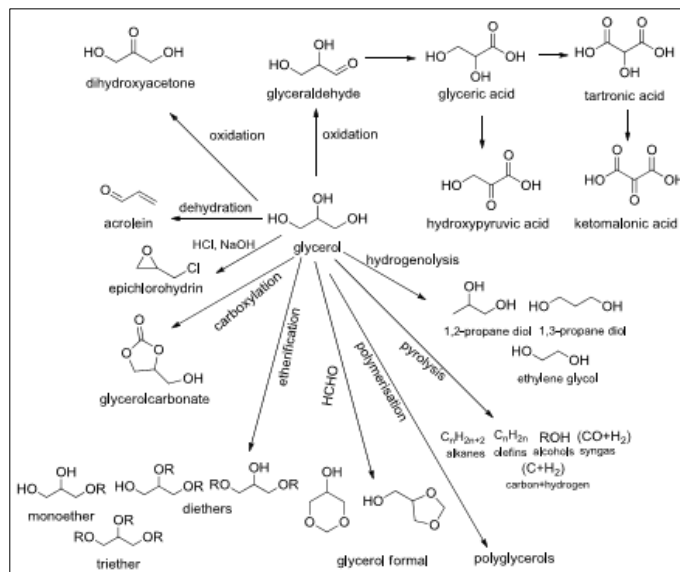


Figure 3.2. Some valuable products obtained from glycerol (Purushothaman., 2014).

3.2 Glycerol Oxidation Mechanism

Oxidation of glycerol has attracted much interest in the last years. Higher value oxygenated products such as glyceric acid, glycolic acid, dihydroxyacetone, glyceraldehyde and oxalic acid can be obtained from glycerol oxidation process. The main possible glycerol oxidation pathway is given in Figure 3.3. When reacted with an oxidation agent, glycerol is converted to many valuable chemicals. Type of the support and active sites, pore shape, crystal phase of the catalysts affect the product selectivity and activity significantly. In the presence of a metal containing catalyst, conversion of glycerol improves. Specific product selectivities can be also enhanced by tuning some catalyst properties or by the selection and designing a suitable catalyst system. Side hydroxyl groups in glycerol are more reactive than the middle that's why formation of glyceraldehyde is more expected than dihydroxyacetone. Dihydroxyacetone, chemical intermediate in organic synthesis, is used in cosmetic and fine chemical industries. To form DHA, middle secondary hydroxyl groups have to be oxidized. For this purpose, double bond formation instead of secondary hydroxyl groups needs to be achieved. This formation occurred over the metal sites of the catalyst. The major challenges in this reaction is to control the products selectivities since the formed products can be converted to another one and carrying out this reaction under base-free conditions. To obtain the maximum DHA selectivity in thermodynamic limitations, shape selective (with optimum pore geometry) metal containing active catalysts should be determined and synthesized. The other favourable product from glycerol oxidation:

glyceraldehyde may be converted to glyceric acid; this may be followed by formic acid formation, which is a valuable chemical and commonly used in leather industry. Oxalic acid and tartronic acid could be also obtained from glyceraldehyde.

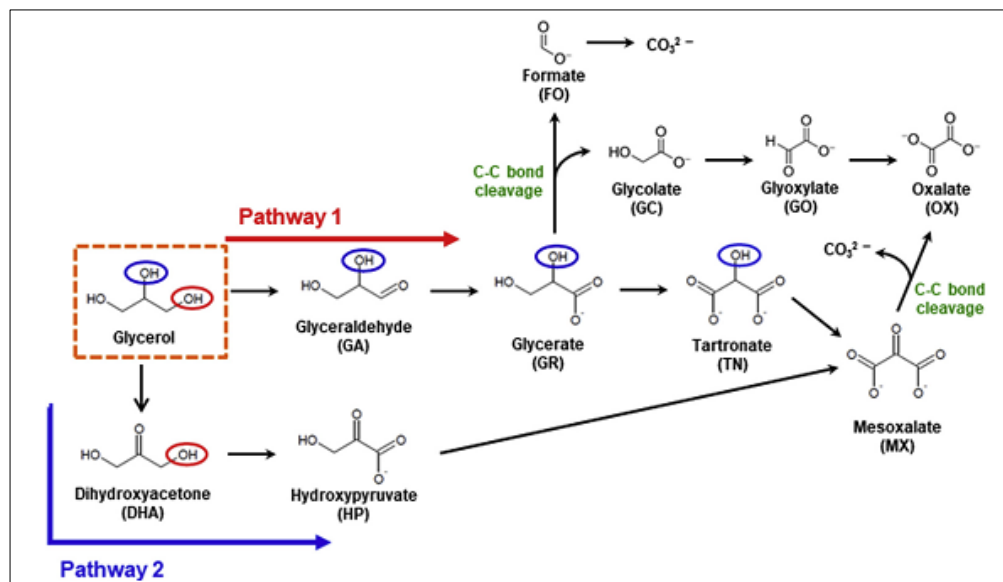


Figure 3.3. Glycerol Oxidation Pathway (Inoue et al., 2018)

Glycerol oxidation mechanism is investigated in three different medium which are alkaline, neutral and acidic medium on Au and Pt metals. There are two possible pathways reported in literature for glycerol oxidation. Figure 3.4 shows possible glycerol oxidation mechanism in alkaline medium. In first pathway, glycerol oxidizes to glyceraldehyde by the transfer of two electrons and then glyceraldehyde oxidizes to glyceric acid again with two electron transfers. Cleavage of C-C bonds of glyceric acid by oxidation occurred by the way formic acid and glycolic acid are formed. Moreover, glyceric acid and glycolic acid are oxidized to tartronic acid and oxalic acid on Pt metal, respectively. In the second pathway, middle -OH groups in glycerol oxidizes to dihydroxyacetone. Then, dihydroxyacetone oxidizes to hydroxypyruvic acid with the two electrons transfer step. Then, ketomalonic acid is also produced by hydroxypyruvic acid oxidation.

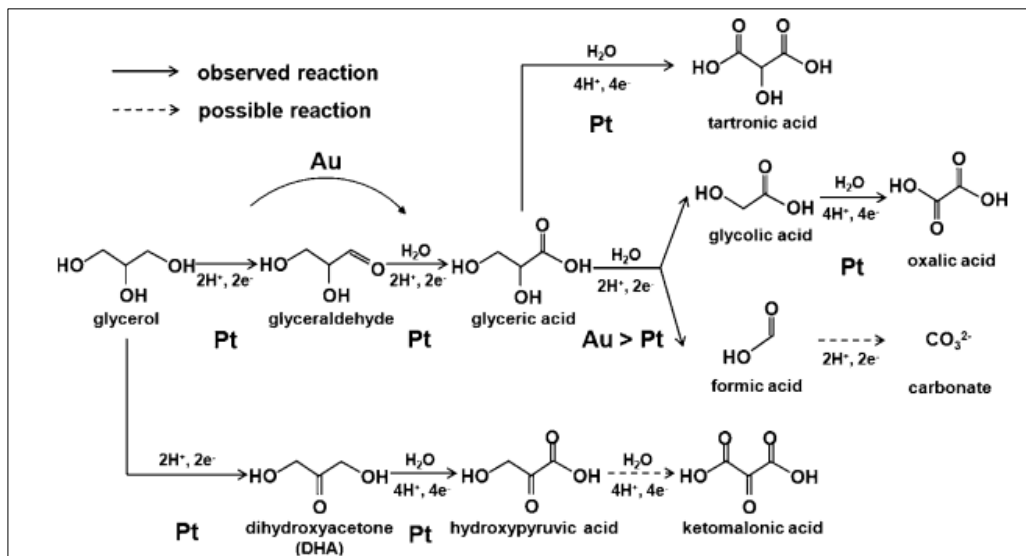


Figure 3.4. Possible Glycerol Oxidation Reaction Mechanism in Alkaline Medium (Kwon et al., 2011).

Mechanism of glycerol oxidation in alkaline and neutral mediums are similar. The sole difference is the absence of oxalic acid and tartronic acid in the neutral medium. The main product of glycerol oxidation over Pt is glyceraldehyde in both mediums. However, glyceraldehyde is unstable in alkaline medium and it can be converted to glyceric acid easily. (Kwon et al., 2011) It was shown in Figure 3.5.

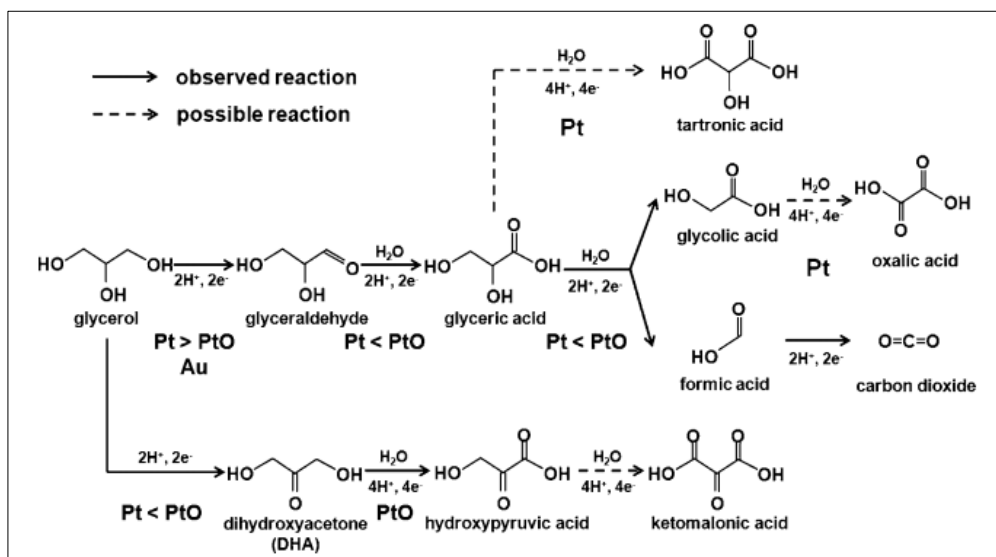


Figure 3.5. Possible Glycerol Oxidation Reaction Mechanism in Neutral Medium (Kwon et al., 2011).

The glycerol oxidation pathways in acidic medium is also similar to other two mediums. It was shown in Figure 3.6. In this case, pH of the medium does not affect the reaction pathways. However, acidity affects the product distribution. The main product is dihydroxyacetone. High concentrations dihydroxyacetone can be obtained in acidic medium (Wcrz et al., 2010; Kimura et al., 1993; Gallezot, 1997; Hu et al., 2010).

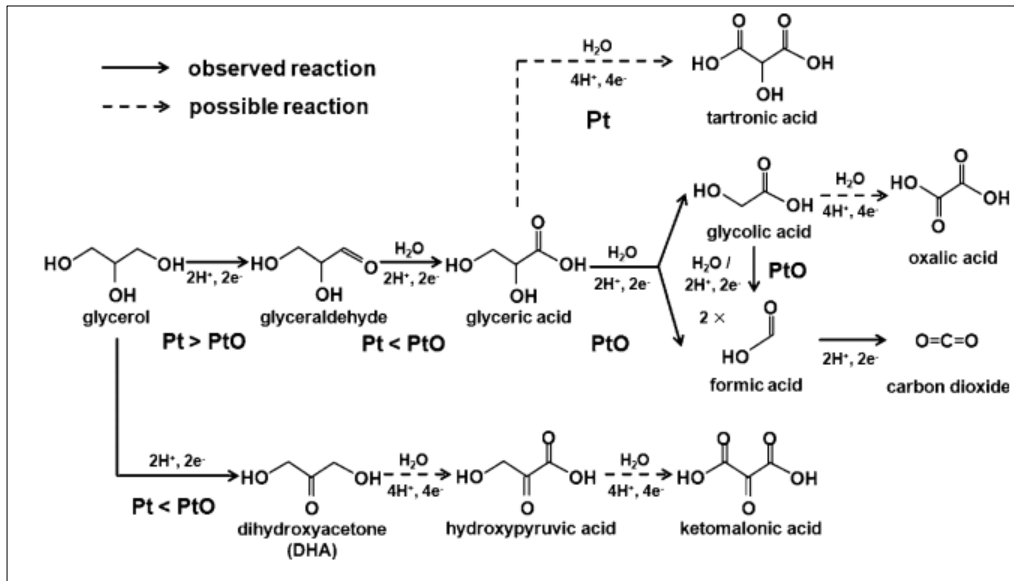


Figure 3.6. Possible Glycerol Oxidation Reaction Mechanism in Acidic Medium (Kwon et al., 2011).

4. LITERATURE REVIEW

4.1 Use of UiO-66 as Catalyst

Today's world needs cleaner and safe industries and reaction systems that is why people are trying to find sustainable reactants and catalysts (non-toxic and reusable) instead of the current ones. The use of homogeneous catalysts involves problems such as toxicity, corrosion, catalyst waste, use of large amount of catalyst, decomposition and reusability. However, heterogeneous catalysts tend to predominate over most of the problems resulting from the use of homogeneous catalysts. Heterogeneous catalysts can easily be separated from the products, can be reused, and their selectivities are higher than the homogeneous catalysts.

Most of the metal organic frameworks exhibited weak thermal and hydrothermal stabilities or had low adsorption capacities due to the narrow pore structure. UiO-66, developed by Prof. Karl Petter Lillerud of the Department of Chemistry at the University of Oslo, is Zr containing octahedral shaped metal organic frameworks with a special structure formed from $Zr_6O_4(OH)_4$ and 1,4-benzenedicarboxylate (BDC) linker (Wang et al., 2015). It has very high surface area (1100-1300 m^2/g), shape selective pores (6 Å), highly packed structure and remarkable stability; (Lu et al., 2014) although other types of MOFs exhibited low stabilities. Strong Zr-O bonds between the metal cluster and carboxylate ligands improved the stability of this material. Decomposition temperature of this catalyst was reported as 500 °C which makes it highly thermally stable and suitable for many reactions. It is also resisted to many chemicals in acidic medium and aqueous solutions. Zr^{+4} ions and carboxylate groups were reported as hard acid and hard base sites, respectively due to the strong affinity between the Zr^{+4} ions and O atom in carboxylate. So, this strong affinity made this catalyst very stable in water and organic solvents also in acidic solutions. On the other hand, it is not stable in basic medium (Affinity between OH groups and Zr is stronger than O atom in carboxylate and Zr^{+4} ion). Given the unsaturated metal sites (Zr) in UiO-66, these sites act as Lewis acids namely electron acceptor. This make the UiO-66 very active catalyst.

Zhang et al. (2017) synthesised the UiO-66 (Zr) metal organic frameworks. UiO-66 (Zr) was found having pentagonal structure, with a high pore volume (2.17 cm^3/g) and high crystalline purity. This catalyst was tested it in the oxidative desulfurization reaction (ODS) at 60 °C for 2.5 h. Effect of catalyst amount (0.06g, 0.08g, 0.10g, 0.12g and 0.14g) was investigated in ODS reaction. Increase in the

catalyst amount loaded, increased the rate of the desulfurization. Ideal amount of the catalyst was reported as 0.1g/10 ml (reaction solution) since there was no change in the conversion over this amount. A complete conversion dibenzothiophene (DBT) was obtained with this catalyst. However, reusability of the catalyst was found low; conversion reduced to 50 % after 5 times of reused. This was attributed to the blocking of the active sites by sulphur ions.

Zhou et al. (2016) investigated synthesis temperatures (100°C, 160°C and 220°C) and different ratio terephthalic acid/ZrCl₄ (BDC/Zr) effects to examine the best UiO-66 catalyst for transesterification of soybean oil with methanol at 140 °C for 5h. They observed that higher synthesis temperatures or BDC/Z ratios caused the higher crystallinities. However, total acid amounts and acid strength were reduced by rising the synthesis temperature and BDC/Zr molar ratio. UiO-66-200-2, which was synthesized at 220 °C and had BDC/Zr molar ratio 2, exhibited lower amount of the acid sites than other catalysts. More acid sites and higher acid strengths were found as very attractive for transesterification reaction to obtain high conversions. The conversion of soybean oil was calculated as 98.5% by using UiO-66-100-1. The product was methyl oleate.

Rasool et al. (2012) prepared Zr-MOF (UiO-66) by solvo-thermal method for the adsorption of hydrogen and carbon dioxide and increased the activity of catalyst with solvent-exchange activation process. After they synthesised the UiO-66 catalyst, the catalyst was immersed in chloroform for 5 days to can remove dimethylformamide (DMF) and terephthalic acid (BDC) residuals from catalyst. Then, filtration and dried process were applied. Activated UiO-66 catalyst had higher surface area and high thermal stability/up to 753K. Using chloroform contributed higher thermal stability because of removing more DMF and nonbonding BDC. UiO-66 had homogeneous particles where the particle size was 100 nm. The BET surface area of catalyst was 1434 m²/g and total pore volume was 0.654 cm³/g. The adsorption capacity of hydrogen and carbon dioxide were found as 1.6 wt % at 1atm, 77K and 79 cc/g at 273 K, 1 atm, respectively. Amount of micropores and average pore sizes were also found as important for H₂ adsorption. 90% of pores of Zr-MOF were micropores and average pore size was 0.9 nm. The pore size distribution of catalyst was in 1.5-5 nm but major pores at 1.5 nm this were good for CO₂ adsorption. It was reported that this catalyst was very effective for the adsorption of these gases due to its high affinities of Zr ions and large pores which improve the mass transfer rate of the molecules to be adsorbed easily.

Li et al. (2018) synthesised Ag/UiO-66 catalyst which was used in oxidation of styrene. Different Ag loading (0.42 wt. %, 1.23 wt. %, 1.86 wt. % and 2.88 wt. %) and solvent types (polar and non-polar solvents) were investigated. Well dispersion of Ag nanoparticles over UiO-66 caused an increase in the catalytic activity. The highest Ag loading caused catalyst agglomeration but provided well dispersion. In addition, particle size raised (1.4 to 5.5 nm) with increasing the loading amount but also conversion increased. This means that high Ag loading was good for catalyst activity but should be in its optimum value to avoid agglomeration. 1.8 wt. % Ag loaded UiO-66 catalyst showed the higher conversion (82%) and selectivity (74%) at 80°C and good recyclability for this reaction in which there was no reduction in catalytic activity up to four times because of the stable catalyst structure. They also investigated solvent effects for this reaction. They used non-polar solvent (n-hexane) but obtained low conversions of styrene then polar solvents (methanol, ethanol and acetonitrile) were tried. Acetonitrile was chosen as a solvent because of the highest conversion value.

Cai et al. (2018) converted 2,3,5-trimethylbenzoquinone (TMBQ) to 2,3,5-trimethylhydroquinone under mild conditions (at 45 °C, 0.4 MPa) by using Pd loaded Hf-based metal organic frameworks (Pd/UiO-66(Hf)). This catalyst was prepared by hydrothermal synthesis method followed by wetness impregnation method. UiO-66(Hf) catalyst had same crystallinity when compared to Pd/UiO-66(Hf). Pd/UiO-66(Hf) had 100 nm to 250 nm range crystal sizes. Pd nanoparticles had highly dispersed and having enough amount of the acid sites. The highest conversion of TMBQ was obtained with 2.0 % Pd/UiO-66(Hf) and this catalyst was reused up to five times hydrogenation of TMBQ to TMHQ and catalytic activity maintained its stability.

Zhao et al. (2018) removed mercury (Hg^0) in flue gas by using Ag nanoparticles loaded UiO-66 catalyst. After loading the Ag, there was no change the crystal structure. Both UiO-66 and Ag-UiO-66 catalyst had cubic structure, so morphology of UiO-66 did not change after treatment; but thermal stabilities and surface area increased. Ag nanoparticles were found as uniformly dispersed on the UiO-66 surface. Mercury adsorption amount was calculated as 3.7 mg/g at 50 °C. Moreover, reusability of the catalyst up to fourth times were very good as performance. Removal amount of the mercury was reported as 85 %.

4.2 Use of UiO-66-NH₂ as Catalyst

Guan et al. (2017) prepared Pd-UiO-66 and Pd-UiO-66-NH₂ catalysts by hydrothermal method which was followed by wetness impregnation. These catalysts were tested in hydrogenation of phenol in water and they also investigated the effects of the NH₂ groups on activity of the catalysts and product selectivities. NH₂ groups affected the crystalline structure of Pd-UiO-66 catalyst negatively and also it reduced the interaction between Zr and Pd ions. Addition of NH₂ groups on the UiO-66 and Pd-UiO-66 catalysts caused a reduction in the surface area. Also, Pd nanoparticles blocked the cavities of UiO-66 and UiO-66-NH₂ so surface area and pore volume decreased but average pore diameter increased. When Pd-UiO-66 catalyst was used in reaction, approximately complete conversion of phenol was obtained at 120 °C for 2h which was higher than Pd-UiO-66-NH₂ catalyst. However, two catalyst shown different selectivities for different products. While selectivity of cyclohexanol (90%) was higher over Pd-UiO-66 where the selectivity of cyclohexanone (>90%) was higher over Pd-UiO-66-NH₂.

Timofeeva et al. (2014) synthesised isorecticular metal organic frameworks which were 2-amino-benzenedicarboxylic acid (NH₂-UiO-66) and 2-nitro-benzenedicarboxylic acid (NO₂-UiO-66). These catalysts were performed in acetalization of benzaldehyde with methanol at 30 °C. Different types and amounts of the functional groups were found to affect the basicity, Lewis acidity and also catalyst activity. NH₂ groups on the UiO-66 raised the strength of the basic sites, however UiO-66-NH₂ catalyst had the highest strength of Lewis acid sites. NO₂ groups withdraw electrons so Lewis acidity rises, however NH₂ groups donates electrons so basicity increases. Lewis acidity can alter stabilization or destabilization of the catalyst due to the electronic properties. The strength of Lewis sites caused an increase in the catalytic activity for acetalization of benzaldehyde which were reported to be carried out over the acid sites of the catalyst. Stability of UiO-66-NO₂ catalyst was high for this reaction. There was no decrease catalytic activity up to 4 times cycles.

Yang et al. (2014) studied Knoevenagel condensation reaction with UiO-66-NH₂ catalyst. They investigated the efficiency, stability and recyclability of the heterogeneous catalysts for the condensation reaction of benzaldehyde with ethyl cyanoacetate or malononitrile. Acid-base properties of the catalysts were important. Type of the polar solvents (DMF, DMSO and ethanol) were found to influence this condensation reaction. The conversion was over 90 % and selectivity of α -

cyanocinnamate was 100 % with DMF at 80 °C for 2 h. When compared to UiO-66-NH₂ catalyst with UiO-66 catalyst, UiO-66-NH₂ exhibited higher performance than UiO-66 due to amino groups lead to the formation of aldimine intermediates from aldehydes since basicity increased the reaction performance. Reusability studies were applied with benzaldehyde and malononitrile. The conversion of benzaldehyde did not reduce too much up to three times. This means, UiO-66-NH₂ catalyst had good chemical resistance.

Krishna et al. (2018) studied with Pd/NH₂-UiO-66 catalyst for hydrogenation of nitrobenzene to aniline using formic acid under mild condition in water medium at 60 °C for 7h. The BET surface area and micropore volume of Pd/NH₂-UiO-66 was lower than NH₂-UiO-66 catalyst due to the encapsulation of Pd nanoparticles. The surface area was decreased from 1052 m²/g to 790 m²/g and micropore volume reduced from 0.43 cm³/g to 0.32 cm³/g when Pd loaded to the NH₂-UiO-66. Pd nanoparticles loading did not affect the crystallinity of catalyst because of high dispersion and low loading (0.7 mol %). Maximum nitrobenzene conversion was found as 98 % and aniline selectivity was calculated as 99%. Pd/NH₂-UiO-66 catalyst was performed by using four times and catalytic activity did not change much but BET surface area reduced from 790 to 534 m²/g. This was attributed to the pore blockage by the residual reactants or products.

Cirujano et al (2015) studied esterification of levulinic acid with ethanol at 78 °C for 8 h. They synthesized UiO-66 and UiO-66-NH₂ catalyst. Levulinic acid converted to ethyl levulinate by esterification with ethanol. The yield of levulinic acid was calculated as 99 % with UiO-66-NH₂ and 64 % with UiO-66. Moreover, these catalysts were reused up to 3 times without losing their catalytic activities.

4.3 Studies on the Synthesis of Bimetallic Metal Organic Frameworks

Wang et al. (2017) synthesised bimetallic organic frameworks. Different amount of Co loaded Cu-BTC (benzene tricarboxylate) MOFs were prepared by thermolysis method in the presence of nitrogen at different calcination temperatures ranging between of 773 K to 1073 K. Co-Cu-BTC catalyst had octahedron morphology. Effect of Co/Cu (0.1, 0.2, 0.3, 0.4 and 0.5) ratio was also studied. Test reaction was selected as hydrogenation of furfural to furfuryl alcohol. The furfural conversion and furfuryl alcohol selectivity were 98.7 % and 97.7 %, respectively at 413 K and 3 MPa. The highest conversion and selectivity were obtained by using

the Cu-Co bimetallic organic framework which was synthesised at 0.4 Co/Cu molar ratio and 873K calcination temperature. After four runs, the conversion of the furfural reduced to 78 % where the selectivity to furfuryl alcohol was 90 %.

Long et al. (2013) synthesized metal organic frameworks (MIL-101) supported Au-Pd alloy nanoparticles by sol-gel method and used this catalyst in the oxidation of cyclohexane to produce cyclohexanone and cyclohexanol. In addition, pure Au and Pd loaded MIL-101 catalysts were also prepared and tested in cyclohexane oxidation. Au-Pd/MIL-101 catalyst had lower BET surface area (2872 m²/g) than Au/MIL-101 (2975 m²/g) and Pd/MIL-101 (3051 m²/g) catalysts. This was attributed to blockage of MIL-101 cavities by metal nanoparticles. The conversion of cyclohexane and selectivity of products were found as 40 % and 80 %, respectively. Au-Pd/MIL-101 (molar ratio Au/Pd=1.4:1) catalyst performance in oxidation of cyclohexane at 150 °C was higher than the pure Au and pure Pd loaded MIL101 catalysts. In oxidation cyclohexane reaction, using the monometallic Pd/MIL-101 or Au/MIL-101 exhibited very low conversions such as 3 % and 16.2 %, respectively. This was due to the strong interaction between two metals and strong support metal interactions that's why using bimetallic catalyst enhanced the catalyst performance. Reusability of the catalysts were also tested. They reused catalysts up to four times without any change in activities and selectivities. Au and Pd metals were found very compatible with each other and exhibited strong support-metal interaction with MIL-101. It was found very stable without any agglomeration or/and leaching.

Poungsombate et al. (2017) synthesised bimetallic Cu-Ni/ZIF-8 metal organic frameworks (MOF). Cu and Ni ions (1/1 ratio) were loaded by incipient wetness impregnation method. Prepared catalysts had cubic-shaped crystals. 5%Cu-Ni/ZIF-8 catalyst had 272 m²/g BET surface area and 0.9125 cm³/g total pore volume. This catalyst was tested in the reaction of CO₂ and MeOH conversion to dimethyl carbonate (DMC) at 20 bar of CO₂, 110 °C and for 12 h. Effects of metal loadings (1, 5, 10, 15 % wt. Cu) and catalyst amount were investigated. The highest DMC yield (6.39%) and MeOH conversion (12.79%) were obtained by using the 5 % Cu containing Cu-Ni/ZIF-8 catalyst. They used this catalyst up to four times without any loss in the catalyst performance.

Wang et al. (2018) synthesised Ni and Co containing SiO₂ supported monometallic and bimetallic organic frameworks. Ni and Co loadings were achieved by impregnation (total metal loading 20 wt. %). Monometallic Ni-

SiO₂/MOF and Co-SiO₂/MOF, bimetallic Ni-Co-SiO₂/MOF were found having similar crystal structures. Textural properties of the catalysts were given in Table 4.1. Ni-SiO₂/MOF and Co-SiO₂/MOF were mesoporous characteristic structure like NiCo-SiO₂/MOF catalyst. Ni and Co particles were obtained highly dispersed on Ni-Co-SiO₂/MOF. These catalysts were tested in hydrogenation of furfuryl alcohol to obtain tetra hydro furfuryl alcohol (THFA). Bimetallic NiCo-SiO₂/MOF was found more active than the monometallic ones. The conversion of furfuryl alcohol was found as 99.8 % where selectivity of THFA was 99.1 % over NiCo-SiO₂/MOF. This was attributed to the attractive synergistic effects between Ni and Co ions. In addition, alloying Ni and Co ions prevented the oxidation of Ni ions during impregnation which made Ni sites remaining reactive. This catalyst was reused up to 5 times with very slight change in activity due to its highly stable crystal structure.

Table 4.1. Textural properties of the catalysts

Catalyst	BET Surface Area (m ² /g)	Total Pore Volume (cm ³ /g)	The Average Mesopore Diameter (nm)
NiCo-SiO ₂ /MOF	340	1.07	12.6
Ni-SiO ₂ /MOF	347	1.05	10.1
Co-SiO ₂ /MOF	445	1.12	10.1

Duan et al. (2017) investigated the performance of the Au-Pd/MOF catalyst on the oxidative carbonylation of amines under mild conditions (at 90 °C, for 20 h at 2 bar O₂ and 6 bar CO). Au and Pd containing MOF-253 catalyst was prepared via impregnation method. Monometallic catalysts were found as less active than bimetallic ones. They also investigated different metal loadings (Au/Pd molar ratio = 0.20:0.80, 0.27:0.73 and 0.69:0.31) on the reaction and the highest catalyst performance was observed over 0.27:0.73 molar ratio Au:Pd/MOF. Au-Pd bimetallic catalyst were found very attractive to activate O₂ and CO in aerobic oxidative carbonylation. Furthermore, gold and palladium had very good synergistic effect for oxidative carbonylation amine reaction.

Li et al. (2017) synthesized Co-Ni alloy nanoparticles loaded in N-doped carbon which was MOF-derived non-noble bimetallic catalyst (Co-Ni@NC) for hydrogenation of phenol to cyclohexanol. Co-Ni@NC had dispersed uniform size nanoparticles (16nm). The BET surface area of the catalyst was found as 1447m²/g

and the total pore volume $0.664 \text{ cm}^3/\text{g}$, showing the highly porous structure. A complete conversion and 100 % selectivity were obtained with molar ratio Co:Ni 1:1.1 Co-Ni@NC at 0.8MPa H_2 and 100 C. It was nearly higher than for 4.3 times Ni@NC catalyst and for 2.8 times Co@NC. Kobalt and nickel metal had strong positive synergistic effects for this reaction. 1Co-1.1Ni@NC catalyst was reused up to five times without any loss in activity.

4.4 Catalysts in Glycerol Oxidation

Diminishing fuel reserves push the researchers to utilize the waste products for the sustainable productions to meet the energy demand of the world. Glycerol is the one of the cheap and popular waste oils from biodiesel industry to be utilized for this purpose. That's why glycerol oxidation has come to an important position for the dihydroxyacetone (DHA) and glyceryl aldehyde production in several years. People investigated many reaction conditions to find the optimum one and searched an effective environmentally friendly catalyst in a green process. Different studies are summarized below to understand the background of this process to determine the best options in this study.

Olmos et al. (2016) synthesized ceria-zirconia ($\text{CeO}_2\text{-ZrO}_2$) supported bimetallic Au and Pd containing catalysts at different Au:Pd molar ratios (0.8 to 6.4) by deposition-precipitation method. They investigated the effects of oxidation temperatures on the reaction; 2.2 Au:Pd (molar ratio) containing catalyst was oxidized at different temperatures (250, 350, 450 and 700 °C). They investigated catalytic activities of these bimetallic catalysts on the selective oxidation of glycerol. The highest catalytic activity (approximately 100%) and the highest glyceric acid selectivity (70%) were obtained over 2.2 Au:Pd containing catalyst. Tartronic acid and glycolic acid selectivities were 40% and 12%, respectively. The highest catalytic activity was obtained at 700°C of catalyst oxidation was obtained over 2.2 Au:Pd catalyst. Particle size of the metals increased after at 700 °C of oxidation but the bimetallic particles became much more homogeneous in composition at above 350 °C. It could be explained by homogeneous formation of bimetallic particles and their contributions for higher catalytic activity in glycerol oxidation.

Zhang et al. (2016) investigated the catalytic performance of Cu-promoted 1.0% Pt/AC (activated carbon) catalyst in glycerol oxidation to lactic acid at 90 C for 4h. The best catalyst for reaction was found as 0.5%Cu-1.0%Pt/AC. They

obtained 80 % glycerol conversion and 69.3 % lactic acid selectivity by using this catalyst. They also tested the reusability of the catalyst up to three times. 0.5%Cu-1.0%Pt/AC catalyst were reused without any change in its activity and slight change (~1 % loss) in lactic acid selectivity. Cu species were found having uniform metal dispersion on the support. However, excess Cu²⁺ caused lower glycerol conversion and lactic acid selectivity. Formation of Pt-Cu interface improved the glycerol conversion and lactic acid selectivity.

Dan et al. (2011) investigated that effects of the activated carbon supported bismuth containing (3.0, 5.0 and 7.0 wt % loadings) and 5.0 wt % platinum loaded catalyst on the glycerol oxidation reaction. This catalyst was synthesized having nanosized particles. Particle size of this catalyst was found as 3.8 nm. They used oxygen as oxidation agent under atmospheric pressure at 60 °C for 6 h. Glycerol conversion of 91.5% and DHA selectivity of 49.0% were obtained by using the 5 % Pt-5% Bi/C catalyst. Well dispersion of Pt-Bi particles on activated carbon enhanced the catalytic performance.

Rodrigues et al. (2011) investigated performance of gold nanoparticles containing multi-walled carbon nanotubes (MWCNT) and also activated carbon (AC) supported catalysts in glycerol oxidation at 60 °C 3 bar. Activated carbon had smaller mesopores (180 m²/g) than MWCNT (285 m²/g) and pores in MWCNT are well distributed. Gold nanoparticles on MWCNT (93% glycerol conversion) exhibited higher catalytic activity than AC supported one (72% glycerol conversion). Larger pores and strong support metal interaction in MWCNT supported catalyst provided higher activity. The glycerol conversion was found as 93 % where the selectivity of dihydroxyacetone was 60 %.

Xiao et al. (2016) investigated five different mono and bimetallic catalysts performance on the glycerol oxidation. Pt-Bi/AC, Pt-Bi/ZSM-5, Pt/MCM-41, Pt-Bi/MCM-41, and Pt/Bi-doped-MCM-41 were used to obtain 1,3-dihydroxyacetone (DHA) from the glycerol oxidation at 75 °C. The highest DHA yield (approximately 55%) was obtained by using Pt-Bi/MCM-41 catalyst because of catalyst's high surface area, uniform pore structure and high Pt dispersion. The specific surface area, average pore diameter and Pt dispersion of Pt-Bi/MCM-41 catalyst were 897 m²/g, 1.9 nm and 39.4%, respectively.

Li et al. (2017) studied metal organic frameworks supported metal nanoparticles in glycerol oxidation. Iron nanoparticles containing MIL-101 type

metal organic frameworks were synthesized and the surface of the catalysts were functionalized with NH_2 . They also prepared Pd-Ce metals containing Fe-MIL-101 and tested this catalyst in glycerol oxidation to convert 1,3-dihydroxyacetone (DHA). They investigated the synthesis time (20h, 40h, 60h and 80h) and also investigated the morphology and structure of metal organic frameworks. When synthesis time increased, the morphology of the catalyst changed whereas crystal structure remained same. When the synthesised time increased, the incidence of octagonal structure increased but crystal size did not change. Therefore, Fe-MIL-101- NH_2 was decided to synthesise at 20 h. Neocuproine ligand was attached to Fe-MIL-101- NH_2 . Glycerol oxidation reactions were carried out at 60 °C, 20 psi for 6h. Pd-Ce/Fe-MIL-101- $\text{N}=\text{CH}_{\text{neocuproine}}$ catalyst exhibited good activity and selectivity to alcohols.

Wang et al. (2015) synthesized mesoporous carbon nitride (MCN) supported Pt catalyst and these catalysts were used in glycerol oxidation at 60 °C for 4 h. Increase in the N content in the support decrease the Pt particle size in catalyst. Mesoporous carbon nitride materials had large surface area, small particle size and tunable pore diameters. Nitrogen atoms in carbon nanostructure increased the catalytic performance, energy-storage properties, mechanical-conductive properties. Glycerol conversion of 63.1%, glyceric acid yield of 58.5% and glyceraldehyde yield of 24.3 % were obtained by using the Pt/MCN which 2.7 g ethylenediamine added catalyst in 60 C for 4h. Reusability of the catalysts were found low; activity dropped after re-tested due to the leaching of N species, oxidation of Pt particles and collapse of the mesoporous structure in carbon nitride support.

Li et al. (2015) studied the performance of silica-supported platinum catalysts on the glycerol oxidation reaction. Moreover, they investigated the shape, size and dispersion of the metal nanoparticles on the support. Three different catalysts were prepared different metal loadings. They used two different solvents which are ethanol and water to synthesis catalyst. According to TEM results, size and dispersion of metal nanoparticles of catalyst, which was prepared with ethanol, was better than with water. The reaction temperature set as 70 °C. Increase in the degree of the metal loading, improved the catalytic activity and product selectivity. Larger nanoparticles provided higher catalytic activity.

Some reaction conditions, activity and product selectivity results for glycerol oxidation from literature are given shown in Table 4.2.

Table 4.2. Glycerol oxidation studies from literature results.

Catalyst	Glycerol Conversion (%)	Selectivity (%)	Reaction Conditions	Reusability	Reference
AuPd-Ce _{0.62} Zr _{0.38} O ₂	100	70 (Glyceric Acid)	60°C, 300 min	-	Olmos et al. (2016)
CuPt-AC	80	69.3 (Lactic Acid)	90°C, 240 min	High	Zhang et al. (2016)
PtBi/C	91.5	49.0 (Dihydroxyacetone)	60°C, 360 min	High	Dan et al. (2011)
Multi-walled carbon nanotubes supported Au	93	60 (Dihydroxyacetone)	60°C, 210 min	-	Rodriguesetal. (2011)
Pt-Bi/MCM-41	-	54.88 (yield)(Dihydroxyacetone)	75°C, 300 min	-	Xiao et al. (2016)
Pd-Ce/Fe-MIL-101-N=CH _{neocuproine}	-	55 (yield)(Dihydroxyacetone)	60°C, 360 min	-	Li et al. (2017)
Mesoporous carbon nitride supported Pt	63.1	58.5 (Glyceraldehyde)	60°C, 240 min	Low	Wang et al. (2015)
Silica-supported Pt	-	80 (Glyceraldehyde)	70°C, 240 min	-	Li et al. (2015)

5. MATERIALS AND METHODS

In this study, the experimental study composed of synthesis and characterization of Zr based metal organic frameworks (UiO-66 and UiO-66-NH₂) and bimetallic metal organic frameworks (Mg@UiO-66 and Mg@UiO-66-NH₂), the catalytic activities of synthesized metal organic frameworks in glycerol oxidation.

5.1 Chemicals

All chemicals and reagents were of high purity and used without further purification. Zirconium chloride (ZrCl₄), terephthalic acid (H₂BDC), 2-amino-terephthalic acid (H₂BDC-NH₂), magnesium acetate, N, N dimethylformamide (DMF), acetic acid and ethanol were used in synthesis of metal organic frameworks. Glycerol and hydrogen peroxide were used as reactants in glycerol oxidation reaction. Also, tartronic acid, glyoxylic acid, glyceric acid, glycolic acid, hydroxyl pyruvic acid, formic acid, lactic acid, acetic acid, oxalic acid, dihydroxyacetone were used as standards for HPLC analysis. The chemicals used in the synthesis of MOF's were listed in Table 5.1.

Table 5.1. Chemicals used in synthesis of different MOFs

MOF	Metal Salt	Organic Ligand	Modulator	Solvent
UiO-66	ZrCl ₄	H ₂ BDC*	Acetic acid	DMF ^{***} /Water
UiO-66-NH ₂	ZrCl ₄	H ₂ BDC-NH ₂ **	Acetic acid	DMF/Water
Mg _x @UiO-66	ZrCl ₄ Mg(CH ₃ COO) ₂	H ₂ BDC	Acetic acid	DMF/Water
Mg _x @UiO-66-NH ₂	ZrCl ₄ Mg(CH ₃ COO) ₂	H ₂ BDC-NH ₂	Acetic acid	DMF/Water

(*) terephthalic acid, (**) amino terephthalic acid, (***) dimethyl formamide

The chemicals used in synthesis of MOFs, glycerol oxidation and calibration curves for HPLC analysis were given in Table 5.2.

Table 5.2. The chemicals used in this study

Chemical Name	Chemical Formula	Source	Purity
Zirconium Chloride	ZrCl ₄	Sigma	99.99%
Magnesium Acetate	Mg(CH ₃ COO) ₂	Sigma	99
Terephthalic Acid	C ₈ H ₆ O ₄	Aldrich	98%
Amino terephthalic acid	C ₈ H ₇ NO ₄	Merck	98%
Acetic acid	CH ₃ COOH	Sigma	99.7%
Dimethyl formamide	C ₃ H ₇ NO	Sigma	98%
Ethanol	C ₂ H ₆ O	Sigma	99%
Glycerol	C ₃ H ₈ O ₃	Sigma	97%
Hydrogen Peroxide	H ₂ O ₂	Aldrich	30%
Tartronic acid	C ₃ H ₄ O ₅	Sigma	97%
Dihydroxyacetone	C ₃ H ₆ O ₃	Sigma	98%
Glycolic acid	C ₂ H ₄ O ₃	Sigma	99%
Glyceraldehyde	C ₃ H ₆ O ₃	Sigma	90%
Glyoxylic acid	C ₂ H ₂ O ₃	Sigma	98%
Formic acid	CH ₂ O ₂	Sigma	98%
Lactic acid	C ₃ H ₆ O ₃	Sigma	>90%
Oxalic acid	C ₂ H ₂ O ₄	Sigma	99%

5.2 Synthesis of Zr Based Metal Organic Frameworks

5.2.1 Synthesis of UiO-66

1 g of $ZrCl_4$, 0.78 g of H_2BDC , 30 mL acetic acid as modulator, 66 mL DMF as solvent and 5 mL of water were mixed. Then the mixture was heated at $120^\circ C$ for 3 hours. The white solid product was obtained after cooling to room temperature and centrifuged at 5000 rpm for 5 min. The product was washed three times with ethanol, then dried and activated at $130^\circ C$ for 4 hours.

5.2.2 Synthesis of UiO-66- NH_2

UiO-66- NH_2 was synthesized in the same way as that of UiO-66 but replacing H_2BDC with $H_2BDC-NH_2$; 1 g of $ZrCl_4$, 0.78 g of $H_2BDC-NH_2$, 30 mL acetic acid, 66 mL DMF and 5 mL of water were mixed. Then the mixture was heated at $120^\circ C$ for 3 hours. The white solid product was obtained after cooling to room temperature and centrifuged at 5000 rpm for 5 min. The product was washed three times with ethanol, then dried and activated at $130^\circ C$ for 4 hours.

5.2.3 Synthesis of $Mg@UiO-66$ and $Mg@UiO-66-NH_2$

Magnesium acetate was used as a source of Mg during the synthesis of $Mg@UiO-66$ and $Mg@UiO-66-NH_2$. In order to compare the structural change different amounts of Mg was added. Table 5.3 shows the amounts of components for the synthesis of Zr based metal organic frameworks

Table 5.3. The synthesis conditions of Zr based metal organic frameworks

Name	ZrCl ₄ (g)	Organic Ligand	Ligand (g)	Acetic acid(mL)	DMF (mL)	Water (mL)	Magnesium acetate(g)
UiO-66	1	H ₂ BDC	0.780	30	66	5	-
UiO-66-NH ₂	1	H ₂ BDC-NH ₂	0.780	30	66	5	-
Mg _{0.15} @UiO-66*	1	H ₂ BDC	0.858	30	73	5	0.348
Mg _{0.225} @UiO-66*	1	H ₂ BDC	0.897	30	76	5	0.522
Mg _{0.3} @UiO-66*	1	H ₂ BDC	0.936	30	79	5	0.695
Mg _{0.15} @UiO-66-NH ₂ *	1	H ₂ BDC-NH ₂	0.858	30	73	5	0.348
Mg _{0.225} @UiO-66-NH ₂ *	1	H ₂ BDC-NH ₂	0.897	30	76	5	0.522
Mg _{0.3} @UiO-66-NH ₂ *	1	H ₂ BDC-NH ₂	0.936	30	79	5	0.695

(*) subscripts of 0.15, 0.225 and 0.3 show the atomic ratio of Mg to Zr.

The metal precursor, organic linker, solvent, water, modulator and Mg were mixed and stirred. The synthesis time and temperature were kept constant at 3 hours and 120°C, respectively. Then product was cooled to room temperature and centrifuged. Then the product was washed with ethanol and activated at 130°C for 4 hours. The schematic description of preparation steps was given in Figure 5.1.

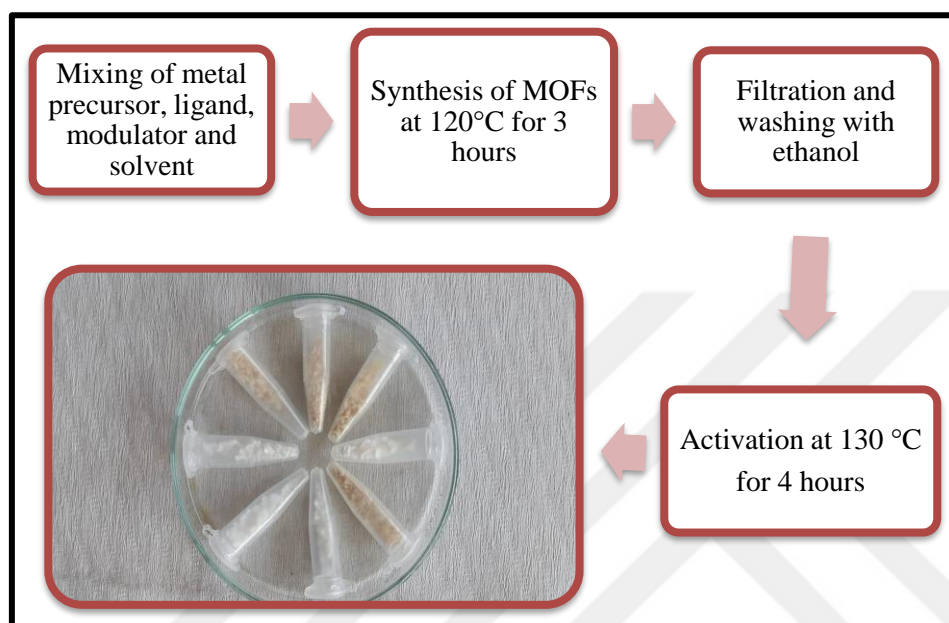


Figure 5.1. The schematic description of preparation steps

The structures of metal precursor, linker and corresponding metal organic frameworks were illustrated in Figures 5.2-5.4.

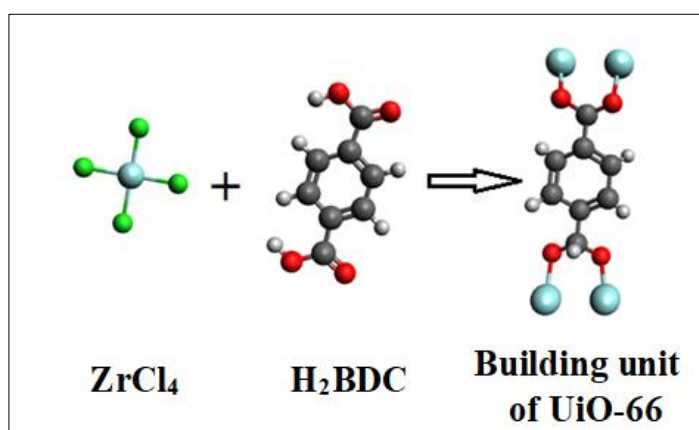


Figure 5.2. Molecular structures of metal precursor, linker and building unit of UiO-66 (Dark grey: carbon; light grey: hydrogen; red: oxygen; blue: zirconium; green: chlorine)

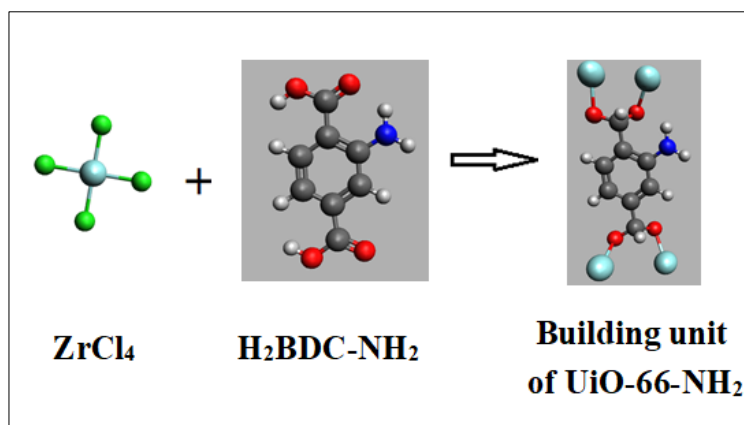


Figure 5.3. Molecular structures of metal precursor, linker and building unit of UiO-66-NH_2 (Dark grey: carbon; light grey: hydrogen; red: oxygen; blue: zirconium; green: chlorine, dark blue: nitrogen).

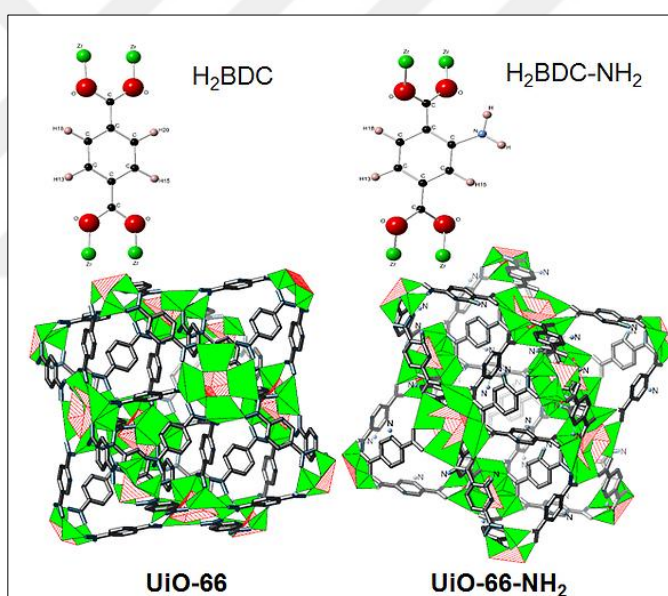


Figure 5.4. Molecular structure of UiO-frameworks (Doan et.al., 2015).

5.3 Characterization Methods

The effect of linker type (H_2BDC and $\text{H}_2\text{BDC-NH}_2$) and Mg addition on the structure of Zr based metal organic frameworks were studied using some instrumental techniques.

The crystal structure and the effect of linker type and Mg addition with different amounts on the crystallinity of the synthesized Zr based metal organic frameworks were analysed using XRD analysis. XRD patterns of the materials were

analysed by a diffractometer of Rigaku Ultima-IV equipped with the graphite monochromatized CuK α radiation($\lambda=1.5406\text{\AA}$) in 2θ angles ranging from 5° to 80° with a step size of 2° and scanning rate 1 minute.

The thermogravimetric analysis is a technique used for measuring the weight change of a material with temperature changes. It is understood that the measured mass of a sample will change when it undergoes sublimation, vaporization, decomposition or loss of water. Thermogravimetric analysis can give information such as at what temperature the mass of samples can change, or how much matter was lost. TG-DTA analysis of the MOFs was performed using a Perkin Elmer Pyris 1 thermal analyser with a range between 30°C and 500°C with a heating rate of $5^\circ\text{C}/\text{min}$ under N_2 flow.

N_2 adsorption-desorption isotherms, surface area and pore volume determination was carried out using a Micromeritics Gemini - 2380 apparatus at -196°C . The surface area was calculated from Brunauer-Emmett-Teller (BET) method.

SEM images were obtained from a scanning electron microscope operating at 20 kV with different magnifications. The elemental composition of Zr based metal organic frameworks was determined by energy dispersive X-ray (EDX) in conjunction with SEM.

5.4 Glycerol Oxidation

The catalytic activity of the catalysts obtained was tested in glycerol oxidation reaction in liquid phase. The experimental setup contains reactor, heater to increase the temperature up to the desired reaction temperature, temperature controller to keep temperature at constant value, stirrer and also condenser to prevent loss of any products. The scheme of the experimental setup was given in Figure 5.5.

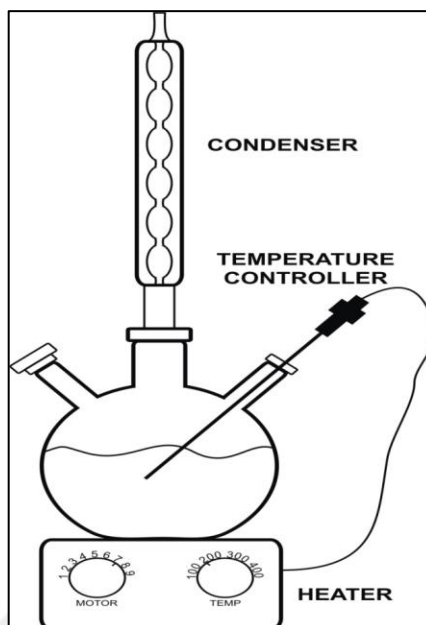


Figure 5.5 The scheme of experimental setup.

In the experimental runs, hydrogen peroxide (H_2O_2) was used as the source of oxygen. The glycerol oxidation reaction was carried out in a 250 mL three-neck flask at atmospheric pressure in an oil bath. Glycerol solution (0.63 g, 0.274 M), and the specified amount of catalyst were mixed together and heated to 90°C in the reactor under constant stirring. Then the desired amount of H_2O_2 was added and the reaction was started. After the reaction, the solution was filtered and analyzed by Agilent 1100 high-performance liquid chromatography (HPLC).

In the experimental study,

- Catalyst Screening
- Parametric study
- Reusability of the selected catalyst were performed.

Catalyst Screening

To observe the effect of acid and basic sites on glycerol conversion, firstly the catalytic activities UiO-66 and UiO-66- NH_2 were compared. Figure 3.6 shows the acidic and basic sites in UiO-66 and UiO-66- NH_2 . Amino groups in amino terephthalic acid increased the basic sites in the synthesized metal organic frameworks.

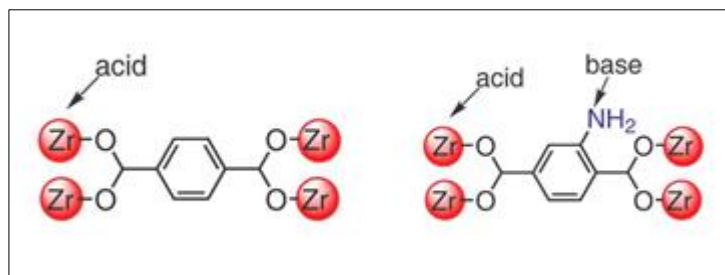


Figure 5.6 Schematic representation of UiO-66 and UiO-66-NH₂.

Then the effect of Mg addition was performed for both UiO-66 and UiO-66-NH₂.

In this study, eight different catalysts were synthesized according to procedure described in Section 3.2. Glycerol oxidation experiments were performed at constant operating parameters to decide the most catalytically active and chemically stable catalyst. The operating conditions were given in Table 5.3.

Table 5.4. The parameters for catalyst screening experiments.

Catalyst	Glycerol (M)	Glycerol (g)	Catalyst Loading (g/L)	T (°C)	H ₂ O ₂ /Glycerol	Time (h)
UiO-66	0.274	0.63	5	90	2.8	3.0
UiO-66-NH ₂	0.274	0.63	5	90	2.8	3.0
Mg _{0.15} @UiO-66*	0.274	0.63	5	90	2.8	3.0
Mg _{0.225} @UiO-66*	0.274	0.63	5	90	2.8	3.0
Mg _{0.3} @UiO-66*	0.274	0.63	5	90	2.8	3.0
Mg _{0.15} @UiO-66-NH ₂ *	0.274	0.63	5	90	2.8	3.0
Mg _{0.225} @UiO-66-NH ₂ *	0.274	0.63	5	90	2.8	3.0
Mg _{0.3} @UiO-66-NH ₂ *	0.274	0.63	5	90	2.8	3.0

(*) subscripts of 0.15, 0.225 and 0.3 show the atomic ratio of Mg to Zr

Parametric Study

The design of experiment (DOE) used a statistical technique to investigate the effects of various parameters included in experimental study and to determine their optimal combination. Taguchi method was used and the parametric study was performed for glycerol oxidation catalyzed by $Mg_{0.3}@UiO-66-NH_2$. DOE using Taguchi approach attempts to extract maximum important information with minimum number of experiments.

Table 5.5. Design experiments with three parameters at three levels for glycerol oxidation

Parameters	Levels		
	-1	0	1
T Temperature (°C)	70	90	50
CL Catalyst Loading. wt%	2.5	5	7.5
MR Molar ratio (H ₂ O ₂ /G)	1.4	2	2.8

During the parametric study, reaction times were kept as 3 hours and the experimental plan was given in Table 5.5.

Table 5.6. The experimental plan for glycerol oxidation catalysed by $Mg_{0.3}@UiO-66-NH_2$

SET	T (°C)	CL (g/L)	MR	t (h)
A1	70	2.5	1.4	3
A2	70	5.0	2.0	3
A3	70	7.5	2.8	3
A4	90	2.5	2.0	3
A5	90	5.0	2.8	3
A6	90	7.5	1.4	3
A7	50	2.5	2.8	3
A8	50	5.0	1.4	3
A9	50	7.5	2.0	3

After deciding the optimum reaction conditions, the effect of time on the conversion of glycerol and selectivity of products were investigated.

5.5 Analysis

Glycerol oxidation reaction was performed in base free medium without sodium hydroxide, so neutralization step was eliminated. Before analyses, catalyst was separated and subsequently filtered over a syringe filter. The liquid sample was diluted and transferred to a HPLC. An injection volume of 10 μL was used for each analysis. The samples were analysed using Agilent 1100 HPLC instrument equipped with an Inerstil column maintained at 70°C using H_3PO_4 (pH=2.3) in ultra-pure water as the eluent with a flow rate of 0.5 mL/min. The components were identified using an UV (210 nm) detector. Concentrations were determined using calibration curves obtained by injecting standard solutions of known concentrations.

The retention times of products obtained in glycerol oxidation were given in Figure 5.7.

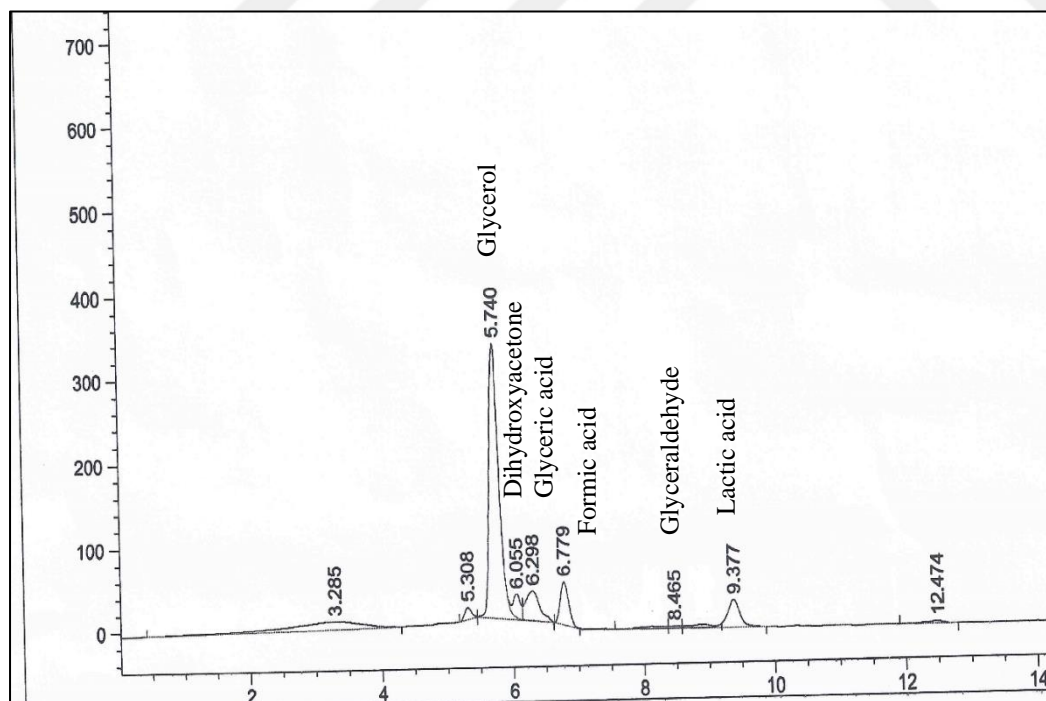


Figure 5.7 The sample HPLC chromatogram

The conversion of glycerol was calculated by the following expression;

$$x = \frac{\text{initial molar concentration of glycerol} - \text{molar concentration of glycerol at time } t}{\text{initial molar concentration of glycerol}}$$

Selectivity of compound i was calculated using the following equation;

$$S_i = \frac{\text{moles of compound } i}{\text{total moles of products}} \times 100$$

6. RESULTS AND DISCUSSION

6.1 Characterization of Zr Based Metal Organic Frameworks

UiO-66, UiO-66-NH₂ and magnesium added zirconium-based metal organic frameworks were analysed using TGA, XRD, SEM and BET techniques. The effects of ligand and also magnesium addition on the structure of zirconium-based metal organic frameworks were tried to highlight.

Thermogravimetric analysis (TGA) of samples was performed by a PerkinElmer STA 6000 from 25°C to 575°C at constant heating rate 5°C/min under N₂ atmosphere. Derivative Thermogravimetric Analysis (DTG) shows the variation of mass of sample with time. This curve is also useful for materials which display multistep decomposition behaviour.

Thermogravimetric analysis of Zirconium based Metal Organic Frameworks including terephthalic acid as ligand

Figure 6.1 illustrates the TGA and DTG curves of terephthalic acid containing zirconium-based metal organic framework. TGA exhibited three weight losses. The initial weight loss stage occurring in the temperature range of 25–100 °C was due to desorption of water (5.5 wt %), whereas the second weight loss (11.1 wt. %) stage observed in the temperature range of 100–450 °C was related to the removal of dimethylformamide (DMF) and the dihydroxylation of the zirconium oxo-clusters (Abid et al., 2012). The third weight loss (20.5 wt %) stage starting at 450 °C was attributed to the decomposition of UiO-66 as a result of the breakdown of organic linkers in the framework (Abid et al., 2012).

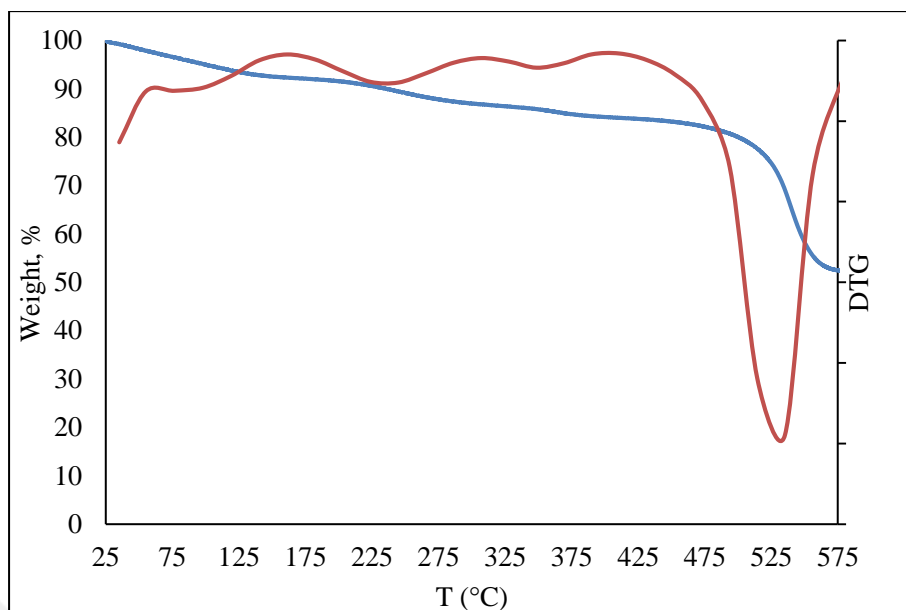


Figure 6.1. TGA and DTG curves for UiO-66.

TGA results of the Mg loaded UiO-66 catalyst is given in Figure 6.2. At the beginning, 5.8 wt% weights loss by water was observed at the range of 25 °C and 100 °C. This was followed by the 9.4 wt % weights loss for Mg_{0.15}@UiO-66 up to 450 °C. This indicated the high thermal stability of the catalyst by the way it can be used at high reaction temperatures. High weight loss (30.6 wt %) from 450 °C to 575 °C indicated the decomposition of organic structure after 450 °C. These results exhibited that loading of Mg into UiO-66 did not affect the thermal stability. Maximum stability temperature was close to the value obtained in literature (Zhao et al., 2018).

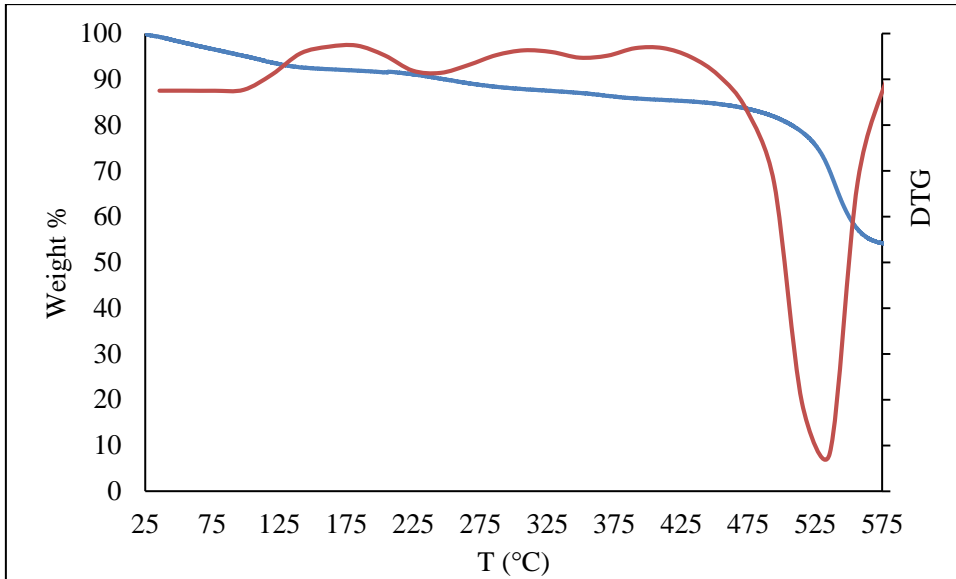


Figure 6.2. TGA and DTG curves for $Mg_{0.15}@UiO-66$.

TGA result of $Mg_{0.225}@UiO-66$ given in Figure 6.3 exhibited similar trends with $Mg_{0.15}@UiO-66$. Weight loss up to 450 °C slightly increased (9.4 to 11.2 wt. %) with the increase in the Mg loading; content of the Mg slightly reduced the stability of the UiO-66. As observed in previous results, decomposition of UiO-66 started above 450 °C, 25.2 % of weight loss was observed above this temperature.

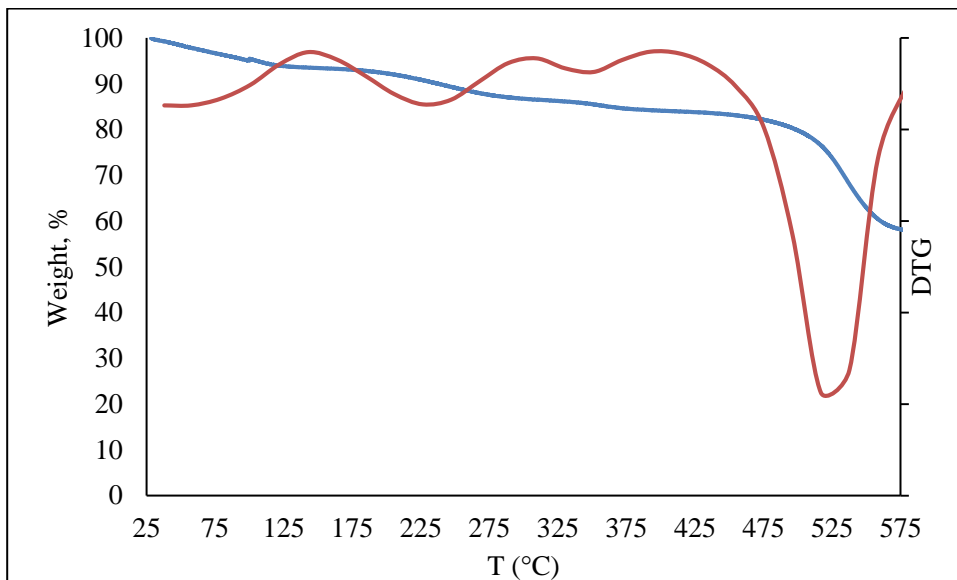


Figure 6.3. TGA and DTG curves for $Mg_{0.225}@UiO-66$.

TGA result of $\text{Mg}_{0.3}\text{@UiO-66}$ is given in Figure 6.4. Same trends with the previous results were observed in weight loss behaviours. Increase in the Mg content slightly decreased the stability (13.3 % weight loss up to 450 °C) as expected. Finally, this catalyst decomposed above 450 °C (weight loss of 29.4 %).

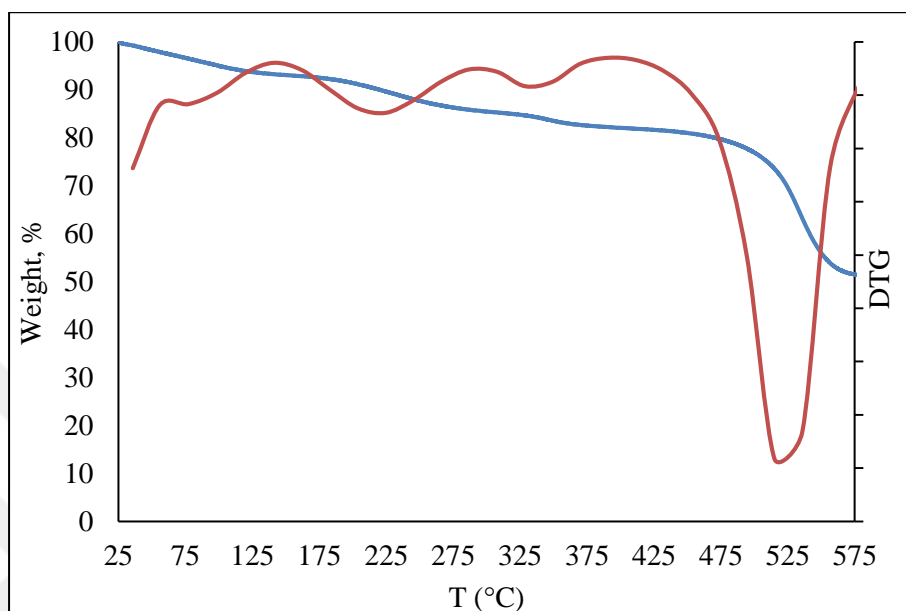


Figure 6.4. TGA and DTG curves for $\text{Mg}_{0.3}\text{@UiO-66}$.

Amount of the weight losses at specific temperature intervals are given in Table 6.1. As mentioned above, stability of UiO-66 catalysts were slightly affected by Mg loading.

Table 6.1. The weight losses of zirconium-based metal organic frameworks including terephthalic acid.

Catalyst	Temperature Intervals		
	25-100°C	100-450°C	450-575°C
UiO-66	5.5	11.1	20.5
$\text{Mg}_{0.15}\text{@UiO-66}$	5.8	9.4	30.6
$\text{Mg}_{0.225}\text{@UiO-66}$	5.5	11.2	25.2
$\text{Mg}_{0.3}\text{@UiO-66}$	5.6	13.3	29.4

Thermogravimetric analysis of Zirconium based Metal Organic Frameworks including amino terephthalic acid as ligand

TGA result of UiO-66, including amino terephthalic acid ligand (UiO-66-NH₂) is given in Figure 6.5. Four steps of weight losses were observed for all samples. First step is in the temperature between 25-150 °C, which occurs due to evaporation of water or solvent molecules inside the pores of zirconium based metal organic frameworks. The TGAs of synthesized materials showed solvent and water loss up to 125°C followed by a drop at 300 °C which was attributed to the dehydration of the Zr₆O₄(OH)₄ nodes to Zr₆O₆ (Luu et al., 2015). The final step around 500 °C was attributed to decomposition of the organic structure.

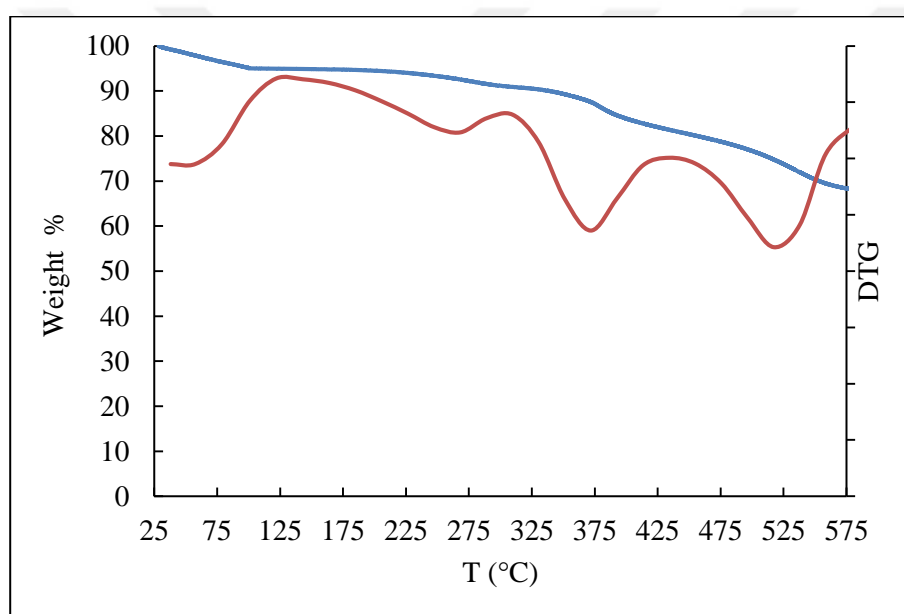


Figure 6.5. TGA and DTG curves for UiO-66-NH₂.

A thermal gravimetric analysis result of Mg_{0.15}@UiO-66-NH₂ is given in Figure 6.6. TGA curve exhibited similar trends with UiO-66-NH₂. Weight loss above 450 °C which is the decomposition of organic framework was 12.45 wt %. Thermal stability was not affected by Mg loading.

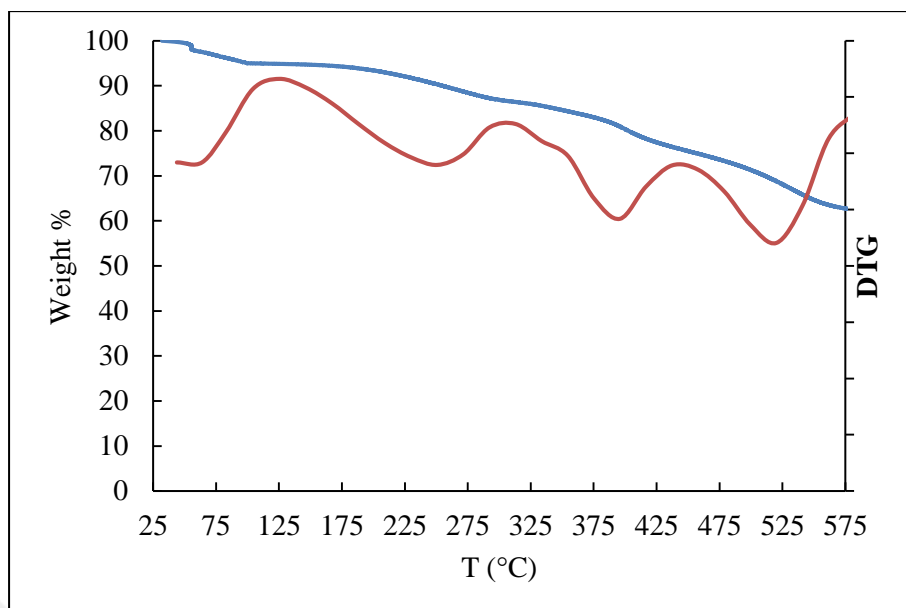


Figure 6.6. TGA and DTG curves for $Mg_{0.15}@UiO-66-NH_2$.

A thermal gravimetric analysis result of $Mg_{0.225}@UiO-66-NH_2$ is given in Figure 6.7. TGA curve exhibited similar trends with the previous $UiO-66-NH_2$ catalysts. Weight loss above 450 °C was 14.50 % indicated the slight decrease in stability by Mg loading.

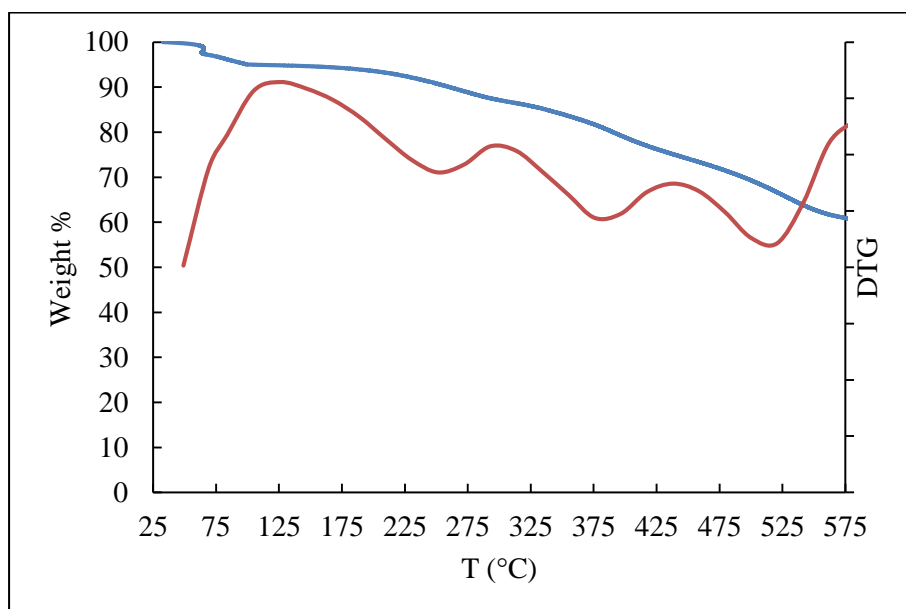


Figure 6.7. TGA and DTG curves for $Mg_{0.225}@UiO-66-NH_2$.

A thermal gravimetric analysis result of $\text{Mg}_{0.3}@ \text{UiO}-66\text{-NH}_2$ is given in Figure 6.8. TGA curve exhibited similar trends with $\text{UiO}-66\text{-NH}_2$. Weight loss above $450\text{ }^\circ\text{C}$ which is the decomposition of organic framework was $12.65\text{ wt}\%$. Thermal stability was not affected by the increase in Mg content.

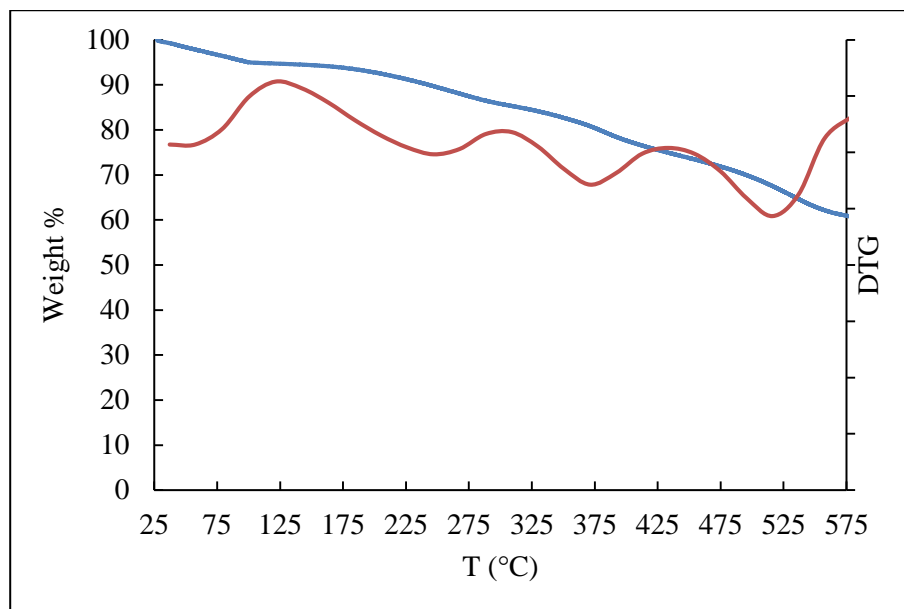


Figure 6.8. TGA and DTG curves for $\text{Mg}_{0.3}@ \text{UiO}-66\text{-NH}_2$.

The weight losses and corresponding temperature intervals are given in Table 6.2. On the whole, there are no big differences between pure $\text{UiO}-66\text{-NH}_2$ and magnesium loaded ones. Total weight losses of $\text{UiO}-66\text{-NH}_2$, $\text{Mg}_{0.15}@ \text{UiO}-66\text{-NH}_2$, $\text{Mg}_{0.225}@ \text{UiO}-66\text{-NH}_2$ and $\text{Mg}_{0.3}@ \text{UiO}-66\text{-NH}_2$ at range $25\text{-}575\text{ }^\circ\text{C}$ was calculated as $31.04\text{ wt}\%$, $37.55\text{ wt}\%$, $39.4\text{ wt}\%$ and $36.67\text{ wt}\%$, respectively. Thermal stability slightly decreased with the addition of Mg.

Table 6.2. The weight losses of zirconium-based metal organic frameworks including amino terephthalic acid

	Temperature Interval			
	25-125°C	125-310°C	310-450°C	450-575°C
Catalyst	The Weight Losses (%)	The Weight Losses (%)	The Weight Losses (%)	The Weight Losses (%)
UiO-66-NH ₂	5.10	4.50	9.52	11.92
Mg _{0.15} @UiO-66-NH ₂	5.15	8.46	11.49	12.45
Mg _{0.225} @UiO-66-NH ₂	5.20	8.42	11.28	14.50
Mg _{0.3} @UiO-66-NH ₂	5.45	9.42	9.15	12.65

The XRD patterns of the synthesized UiO-66 and its modified forms are given in Figure 6.9. The crystal structure of synthesized UiO-66 was found similar with UiO-66 materials in literature (Cai et al., 2018). UiO-66 materials preserved its crystalline structure after Mg loading. Severity of the loading also did not change the crystalline structure of this material; peak positions were same with the parent material (Guan et al., 2017). On the other hand, crystallinity slightly reduced with Mg amount loaded. In addition, there was no MgO crystallites observed after loading. This was attributed to the well dispersion of Mg ions in the framework of UiO-66 (Pourkhosravani et al., 2015).

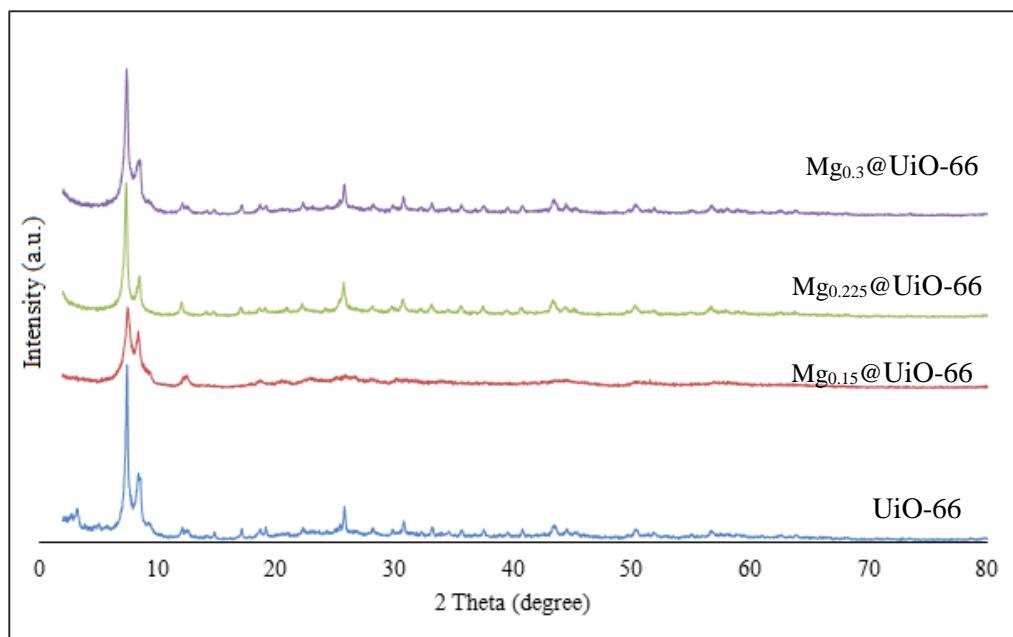


Figure 6.9. XRD pattern for synthesized UiO-66 and UiO-66 by loading different amount of Mg

The XRD patterns of UiO-66-NH₂ and its modified forms are given in Figure 6.10. UiO-66-NH₂ was synthesized successfully with characteristic peaks of UiO-66 at $2\theta = 7.4^\circ$ and 8.6° and 25.8° attributed to (111) (200) and (600) crystal planes. Crystalline structure of catalysts was in good agreement with previously reported UiO-66-NH₂ materials in literature (Guan et al., 2017). Similar to the UiO-66 materials reported above, concentration of Mg loaded did not affect the crystalline structure, peak positions of the material. Slight reduction in crystallinity was observed after Mg loading. However, no peaks of specific MgO crystals observed, was due to the well dispersion of Mg ions in UiO-66 framework (Burton et al., 2011).

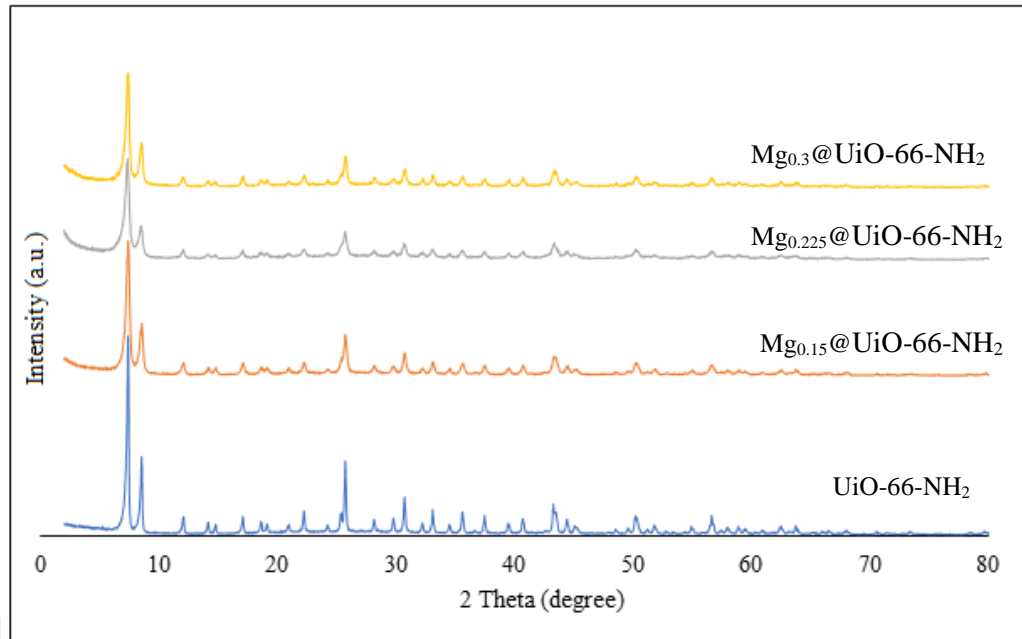


Figure 6.10. XRD pattern for synthesized UiO-66-NH₂ and UiO-66-NH₂ by loading different amount of Mg

The crystal sizes of all zirconium-based metal organic frameworks (UiO-66, UiO-66-NH₂ and their modified forms) were found using Scherrer's equation;

$$B(2\theta) = \frac{K\lambda}{L\cos\theta}$$

where;

B: Peak Width

K: Scherrer Constant

L: Crystalline Size

λ : Wavelength of X-ray

The crystal sizes of samples were determined by taking average of most intense three peaks at 7.4°, 8.6° and 25.8°. According to Scherrer's equation the crystal sizes of UiO-66 and UiO-66-NH₂ were found as 38.73 nm and 49.17 nm, respectively. The widths of the diffraction peaks were found smaller in pure UiO-

66 compared to its NH_2 forms. So, the crystal sizes of UiO-66 derivatives were smaller than that of UiO-66- NH_2 and its modified forms. During the synthesis of MOFs, modulators play two important roles; (i) to facilitate the formation of $\text{Zr}_6\text{O}_4(\text{OH})_4$ clusters and thus the growth of crystals (ii) to slow down the crystal growth rate avoiding fast precipitation of amorphous products (Schaate et al., 2011, Hu et al., 2015). In literature, when acetic acid was used as modulator, the crystal size was found between 150 and 400 nm. But in this study, the obtained crystal sizes were obtained as 38.73 nm and 49.17 nm for UiO-66 and UiO-66- NH_2 , respectively. This difference may have come from the water addition during the synthesis (Schaate et al., 2011).

Scanning Electron Microscopy Analysis

Figures 6.11-6.14 illustrate SEM images of terephthalic acid containing zirconium based metal organic frameworks; UiO-66, $\text{Mg}_{0.15}@$ UiO-66, $\text{Mg}_{0.225}@$ UiO-66 and $\text{Mg}_{0.3}@$ UiO-66.

SEM images showed octahedral structure and homogeneity of UiO-66 materials having average particles sizes 100 nm with a uniform shape. In literature, particle sizes of UiO-66 materials ranged from 100 nm to 200 nm. Slight difference was attributed to the difference in the ratio of ZrCl_4 :BDC:DMF which increased the particle sizes of UiO-66 forms. (Abid et al., 2012). The average particle size of $\text{Mg}_{0.15}@$ UiO-66 was found as 90 nm which was smaller than UiO-66 materials. However, this material slightly aggregated due to magnesium loading. When magnesium loading amount was increased, increase in the severity of agglomeration was observed.

To determine content of elements in UiO-66, analysis using SEM-EDX was performed. Detected elements were carbon (C), nitrogen (N), oxygen (O) and zirconium (Zr) and they were found similar to its modified forms. At UiO-66, the composition of C, N, O and Zr were 50.82%, 1.75%, 31.28% and 15.58%, respectively.

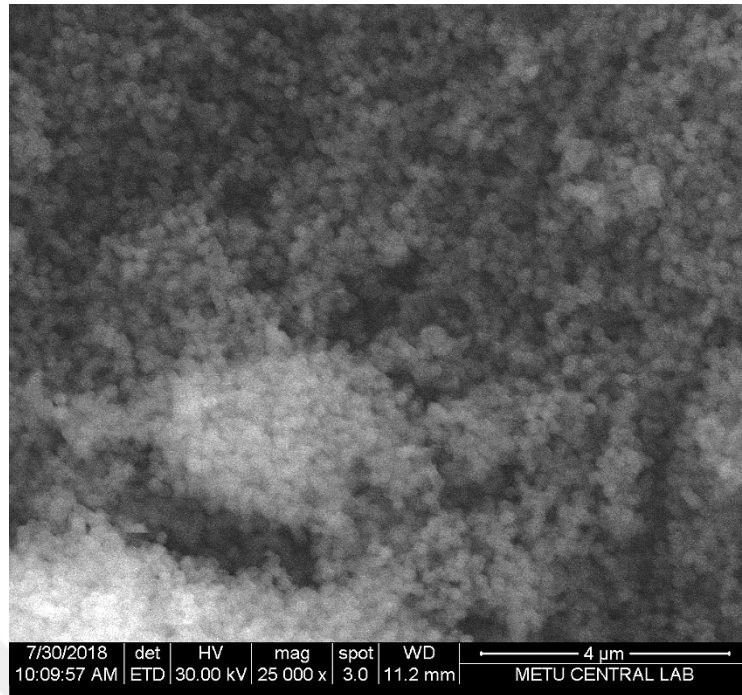
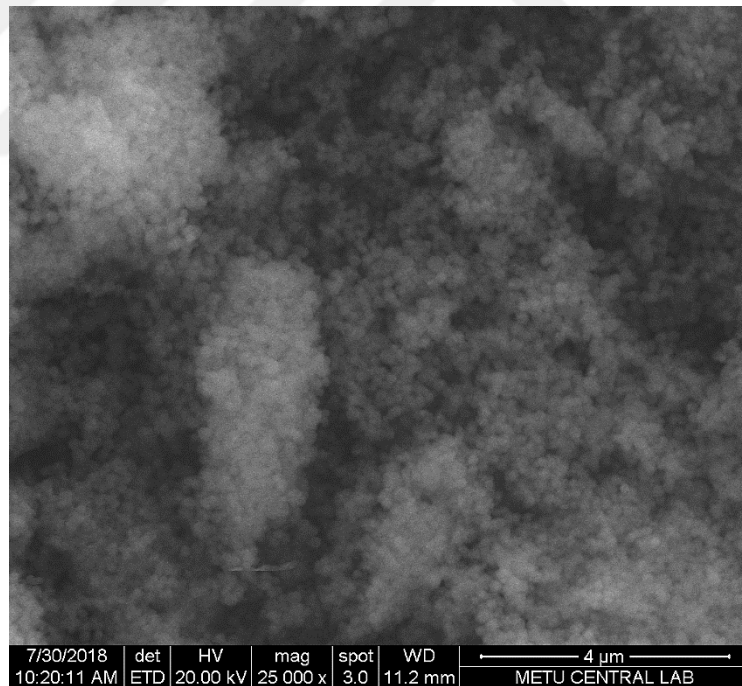


Figure 6.11. SEM image of UiO-66

Figure 6.12. SEM image of Mg_{0.15}@UiO-66

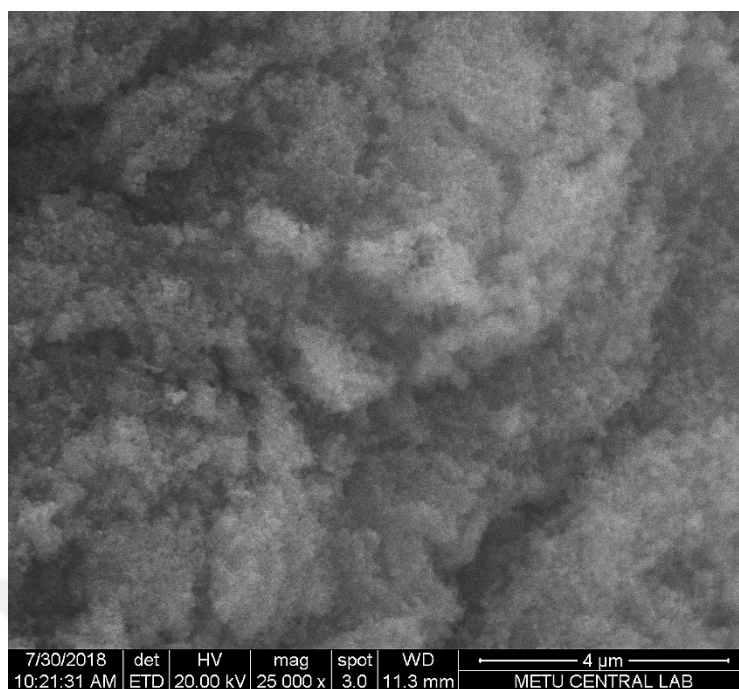


Figure 6.13. SEM image of Mg_{0.225}@UiO-66

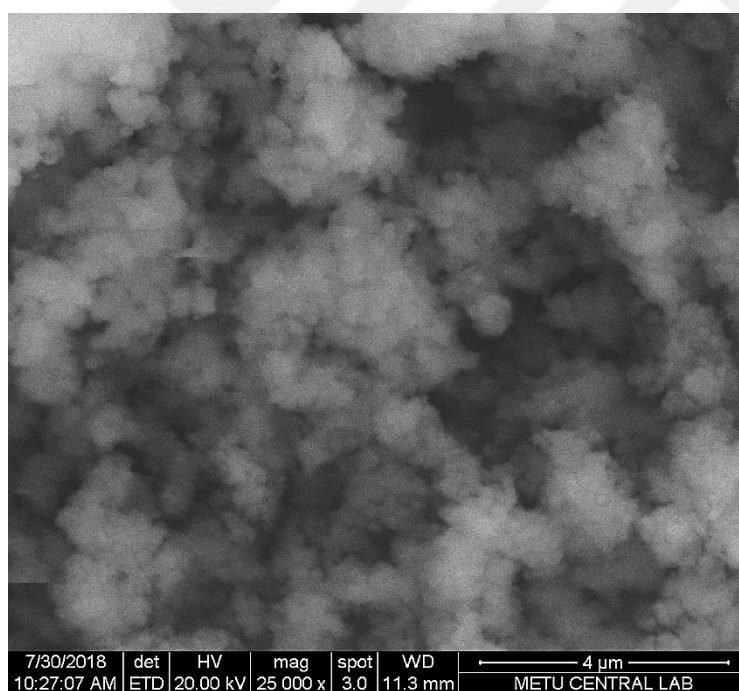


Figure 6.14. SEM image of Mg_{0.3}@UiO-66

Similarly Figures 6.15-6.18 indicate the SEM images of amino terephthalic acid containing zirconium based metal organic frameworks; UiO-66-NH₂, Mg_{0.15}@UiO-66-NH₂, Mg_{0.225}@UiO-66-NH₂ and Mg_{0.3}@UiO-66-NH₂ Figures

showed the morphology of UiO-66-NH₂ with uniform shapes having octahedral structure which is in compatible with literature.

Compared to UiO-66, UiO-66-NH₂ possessed smaller particle sizes which are observed that around 60 nm. Addition of Mg caused slight agglomeration in UiO-66-NH₂ materials. To determine content of elements in UiO-66-NH₂, analysis SEM-EDX was performed. Detected elements were carbon (C), nitrogen (N), oxygen (O) and zirconium (Zr). The amount of nitrogen in UiO-66-NH₂ was greater than that of UiO-66 because of the amino group. The composition of C, N, O and Zr were 45.23%, 6.27%, 22.47% and 24.95%, respectively.

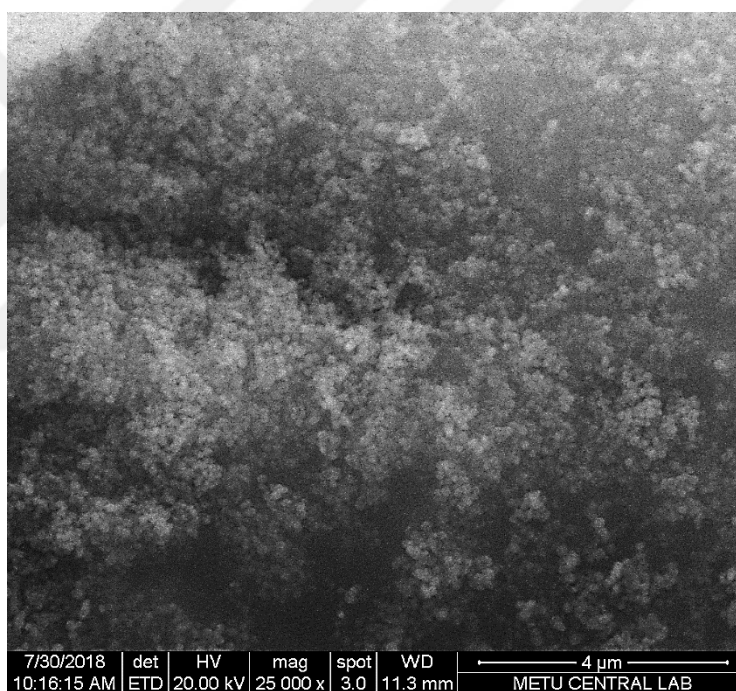


Figure 6.15. SEM image of UiO-66-NH₂

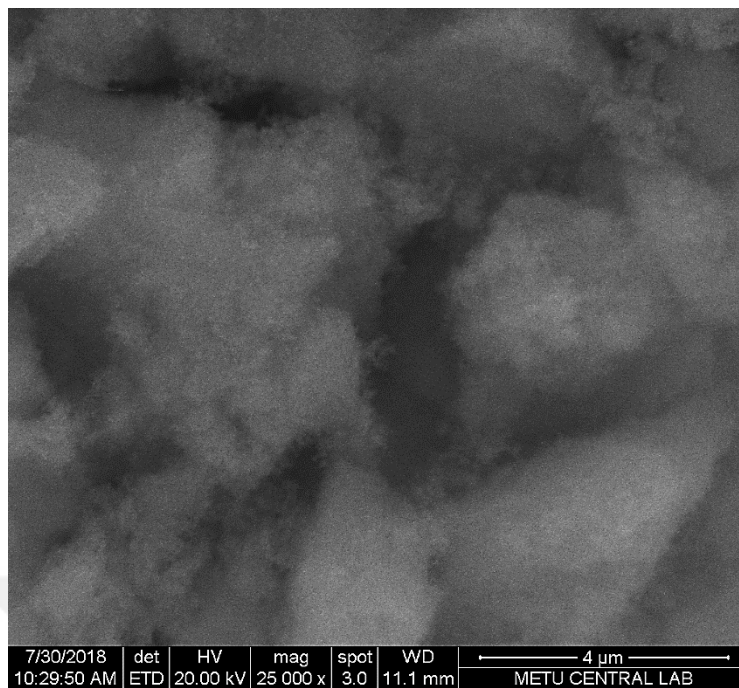


Figure 6.16. SEM image of Mg_{0.15}@UiO-66-NH₂

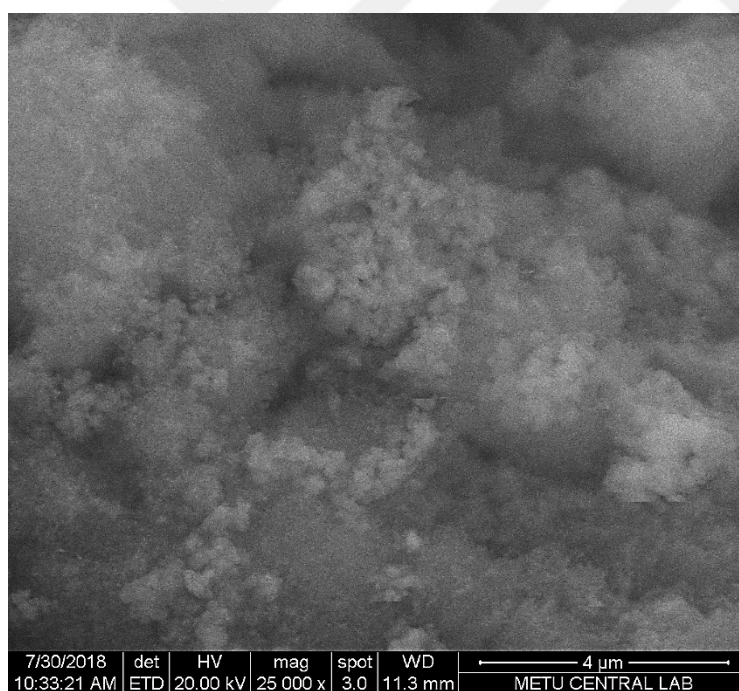


Figure 6.17. SEM image of Mg_{0.225}@UiO-66-NH₂

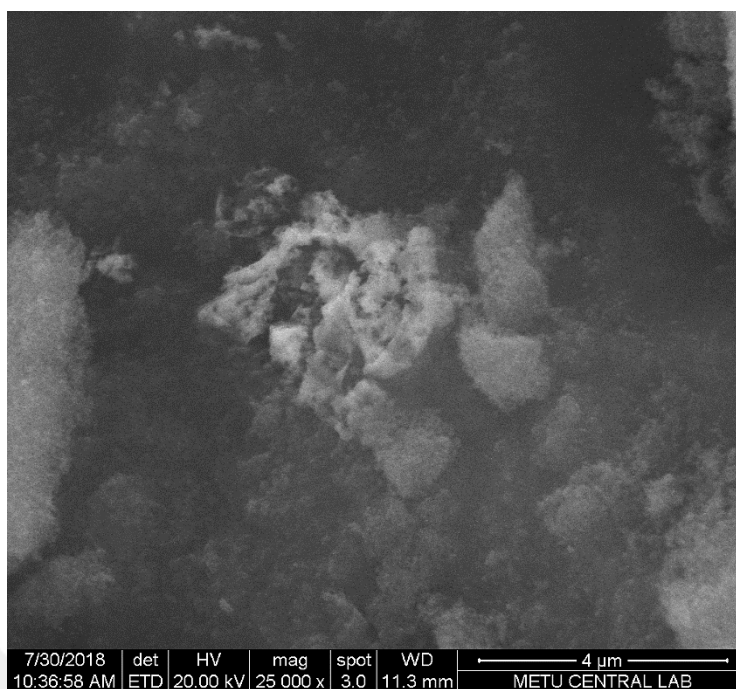


Figure 6.18. SEM image of $Mg_{0.3}@UiO-66-NH_2$

Analysis of Surface Area and Textural Properties

Surface area results of Zr-based metal organic frameworks and amino including Zr based metal organic frameworks are given in Table 6.3. Surface area of UiO-66 and UiO-66-NH₂ was found as 1057 m²/g and 950.2 m²/g, respectively. This was very close to literature values which were 1200 m²/g for UiO-66 and 1052 m²/g for UiO-66-NH₂. (Li et al., 2017, Neeli et al., 2018). The surface area of UiO-66-NH₂ was found lower than that of UiO-66 as expected. This was due to the amino groups which caused a decrease in surface area.

Table 6.3. Surface area of the synthesis Zr-based metal organic frameworks

Sample	Surface Area (m ² /g)
UiO-66	1057
Mg _{0.15} @UiO-66	820.6
Mg _{0.225} @UiO-66	799
Mg _{0.3} @UiO-66	684.6
UiO-66-NH ₂	950.2
Mg _{0.15} @UiO-66-NH ₂	810.2
Mg _{0.225} @UiO-66-NH ₂	689
Mg _{0.3} @UiO-66-NH ₂	676.1

6.2 Catalytic Activities of Zirconium Based Metal Organic Frameworks in Glycerol Oxidation

The catalytic activities of synthesized zirconium based metal organic frameworks were tested in liquid phase oxidation of glycerol. Hydrogen peroxide was used as oxidant and NaOH-free experiments were carried out. The catalytic activity of synthesized eight different zirconium based metal organic frameworks were studied at constant reaction conditions. Initially, the most catalytically active catalyst was chosen, reaction mechanism was highlighted and the parametric studies were carried out using the selected catalyst.

Catalyst Screening

Experiments were carried out at a temperature of 70°C, catalyst loading of 5 g/L and hydrogen peroxide/glycerol molar ratio of 2.8. The conversion of glycerol was calculated using initial and final concentrations of glycerol. Figure 6.19 illustrates the catalytic activities of zirconium based metal organic frameworks.

The liquid phase oxidation of glycerol was performed without catalyst and 1.5% of glycerol converted into products at a temperature of 70°C, catalyst loading of 5 g/L and hydrogen peroxide/glycerol molar ratio of 2.8.

Using UiO-66 as catalyst improved the conversion of glycerol from 1.5% to 11% at the same conditions and also UiO-66-NH₂ provided 12.2% of conversion. Amino group in the framework serve as Bronsted basic sites which accelerates the conversion of glycerol.

Although, the crystallinity of UiO-66 catalyst reduced after Mg addition, conversion of the glycerol doubled. This may be attributed to the formation of the active sites by Mg oxide molecules.

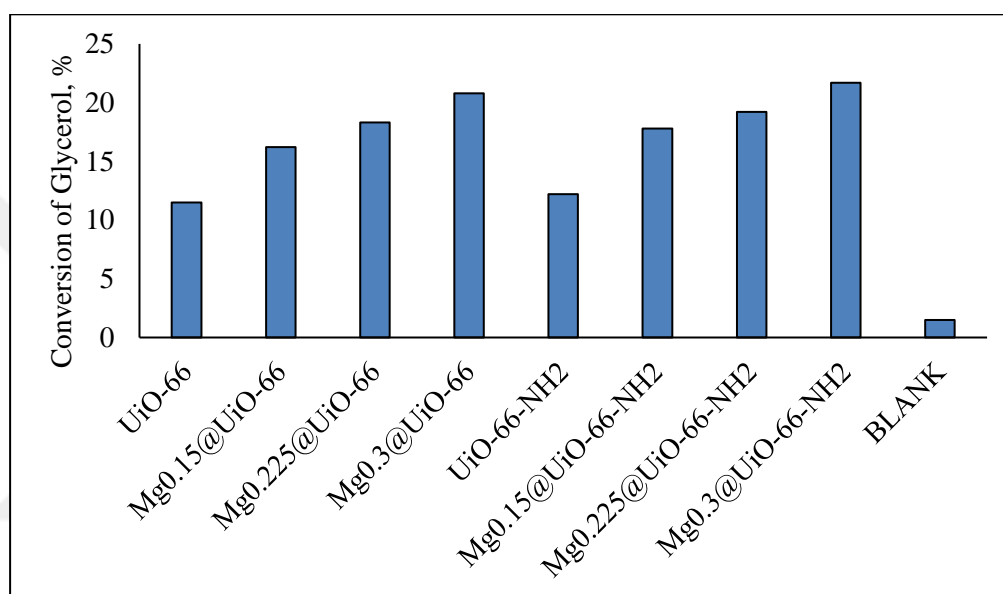


Figure 6.19. Catalytic activities of zirconium based metal organic frameworks

Different amounts of magnesium were added during the synthesis of metal organic framework, and the catalytic activities were compared with parent samples. The addition of magnesium increased the conversion of glycerol due to the interaction between zirconium and magnesium and also formation of Lewis basic sites. The maximum conversion of glycerol was achieved using Mg_{0.3}@UiO-66-NH₂. The glycerol conversion increased from 12.1% to 21.7% due to magnesium addition into the framework. UiO-66-NH₂ acts as a bifunctional catalyst with Lewis acid Zr-sites and Bronsted base -NH₂ sites (Hajek et al., 2015).

Figure 6.20 shows the product distribution over Mg_{0.3}@UiO-66-NH₂ after reaction period of 3 hours. Because glycerol is a highly functionalized molecule containing three hydroxyl groups, it is feasible to convert glycerol into valuable oxygenated derivatives via catalytic oxidation, such as tartronic acid, glyceric acid,

and dihydroxyacetone. More basic sites promote the oxidation of glycerol and also it promotes sequential oxidation of glyceraldehyde to glyceric acid (Wang et al., 2015). Therefore, glyceraldehyde might have been converted to glyceric acid in this reaction condition. In addition, there could be side reaction of C-C bond cleavage.

In literature, gold impregnated metal oxides, gold nanoparticles and platinum impregnated oxides were most used catalyst types. In the study of Zhang et al (2016), they used Cu and Pt loaded activated carbon supported catalysts. They increased the Cu content from 0.1 % to 2 wt. %, at constant Pt ratio (1 wt. %). Increase in the Cu content improved the glycerol conversion to some extent (80 %), then reduced and formic acid yield was maximized at 2 wt. % Cu loading. Reduction in conversion was related to the decrease in the surface Cu species (XPS results) when Cu content increased. That is why promoter Mg metal was loaded at the specified optimum amount in our study. On the other hand, in Zhang et al (2016) study, they used base (LiOH) in the reaction solution. Although used catalysts provided 80 % glycerol conversion, high cost of the Pt metal and negative environmental effects of base (LiOH) usage limited the application of this catalyst in industry. Another study on glycerol oxidation using Pd and Au containing activated carbon and graphite supported catalyst was published by Villa et al (2015). The gold particles were found having nanosized. Complete conversion was obtained at 60 °C. Same comments similar to Zhang et al (2016) can be made with this study; use of high amount of NaOH in reaction limited its usage in real processes in spite of the high activity. Gold-Copper bimetallic catalyst loaded ZnO was tested in glycerol oxidation at 60 °C by Kaskow et al (2018). High conversion results (95 %) was also reported in the presence of NaOH. In order to obtain high products yields, harsh reaction conditions for glycerol oxidation (using bases for high pH or high reaction temperatures) were used in literature. Good results were also achieved by expensive catalysts (Ru, Pt or Au metal containing ones). However, aim of our study is based on finding cost effective catalyst works at environmental conditions and low temperatures. Metal organic frameworks called as future-green catalyst was selected in this study for high product yields and activities. Promising results can be obtained by increasing the reaction temperature and optimising the reaction conditions which was confirmed by experimental design studies; 55 % of glycerol conversion was found at 90 °C.

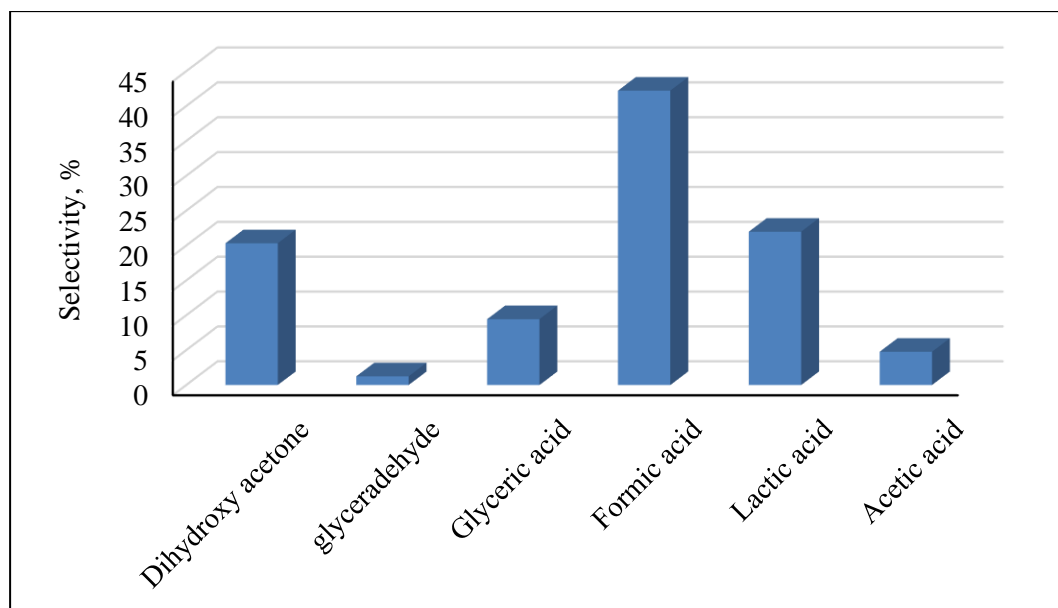


Figure 6.20. The product distribution of glycerol oxidation using $Mg_{0.3}@UiO-66-NH_2$ after 3 hours

Proposed reaction mechanism of glycerol oxidation is given in Figure 6.21. According to the Figure, firstly glycerol was converted to dihydroxyacetone and glyceraldehyde in the presence of oxidant and suitable catalyst. Then further oxidation reactions occurred according to the operating conditions.

The reaction mechanism was highlighted for the liquid phase glycerol oxidation;

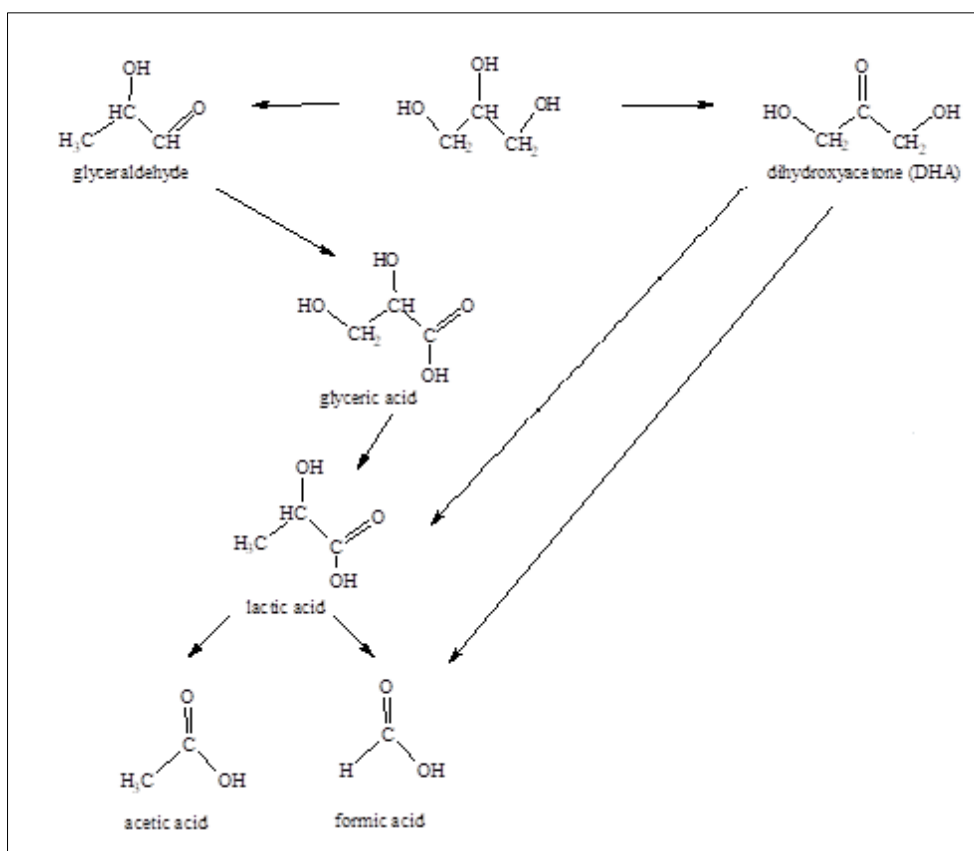


Figure 6.21. The proposed mechanism of glycerol oxidation

Parametric Study

The parametric study was investigated using Mg_{0.3}@UiO-66-NH₂ as catalyst at different temperatures, catalyst loadings and hydrogen peroxide/glycerol molar ratios. The effects of these operating conditions were investigated using Anova software. To see the effects of parameters on the conversion, reaction times were kept as 3 hours and results were summarized in Table 6.4.

Table 6.4. The results of parametric study performed using $Mg_{0.3}@UiO-66-NH_2$

SET	T (°C)	CL (g/L)	H/G (Molar Ratio)	t (h)	Conversion (%)
A1	70	2.5	1.4	3	35.1
A2	70	5.0	2.0	3	28.0
A3	70	7.5	2.8	3	22.1
A4	90	2.5	2.0	3	36.1
A5	90	5.0	2.8	3	23.4
A6	90	7.5	1.4	3	55.5
A7	50	2.5	2.8	3	14.1
A8	50	5.0	1.4	3	24.2
A9	50	7.5	2.0	3	21.3

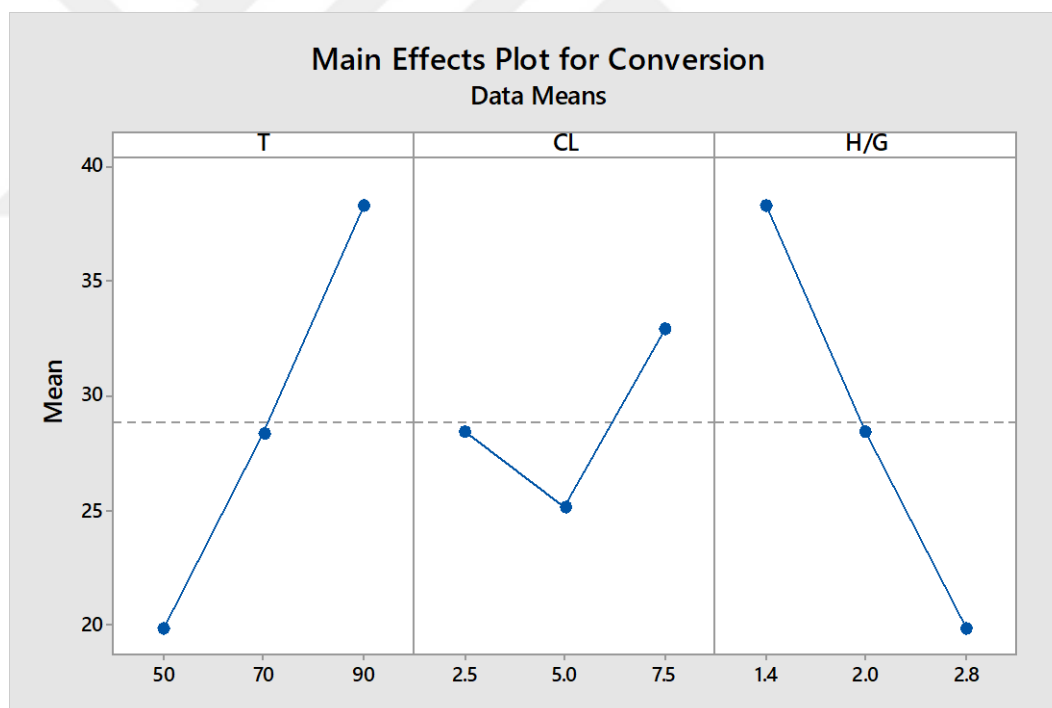


Figure 6.22. Main effects of parameters

Figure 6.22 exhibited that reaction temperature directly affected the conversion of glycerol and also inversely affected the hydrogen peroxide/glycerol molar ratio. The effect of catalyst loading was negligible when compared to

temperature and hydrogen peroxide/glycerol molar ratio. This can be understood from the linearity of the line, which was confirmed T and H/G lines. Analysis of variance (ANOVA) was carried out to check the significant effect of independent variables on the response variables. ANOVA was summarized in Table 6.5.

Determining the degree of parameters affecting the glycerol oxidation was simulated by ANOVA software and results are tabulated in Table 6.5. Effect of parameters can be discussed by P values. Lowest P values mean highest effects in the reaction. P values of 0.004 (the main parameters should be <0.05 according to the statistical regression analysis) for both temperature and hydrogen peroxide/glycerol ratio confirmed that these parameters were the main factors for glycerol oxidation. According to the table, catalyst loading is not significant for this reaction and slightly affects the mechanism. In the study of Sankar et al (2017), experimental design studies were also performed in glycerol oxidation. Similar to our findings, reaction temperature (30 °C and 80 °C) was also found the main factor for glycerol oxidation after ANOVA analysis (Sankar et al., 2017).

Table 6.5. Anova Results for conversion of limiting reactant

	Adj SS	F value	P value
T (°C)	479.78	262.20	0.004
CL (g/L)	36.94	20.19	0.046
H/G (Molar Ratio)	505.27	276.13	0.004
T*CL	4.19	2.29	0.269
T*H/G	63.95	34.95	0.027
CL*H/G	0.00	0	0.984

The product selectivities for glycerol oxidation over $Mg_{0.3}@UiO-66-NH_2$ simulated by ANOVA software was given in Table 6.6.

Table 6.6. Product selectivity of liquid phase glycerol oxidation catalyzed by Mg_{0.3}@UiO-66-NH₂

SET	T (°C)	CL (g/L)	H/G (Molar Ratio)	Conversion (%)	DHA (%)	GAL (%)	GA (%)	FA (%)	LA (%)
A1	70	2.5	1.4	35.1	34.833	3.476	4.907	32.598	24.186
A2	70	5.0	2.0	28	26.978	12.053	1.232	38.315	21.423
A3	70	7.5	2.8	22.1	21.350	3.460	2.880	44.949	27.361
A4	90	2.5	2.0	36.1	27.650	10.250	3.520	28.370	30.210
A5	90	5.0	2.8	23.4	29.580	8.520	4.540	24.150	33.210
A6	90	7.5	1.4	55.5	32.210	7.520	5.140	26.550	28.580
A7	50	2.5	2.8	14.1	14.000	0.000	0.000	86.000	0.000
A8	50	5.0	1.4	24.2	18.000	0.000	0.000	82.000	0.000
A9	50	7.5	2.0	21.3	17.000	0.000	0.000	83.000	0.000

(*) DHA= dihydroxyacetone; GAL=glyceraldehyde; GA= glyceric acid; FA=formic acid; LA: lactic acid

During the experiments, hydrogen peroxide was used as an oxidant and the amount of hydrogen peroxide was increased to investigate its effects. At lower amount of hydrogen peroxide, glycerol oxidized to a mixture of dihydroxyacetone and glyceraldehyde, but at higher amounts of hydrogen peroxide, the main product was formic acid due to the further oxidation of intermediates.

Another important parameter was temperature, at 50°C, the conversion of glycerol was very low and there was no effect of amounts of catalyst and hydrogen peroxide. Due to the low conversion of glycerol, there were no other oxidation products, the main product was formic acid. At 90°C, the conversion of glycerol was higher, but the selectivity of dihydroxyacetone was lower because of the further oxidation reactions which lead to formation of lactic acid and formic acid. By considering converted amount of glycerol and selectivity of dihydroxyacetone, the optimum operating conditions were; temperature of 90°C, catalyst loading of 7.5 g/L and hydrogen peroxide/glycerol molar ratio of 1.4.

Effect of Time

The effect of reaction time on the conversion of glycerol and the selectivity of products were investigated at a temperature of 90°C, catalyst loading of 7.5 g/L and hydrogen peroxide/glycerol molar ratio of 1.4. The conversion of glycerol was increased with reaction time as expected. The glycerol conversion was obtained as 94.8% up to 6 hours. This indicating that the catalyst signed to be active after 6 hours. It was shown in Figure 6.23.

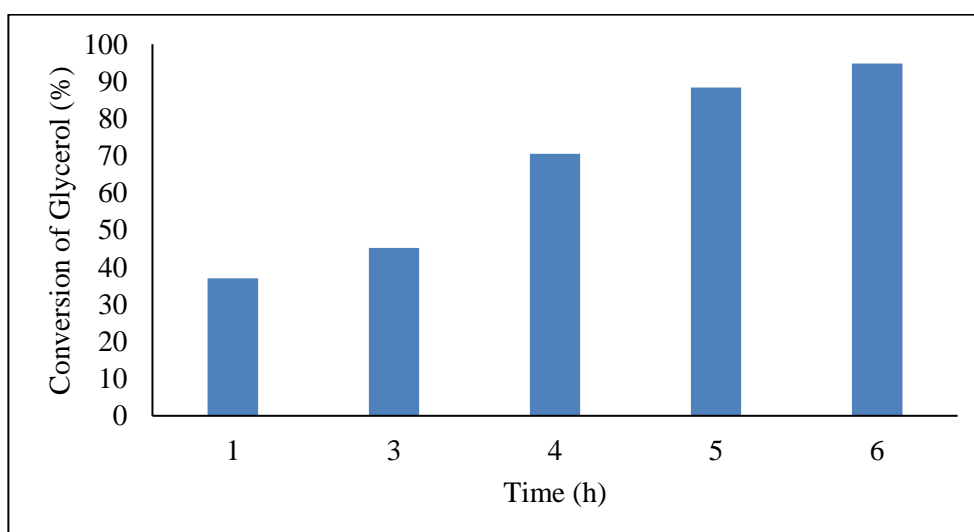


Figure 6.23. The effects of the reaction time on the conversion of glycerol.

Selectivity of products at different reaction times are given in Figure 6.24. For the liquid phase oxidation of glycerol, after one hour 37% of glycerol converted to mainly dihydroxyacetone, glyceraldehyde, glyceric acid, lactic acid and formic acid. After 6 hours, the conversion of glycerol was achieved as 94.8%. The amounts of dihydroxyacetone and glyceraldehyde decreased and converted to lactic acid and formic acid as the reaction time progresses. This was due to the presence of H_2O_2 in the solution which oxidizes the dihydroxyacetone to lactic acid and formic acid over metal sites (Zr and Mg in UiO-66) (Farnetti et al., 2016).

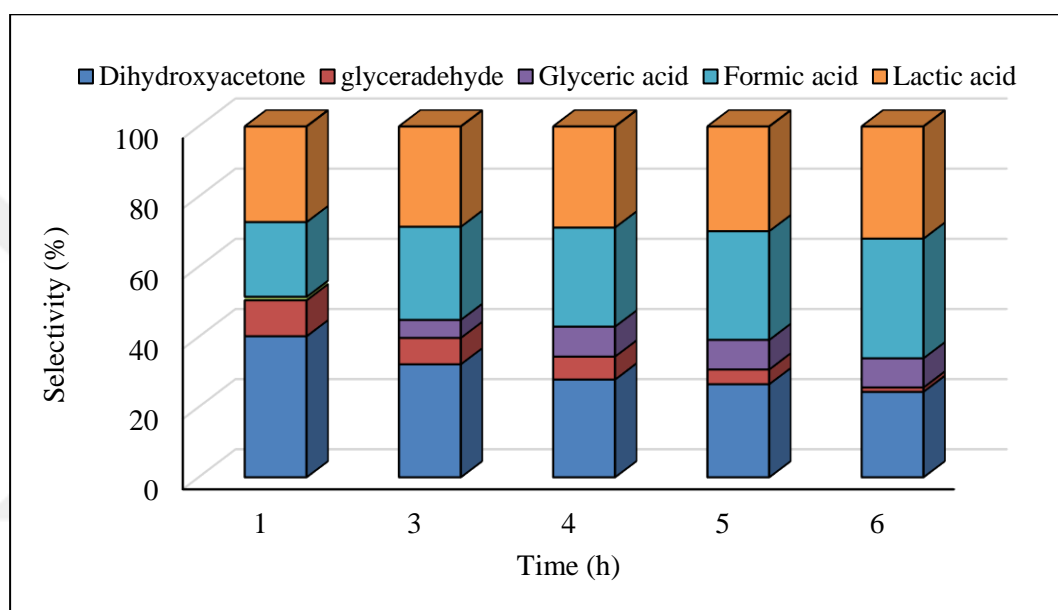


Figure 6.24. The selectivity of products with different reaction time.

7. CONCLUSION

Glycerol was oxidized by using hydrogen peroxide over synthesized Zr-based metal organic frameworks (UiO-66, $Mg_x@UiO-66$, UiO-66-NH₂, $Mg_x@UiO-66-NH_2$) effectively.

The synthesized catalysts were characterized to find the stability, crystallinity and morphology by using TGA, BET, XRD and SEM analysis, respectively. UiO-66 and its modified forms were found thermally stable up to 450°C. It was also similar in UiO-66-NH₂. There were no big differences in thermal stabilities between pure UiO-66-NH₂ and magnesium loaded ones. Addition of magnesium into frameworks didn't change the thermal stabilities.

According to XRD results, UiO-66 materials preserved its crystalline structure after Mg loading. MgO crystals were not observed in XRD results for all samples. It was attributed to the high uniform distribution of Mg ions in the frameworks of UiO-66. According to Scherrer's equation, crystal sizes of UiO-66 and UiO-66-NH₂ were found as 38.73 nm and 49.17 nm, respectively.

SEM-EDX analysis indicated the octahedral structure and homogeneity of Zr-based metal organic frameworks. Mg loading caused slight agglomeration in these materials. In addition, EDX analysis gave the composition of C, N, O and Zr.

The surface area and pore volume of catalysts decreased after the addition of Mg. Also, the use of amino terephthalic acid as linker caused to decrease in the surface area and pore volume due to blockage of pores.

Glycerol conversion of 21.7 % was obtained with $Mg_{0.3}@UiO-66-NH_2$ which was the most active catalyst. $Mg_{0.3}@UiO-66-NH_2$ acted as the bifunctional catalyst with Lewis acid Zr-sites and Bronsted base -NH₂ sites. When severity of magnesium loading increased, the conversion of glycerol was also increased for both UiO-66 and UiO-66-NH₂ because of the strong interaction between zirconium and magnesium. The selectivity of main products, which were formic acid, lactic acid and dihydroxy acetone, were 42.2 %, 21.9 % and 20.3 %, respectively. The parametric study was performed with the most active catalyst ($Mg_{0.3}@UiO-66-NH_2$). The effects of different temperatures, catalyst loadings and hydrogen peroxide/glycerol (H/G) molar ratio were investigated by Anova software program.

55.5 % of glycerol conversion was obtained at 90°C, 7.5 g/L catalyst loading and 1.4 H/G molar ratio. The effect of reaction time on the conversion of glycerol was investigated at 90°C. After 6 hours, the glycerol conversion was found as 94.8 %.



REFERENCES

- Abid, H., Tian, H., Ang, M., Tade, M., Buckley, C. and Wang, Shaobin,** 2012, Nanosize Zr-metal organic framework (UiO-66) for hydrogen and carbon dioxide storage, *Chemical Engineering Journal*, 187:415–420 pp.
- Bai, Y., Dou, Y., Xie, L., Rutledge, W., Li, J., and Zhou, H.,** 2016, Zr-based metal-organic frameworks: design, synthesis, structure and applications, *Chemical Society Reviews*, 45:2327–2367 pp.
- Beltra, J. C., Pecha, J., Kasparkova, V. and Kolomaznik, K.,** 2013, Development of an hplc method for the determination of glycerol oxidation products, *Journal of Liquid Chromatography and Related Technologies*, 36:2758–2773 pp.
- Burton, P. D., Boyle T.J., Datye, A.K.,** 2011, Facile, surfactant-free synthesis of Pd nanoparticles for heterogeneous catalysis, *Journal of Catalysis*, 280:145–149 pp.
- Cai, X. et al.,** 2018, Pd/UiO-66 (Hf): A highly efficient heterogeneous catalyst for the hydrogenation of 2, 3, 5-trimethylbenzoquinone. *Catalysis Communications*, 113:23–26 pp.
- Cavka, J. H., Jakobsen, S., Olsbye, U., Guillou, N., Lamberti, C., Bordiga, S., and Lillerud, K. P.,** 2008, A new zirconium inorganic building brick forming metal organic frameworks with exceptional stability, *Journal of the American Chemical Society*, 130:13850–13851 pp.
- Chui, S. S.Y., Lo, S. M. F., Charmant, J. P. H., Orpen, A. G. and Williams, I. D.,** 1999, A chemically functionalizable nanoporous material [Cu-3(TMA)(2)(H₂O)(3)](n), *Science*, 283:1148 pp.
- Cirujano, F. G., Corma, A. & Xamena, F. X. L.,** 2015, Zirconium-containing metal organic frameworks as solid acid catalysts for the esterification of free fatty acids : Synthesis of biodiesel and other compounds of interest. *Catalysis Today*, 257:213–220 pp.
- Dan, L., Shiyu, C., Jing, G., Junhua, W., Ping, C. and Zhaoyin, H.,** 2011, Glycerol oxidation with oxygen over bimetallic Pt-Bi catalysts under atmospheric pressure, *Chinese Journal of Catalysis* 32:1831–1837 pp.

REFERENCES (continued)

- Duan, H., Zeng, Y., Yao, X., Xing, P., Liu, J. and Zhao, Y.,** 2017, Tuning synergistic effect of Au–Pd bimetallic nanocatalyst for aerobic oxidative carbonylation of amines, *American Chemical Society*, 29:3671-3677 pp.
- Eddaoudi, M., Kim, J., Rosi, N., Vodak, D., Wachter, J., O’Keeffe M. and O. M. Yaghi,** 2002, Systematic design of pore size and functionality in isoreticular MOFs and their applications in methane storage, *Science*, 295:469- 472 pp.
- Eddaoudi, M., Moler, D. B. and Li, H.,** Chen, B., Reineke, T.M., O’Keeffe, M. and Yaghi, O.M., 2001, Modular chemistry: secondary buildings units as a basis for the design of highly porous and robust metal-organic carboxylate frameworks, *Accounts of Chemical Research*, 34:319-330 pp.
- Falcaro, P., Ricco, R., Yazdi, A., Imaz, I., Furukawa, S., Maspoeh, D., Ameloot, R., Evans, J. D. and Doonan, C. J.,** 2016, Application of metal and metal oxide nanoparticles@MOFs, *Coordination Chemistry Reviews*, 307:237–254 pp.
- Farnetti, E. and Crotti, C.,** 2016, Selective oxidation of glycerol to formic acid catalysed by iron salts, *Catalysis Communications*, 84: 1-4 pp.
- Feng, D., Gu, Z.Y., Li, J.R., Jiang, H.L., Wei, Z. and Zhou, H.C.,** 2012, Zirconium-metalloporphyrin PCN-222:mesoporous metal-organic frameworks with ultrahigh stability as biomimetic catalysts, *Angewandte Chemie International Edition*, 51:10307–10310 pp.
- Ferey, G.,** 2008, Hybrid porous solids: past, present, future, *Chemical Society Reviews*, 37:191 –214 pp.
- Férey, G., Drazniekes, C. M., Serre, C., Millange, F., Dutour, J., Surblé, S. and Margiolaki, I.,** 2005, A chromium terephthalate-based solid with unusually large pore volumes and surface area, *Science*, 309: 2040-2042 pp.
- Fu, Y., Xu, L., Shen, H., Yang, H., Zhang, F., Zhu, W., and Fan, M.,** 2016, Tunable catalytic properties of multi-metal – organic frameworks for aerobic styrene oxidation, *Chemical Engineering Journal*, 299:135–141 pp.
- Fulajtarova, K., Sotak, T., Hronec, M., Vavra, I., Dobrocka, E. and Omastova, M.,** 2015, Aqueous phase hydrogenation of furfural to furfuryl alcohol over Pd-Cu catalysts, *Applied Catalysis A: General*, 502:78–85 pp.
- Furukawa, H., Cordova, K. E., O’Keeffe, M. and Yaghi, O. M.,** 2013, The chemistr and applications of metal-organic frameworks, *Science*, 341:6149 pp.

REFERENCES (continued)

- Gallezot, P.**, 1997, Selective oxidation with air on metal catalysts, *Catalysis Today*, 37:405–418 pp.
- Gedanken, A.**, 2004, Using sonochemistry for the fabrication of nanomaterials, *Ultrason Sonochem*, 11: 47-55 pp.
- Guan, Q., Wang, B., Chai, X., Liu, J., Gu, J. and Ning, P.**, 2017, Comparison of Pd-UiO-66 and Pd-UiO-66-NH₂ catalysts performance for phenol hydrogenation in aqueous medium, *Fuel*, 205:130–141 pp.
- Hajek, J., Vandichel, M., Voorde, B. Van De, Bueken, B., Vos, D. De, Waroquier, M., and Speybroeck, V. Van.**, 2015, Mechanistic studies of aldol condensations in UiO-66 and UiO-66-NH₂ metal organic frameworks, *Journal of Catalysis*, 331:1–12 pp.
- Hou, J., Luan, Y., Tang, J., Wensley, A. M., Yang, M., and Lu, Y.**, 2015, Journal of molecular catalysis a: chemical synthesis of UiO-66-NH₂ derived heterogeneous copper (II) catalyst and study of its application in the selective aerobic oxidation of alcohols, *Journal of Molecular Catalysis A: Chemical*, 407:53–59 pp.
- Hu, W., Knight, D., Lowry, B., and Varma, A.**, 2010, Catalytic oxidation of glycerol to high-value chemicals, *Industrial and Engineering Chemistry Research*, 49: 10876 –10882 pp.
- Hu, Z., Peng, Y., Kang, Z., Qian, Y. and Zhao, D. A.**, 2015, Modulated hydrothermal (MHT) approach for the facile synthesis of UiO-66-type MOFs, *Inorganic Chemistry*, 54: 4862 –4868 pp.
- Inoue, H., Kimura, S., Teraoka, Y., Chiku, M., and Pd, A.**, 2018, Mechanism of glycerol oxidation reaction on silver-modified palladium electrode in alkaline medium, *International Journal of Hydrogen Energy*, 1–8 pp (unpublished).
- Javadian, P., Zlotea, C., Ghimbeu, C.M., Latroche, M. and Jensen, T.R.**, 2015, Hydrogen storage properties of nanoconfined LiBH₄-Mg₂NiH₄ reactive hydride composites, *The Journal of Physical Chemistry C*, 119:5819 -5826 pp.
- Jhung, S. H., Lee, J. H., Yoon, J. W., Serre, C., Férey, G. and Chang, J. S.**, 2007, Microwave synthesis of chromium terephthalate MIL-101 and its benzene sorption ability, *Advanced Materials*, 19:121-124 pp.

REFERENCES (continued)

- Kaskow, I., Decyk, P. and Sobczak, I.,** 2018, The effect of copper and silver on the properties of Au-ZnO catalyst and its activity in glycerol oxidation, *Applied Surface Science*, 444:197-207.
- Kim, M. and Cohen, S. M.,** 2012, Postsynthetic modification of coordination networks, *CrystEngComm*, 14: 4096 –4104 pp.
- Kimura, H.,** 1993, Selective oxidation of glycerol on a platinum-bismuth catalyst by using a fixed bed reactor, *Applied Catalysis A: General*, 105:147–158 pp.
- Kimura, H., Tsuto, K., Wakisaka, T., Kazumi, Y. and Inaya, Y.,** 1993, Selective oxidation of glycerol on a platinum-bismuth catalyst, *Applied Catalysis A: General*, 96:217–228 pp.
- Kitagawa, S., Kitaura, R. and Noro, S.,** 2004, Functional porous coordination polymers, *Angewandte Chemie International Edition*, 43:2311-2453 pp.
- Krishna, C., Neeli, P., Puthiaraj, P., Lee, Y. and Chung, Y.,** 2018, Transfer hydrogenation of nitrobenzene to aniline in water using Pd nanoparticles immobilized on amine-functionalized UiO-66, *Catalysis Today*, 303:227–234 pp.
- Kwon, Y., Schouten, K. J. P., and Koper, M. T. M.,** 2011, Mechanism of the Catalytic Oxidation of Glycerol on Polycrystalline Gold and Platinum Electrodes, 7: 1085-1215 pp.
- Lee, J., Farha, O. K., Roberts, J., Scheidt, K. A., Nguyen, S. and Hupp, T.,** 2009, Metal-organic framework materials as catalysts, *Chemical Society Reviews*, 38: 1450 –1459 pp.
- Lee, Y., Kim, J. and Ahn, W.,** 2013, Synthesis of metal-organic frameworks : A mini review, *Korean Journal of Chemical Engineering*, 30:1667–1680 pp.
- Lee, Y., Kim, S., Kang, J. K. and Cohen, S.M.,** 2015, Photocatalytic CO₂ reduction by a mixed metal (Zr/Ti) mixed ligand metal-organic framework under visible light irradiation, *Chemical Communications*, 51:5735 –5738 pp.
- Li, A., Shen, K., Chen, J., Li, Z. and Li, Y.,** 2017, Highly selective hydrogenation of phenol to cyclohexanol over MOF-derived non-noble Co-Ni @ NC catalysts, *Chemical Engineering Science*, 166:66–76 pp.
- Li, H., Eddaoudi, M., O’Keeffe, M. and Yaghi, O. M.,** 1999, Design and synthesis of an exceptionally stable and highly porous metal-organic framework, *Nature*, 402:276- 279 pp.

REFERENCES (continued)

- Li, J., Li, X., Hayat, T., Alsaedi, A., and Chen, C.,** 2017, Screening of zirconium-based metal–organic frameworks for efficient simultaneous removal of antimonite (Sb(III)) and antimonate (Sb(V)) from aqueous solution, *ACS Sustainable Chemistry and Engineering*, 5:11496-11503 pp.
- Li, X., Kaizen, A., Ding, J., Min, J. and Zhu, Y.,** 2017, Pd-Ce nanoparticles supported on functional Fe-MIL-101-NH₂ : An efficient catalyst for selective glycerol oxidation, *Catalysis Today*, 279:77–83 pp.
- Li, Y. and Zaera, F.,** 2015, Sensitivity of the glycerol oxidation reaction to the size and shape of the platinum nanoparticles in Pt/SiO₂ catalysts, *Journal of Catalysis*, 326:116–126 pp.
- Li, Y., Wei, Z., Liu, L., Gao, M. and Han, Z.,** 2018, Ag nanoparticles supported on UiO-66 for selective oxidation of styrene, *Inorganic Chemistry Communications*, 88:47–50 pp.
- Liang, Q., Zhang, M., Zhang, Z., Liu, C., Xu, S., and Li, Z.,** 2017, Zinc phthalocyanine coupled with UiO-66 (NH₂) via a facile condensation process for enhanced visible-light-driven photocatalysis. *Journal of Alloys and Compounds*, 690: 123–130 pp.
- Lin, K. A., Liu, Y. and Chen, S.,** 2016, Adsorption of fluoride to UiO-66-NH₂ in water: stability, kinetic, isotherm and thermodynamic studies, *Journal of Colloid and Interface Science*, 461: 79–87 pp.
- Long, J., Liu, H., Wu, S., Liao, S. and Li, Y.,** 2013, Selective oxidation of saturated hydrocarbons using Au – Pd alloy nanoparticles supported on metal–organic frameworks, *ACS Catalysis*, 3: 647-654 pp.
- Lu, P., Wu, Y., Kang, H., Wei, H., Liu, H. and Fang, M.,** 2014, What can pKa and NBO charges of the ligands tell us about the water and thermal stability of metal organic frameworks?, *Journal of Materials Chemistry A*, 2:16250–16267 pp.
- Lu, W., Wei, Z., Gu, Z., Li, T., Park, J., Tian, J., Zhang, M., Zhang, Q., Gentle, T., Bosch, M. and Zhou, H.,** 2014, Tuning the structure and function of metal-organic frameworks via linker design, *Chemical Society Reviews*, 43: 5561–5593 pp.
- Luu, C. L., Nguyen, T. T. Van, Nguyen, T., and Hoang, T. C.,** 2015, Synthesis, characterization and adsorption, *Advances in Natural Sciences: Nanoscience and Nanotechnology*, 6: 025004.

REFERENCES (continued)

- Maris, E. P., Ketchie, W. C., Murayama, M., & Davis, R. J.**, 2007, Glycerol hydrogenolysis on carbon-supported Pt-Ru and Au-Ru bimetallic catalysts, *Journal of Catalysis*, 251: 281–294 pp.
- Mondloch, J.E., Bury, W., Fairen-Jimenez, D., Kwon, S., DeMarco, E.J., Weston, M.H., Sarjeant, A.A., Nguyen, S.T., Stair, P.C., Snurr, R.Q., Farha, O.K. and Hupp, J.T.**, 2013, Vapor-phase metalation by atomic layer deposition in a metal-organic framework, *Journal of American Chemical Society*, 135:10294–10297 pp.
- Mueller, U., Schubert, M., Teich, F., Puetter, H., Schierle-Arndt K. and Pastre, J.**, 2006, metal-organic frameworks-prospective industrial applications, *Journal of Materials Chemistry*, 16:626-636 pp.
- Müller, M., Harvey, G. and Prins, R.**, 2000, Comparison of the dealumination of zeolites beta, mordenite, ZSM-5 and ferrierite by thermal treatment, leaching with oxalic acid treatment with Si Cl₄ by ¹H, ²⁹Si, ²⁷Al MAS NMR, *Microporous Mesoporous Materials*, 34:135–147 pp.
- Nale, A., Pendolino, F., Maddalena, A. and Colombo, P.**, 2016, Enhanced hydrogen release of metal borohydrides M(BH₄)_n (M = Li, Na, Mg, Ca) mixed with reduced graphene oxide, *International Journal of Hydrogen Energy* 41:11225-11231 pp.
- Ni, Z. and Masel, R.I.**, 2006, Rapid production of metal-organic frameworks via microwave-assisted solvothermal synthesis, *Journal of the American Chemical Society*, 128:12394- 12395 pp.
- Olmos, C. M., Chinchilla, L.E., Rodrigues E.G., Delgado, J.J., Hungria, A. B., Blanco, G., Pereira, M. F. R., Orfao, J. J. M., Calvino, J.J. and Chen, X.**, 2016, Environmental Synergistic effect of bimetallic Au-Pd supported on ceria-zirconia mixed oxide catalysts for selective oxidation of glycerol. *Applied Catal. B, Environ.* 197:222–235 pp.
- Oozeerally, R., Burnett, D. L., Chamberlain, T. W., Walton, R. I. and Degirmenci, V.**, 2017, Exceptionally efficient and recyclable heterogeneous metal-organic framework catalyst for glucose isomerization in water, *ChemCatChem*, 10:706–709 pp.
- Pagliaro, M.**, 2010, *The future of Glycerol*, RSC Publishing, Cambridge, 170 p.

REFERENCES (continued)

- Plerdsranoy, P., Kaewsuwan, D., Chanlek, N. and Utke, R.,** 2017, Effects of specific surface area and pore volume of activated carbon nanofibers on nanoconfinement and dehydrogenation of LiBH₄, *International Journal of Hydrogen. Energy* 42:6189 -6201 pp.
- Ponomareva, V. G., Kovalenko, K. A., Chupakhin, A. P., Dybtsev, D. N., Shutova, E. S. and Fedin, V. P.,** 2012, Imparting high proton conductivity to a metal–organic framework material by controlled acid impregnation, *Journal of the American Chemical Society*, 134:15640 –15643 pp.
- Poungsombate, A., Imyen, T., Dittanet, P., Embley, B. and Kongkachuichay, P.,** 2017, Direct synthesis of dimethyl carbonate from CO₂ and methanol by supported bimetallic Cu–Ni/ZIF-8 MOF catalysts, *Journal of the Taiwan Institute of Chemical Engineers*, 80:16–24 pp.
- Pourkhosravani, M., Dehghanpour, S. and Farzaneh, F.,** 2015, Palladium nanoparticles supported on zirconium metal organic framework as an efficient heterogeneous catalyst for the suzuki-miyaura coupling reaction, *Catalysis Letters*, 146: 499–508 pp.
- Purushothaman, R. K. P.,** 2014, Oxidation of glycerol to bio-based chemicals using supported mono- and bimetallic noble metal catalysts, PhD thesis, University of Groningen, 156p.
- Rademann, K., Klimakow, M., Klobes, P., and Th, A. F.,** 2010, Mechanochemical synthesis of metal-organic frameworks: a fast and facile approach toward quantitative yields and high specific surface areas, *American Chemical Society*, 22: 5216–5221 pp.
- Rodrigues, E. G., Pereira, M. F. R., Delgado, J. J., Chen, X. and Órfão, J. J. M.,** 2011, Enhancement of the selectivity to dihydroxyacetone in glycerol oxidation using gold nanoparticles supported on carbon nanotubes, *CATCOM*, 16:64–69 pp.
- Rösler, C., Dissegna, S., Rechac, V. L., Kauer, M., Guo, P., Turner, S. and Tendeloo, G.,** 2017, Encapsulation of bimetallic metal nanoparticles into robust zirconium-based metal–organic frameworks: evaluation of the catalytic potential for size-selective hydrogenation, *Chemistry: A European Journal*, 23: 3583–3594 pp.
- Sankar, J., Onyeozili, E.N. and Kalu, E.E.,** 2017, Oxidation of glycerol with unactivated electroless CuNiMoP catalyst, *ChemEngineering*, 1:11 p.

REFERENCES (continued)

- Schaate, A., Roy, P., Godt, A., Lippke, J., Waltz, F., Wiebcke, M. and Behrens, P.**, 2011, Modulated synthesis of Zr-based metal-organic frameworks: from nano to single crystals, *Chemistry: A European Journal*, 17: 6643 –6651 pp.
- Sharma, G., Kumar, A., Sharma, S., Naushad, M., Prakash, R., Alothman, Z. A., and Tessema, G.**, 2017, Science novel development of nanoparticles to bimetallic nanoparticles and their composites: a review, *Journal of King Saud University – Science* (in press).
- Silaghi, M., Chizallet, C., and Raybaud, P.**, 2014, Microporous and mesoporous materials challenges on molecular aspects of dealumination and desilication of zeolites, *Microporous and Mesoporous Materials*, 191:82-96 pp.
- Stock, N. and Biswas, S.**, 2012, Synthesis of metal-organic frameworks (MOFs): routes to various MOF topologies, morphologies and composites, *Chemical Reviews*, 112:933-969 pp.
- Surrey, A., Minella, C.B., Fechler, N., Antonietti, M., Grafe, H.J., Schultz, L. and Rellinghaus, B.**, 2016, Improved hydrogen storage properties of LiBH₄ via nanoconfinement in micro- and mesoporous aerogel-like carbon, *International Journal of Hydrogen Energy*, 41:5540-5548 pp.
- Suslick, K. S., Choe, S. B., Cichowlas, A. A. and Grinstaff, M. W.**, 1991, Sonochemical synthesis of amorphous iron, *Nature*, 353:414-416 pp.
- Taddei, M.**, 2017, When defects turn into virtues: the curious case of zirconium-based metal-organic frameworks, *Coordination Chemistry Reviews*, 343:1–24 pp.
- Timofeeva, M. N., Panchenko, V.N., Jun, J. W., Hasan, Z., Matrosova, M.M. and Jhung, S.H.**, 2014, Effects of linker substitution on catalytic properties of porous zirconium terephthalate UiO-66 in acetalization of benzaldehyde with methanol, *Applied Catalysis A: General*, 471: 91–97 pp.
- Tranchemontagne, D. J., Mendoza-Cortes, J. L., O’Keeffe, M. and Yaghi, O. M.**, 2009, Secondary building units, nets and bonding in the chemistry of metal-organic frameworks, *Chemical Society Reviews*, 38:1257-1283 pp.
- Vershon, D. and Purushothaman, P.**, 2014, Oxidation of glycerol to biobased chemicals using supported mono- and bimetallic noble metal catalysts, 156 p.
- Villa, A., Dimitratos, N., Chan-Thaw, C.E., Hammond, C., Prati, L. and Hutchings G.J.**, 2015, Glycerol oxidation using gold-containing catalysts, *American Chemical Society*, 48:1403-1412 pp.

REFERENCES (continued)

- Wang, F. et al.**, 2015, Selective oxidation of glycerol over Pt supported on mesoporous carbon nitride in base-free aqueous solution, *Chemical Engineering Journal*, 264: 336–343 pp.
- Wang, H., Li, X., Lan, X. and Wang, T.**, 2018, Supported ultra fine NiCo bimetallic alloy nanoparticles derived from bimetal–organic frameworks : a highly active catalyst for furfuryl alcohol hydrogenation, *ACS Catalysis*, 8: 2121-2128 pp.
- Wang, S., Wang, J., Cheng, W., Yang, X., Zhang, Z., Xu, Y., Liu, H., Wu Y. and Fang, M.**, 2015, A Zr-metal-organic frameworks based on tetrakis(4-carboxyphenyl) silane and factors affecting the hydrothermal stability of Zr-MOFs, *Dalton Transactions*, 44:8049–8061 pp.
- Wang, Y., Miao, Y., Li, S., Gao, L. and Xiao, G.**, 2017, Metal-organic frameworks derived bimetallic Cu-Co catalyst for efficient and selective hydrogenation of biomass-derived furfural to furfuryl alcohol, *Molecular Catalysis*, 436:128–137 pp.
- Wang, Y.T., Wan, C.B., Meng, X.H. and Ju, X.**, 2015, Improvement of the LiBH₄ hydrogen desorption by confinement in modified carbon nanotubes, *Journal of Alloys and Compounds*, 645 (1):112-116 pp.
- Węrz, N., Brandner, A. and Claus, P.**, 2010, A theoretical study of CO₂ anions on anatase (101) surface, *The Journal of Physical Chemistry*, 114:1164 – 1172 pp.
- Wu, H., Chua, Y. S., Krungleviciute, V., Tyagi, M., Chen, P., Yildirim, T. and Zhou, W.**, 2013, Unusual and highly tunable missing-linker defects in zirconium metal –organic framework UiO-66 and their important effects on gas adsorption. *Journal of the American Chemical Society*, 135 (28):10525 –10532 pp.
- Xiao, Y., Greeley, J. and Varma, A.**, 2016, An experimental and theoretical study of glycerol oxidation to 1,3-dihydroxyacetone over bimetallic Pt-Bi catalysts, *AIChE Journal*, 63:397-854 pp.
- Yaghi, O.M., O'Keeffe, M., Ockwig, N.W., Chae, H.K., Eddaoudi, M. and Kim, J.**, 2003, Reticular synthesis and the design of new materials, *Nature* 423:705 pp.

REFERENCES (continued)

- Yang, Y., Yao, H., Xi, F. and Gao, E.,** 2014, Amino-functionalized Zr (IV) metal–organic framework as bifunctional acid–base catalyst for Knoevenagel condensation, *Journal of Molecular Catalysis A : Chemical*, 390:198–205 pp.
- Yee, K. K., Reimer, N., Liu, J., Cheng, S. Y., Yiu, S. M., Weber, J., Stock, N. and Xu, Z.,** 2013, Effective mercury sorption by thiol-laced metal organic frameworks: in strong acid and the vapor phase, *Journal of the American Chemical Society*, 135:7795–7798 pp.
- Yu, X., Tang, Z., Sun, D., Ouyang, L. and Zhu, M.,** 2017, Recent advances and remaining challenges of nanostructured materials for hydrogen storage applications, *Progress in Materials Science*, 88:1-48 pp.
- Yuan, S., Qin, J., Lollar, C. T., and Zhou, H.,** 2018, Stable metal–organic frameworks with group 4 metals: current status and trends, *American Chemical Society*, 4:440-450 pp.
- Zhang, C., Wang, T., Liu, X. and Ding, Y.,** 2016, Cu-promoted Pt/activated carbon catalyst for glycerol oxidation to lactic acid, *Journal of Molecular Catalysis A : Chemical*, 424: 91–97 pp.
- Zhang, F., Zhang, T., Zou, X., Liang, X., Zhu, G., and Qu, F.,** 2017, Electrochemical synthesis of metal organic framework films with proton conductive property, *Solid State Ionics*, 301:125–132 pp.
- Zhang, X., Huang, P., Liu, A. and Zhu, M.,** 2017, A metal–organic framework for oxidative desulfurization: UiO-66 (Zr) as a catalyst, *Fuel*, 209: 417–423 pp.
- Zhao, S., Chen, D., Xu, H., Mei, J., Qu, Z., Liu, P., Cui, Y. and Yan, N.,** 2018, Chemosphere combined effects of Ag and UiO-66 for removal of elemental mercury from flue gas, *Chemosphere*, 197:65–72 pp.
- Zheng, J., Wu, M., Jiang, F., Su, W. and Hong, M.,** 2015, Stable porphyrin Zr and Hf metalorganic frameworks featuring 2.5 nm cages: high surface areas, SCSC transformations and catalyses, *Chemical Science*, 6:3466 –3470 pp.
- Zhou, F., Lu, N., Fan, B., Wang, H. and Li, R.,** 2016, Zirconium-containing UiO-66 as an efficient and reusable catalyst for transesterification of triglyceride with methanol, *Journal of Energy Chemistry*, 25:874–879 pp.

REFERENCES (continued)

Zhu, X. Y., Li, B., Yang, J., Li, Y. S., Zhao, W. R., Shi, J. L. and Gu, J. L., 2015, Effective adsorption and enhanced removal of organophosphorus pesticides from aqueous solution by Zr-Based MOFs of UiO-67, *ACS Applied Materials and Interfaces*, 7: 223 –231 pp.



CURRICULUM VITAE

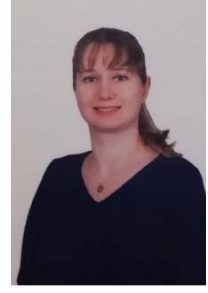
Hülya AÇAR KILIÇ

Cumhuriyet Neighborhood Uğur Mumcu Street No:135/7

Uşak TURKEY

0506 393 96 17

E-mail: hulyaacar13@gmail.com



PERSONAL DATA

Date of birth : 13.09.1987
 Place of Birth : Edirne
 Nationality : Turkish
 Marital Status : Married
 Driver's License : Class B Driving License

EDUCATION INFORMATION

2007-2012 Izmir Institute of Technology- İzmir
 License, Engineering Faculty,
 Department of Chemical Engineering (English),
 Degree Note: 3,10/4

2002-2006 Edirne Anatolian High School-Edirne
 Science Department,
 Degree Note: 4,74/5

JOB EXPERIENCE

2013-2014 Pharmactive Pharmaceuticals Industry Trade Inc.-
 Tekirdağ

- R&D Laboratory, Analytic Expert Assistant

(07-08)-2011 Olmuksan International Paper Packing Industry and Trade
 Inc.- Edirne

- Product Department, Trainee

JOB EXPERIENCE

- (01-02)-2011 Edirne Oil Industry and Trade Inc.- Edirne
- Laboratory Department, Trainee
- (06-07)-2011 Pharmaceuticals Industry Trade Inc.- Tekirdağ
- Laboratory and Production Department, Trainee

LANGUAGES

English	Advanced Level (Speaking and Writing)
French	Beginner
German	Beginner

COMPUTER SKILLS

MS Office Program	High Level
Polymath	Intermediate
Matlab, Chemeq	Intermediate
Minitab	Beginner
Microsoft Office Project Program	Beginner
Aspen, Chemcaq	Beginner

USED DEVICES

HPLC, GC (EID), UV Device, Dissolution Device, Genel Laboratory Devices.

PROJECTS

Undergraduate Thesis

(2011-2012) Biomass Conversion to Valuable Chemical

PROJECTS

ISPARTEK 2012 Project Competition First Prize**(Biomass Valuable Chemicals)**

Design Project

(2011-2012)	The Clean Coal Power Plant Design
Autumn 2011-2012	Absorption Column Design
Spring 2010-2011	Ethylene Oxide Production Reactor Design
Autumn 2010-2011	Heat Exchanger- Condenser Design
Spring 2009-2010	Natural Fiber Reinforces Polymer Composite and Application
Autumn 2009-2010	Production and Characterization of Autoclaved Aerated Concrete

CONFERENCES

04.2012 4th National Catalysis Conference - Kocaeli

- Kılıç E., Açar H., İşeri N., Yılmaz S. "Selective Dehydration of Fructose over different catalysts and solvents" NCC 4 National Congress of Catalysis, Kocaeli Turkey, March 2012.

05.2012 ISPARTEK 2012 Project Competition - Isparta

- Kılıç E., Açar H., İşeri N., Yılmaz S. "Production of Valuable Chemicals from Fruit Sugars" ISPARTEK 2012 Project Competition, (Championship Award), Isparta Turkey, May 2012.

CONFERENCES**07.2012 CAT4BIO International Conference Thessaloniki/ Greece**

- Kılıç E., Açar H., İşeri N., Yılmaz S. "Fructose Dehydration to 5-Hydroxymethylfurfural over Catalysts Prepared by Sulfonation" Cat 4 Bio Conference, Thessaloniki Greece, June, 2012.

06.2017 Humanitarian Engineering Symposium at the University of Warwick Coventry/England.**REFERENCES**

- Prof. Dr. Selahattin Yılmaz
Izmir Institute of Technology- İzmir
Phone Number: 0232 750 66 59
E-mail: selahattinyilmaz@iyte.edu.tr
- Prof. Dr. Erol Şeker
Izmir Institute of Technology- İzmir
Phone Number: 0232 750 66 46
E-mail: erolseker@iyte.edu.tr